Sensoriamento Remoto da Atmosfera com Lasers

Eduardo Landulfo

elandulf@ipen.br

TÓPICOS

- INTRODUÇÃO
- ESPALHAMENTO
  - RAYLEIGH
  - MIE
- INSTRUMENTAÇÃO LIDARS
  - ÓPTICA
  - LASERS
  - ELETRÔNICA
- ESTUDOS ATMOSFÉRICOS COM LASERS
  - AEROSSÓIS
  - VAPOR D'ÁGUA
  - GEE

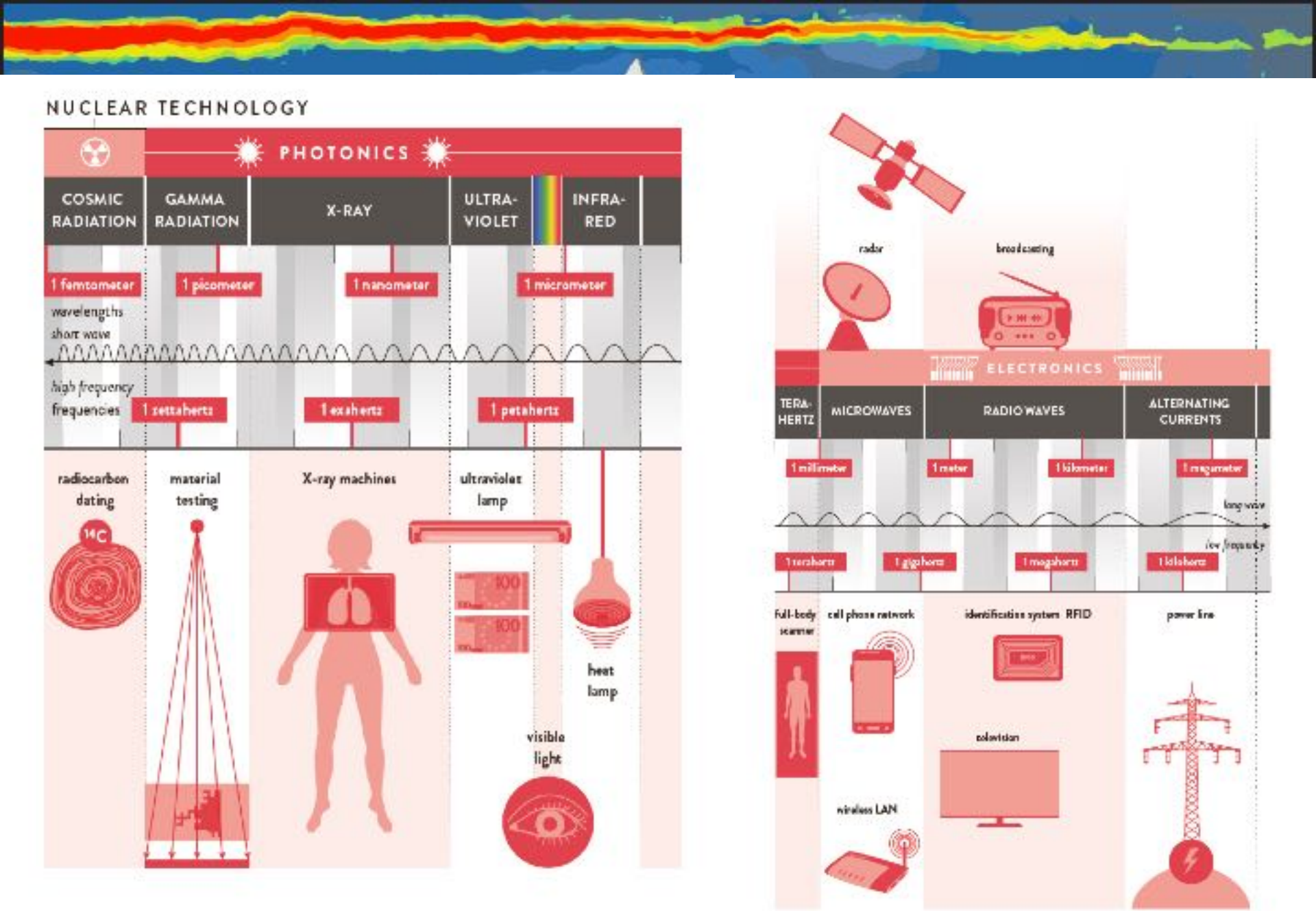

Sensoriamento Remoto da Atmosfera com Lasers

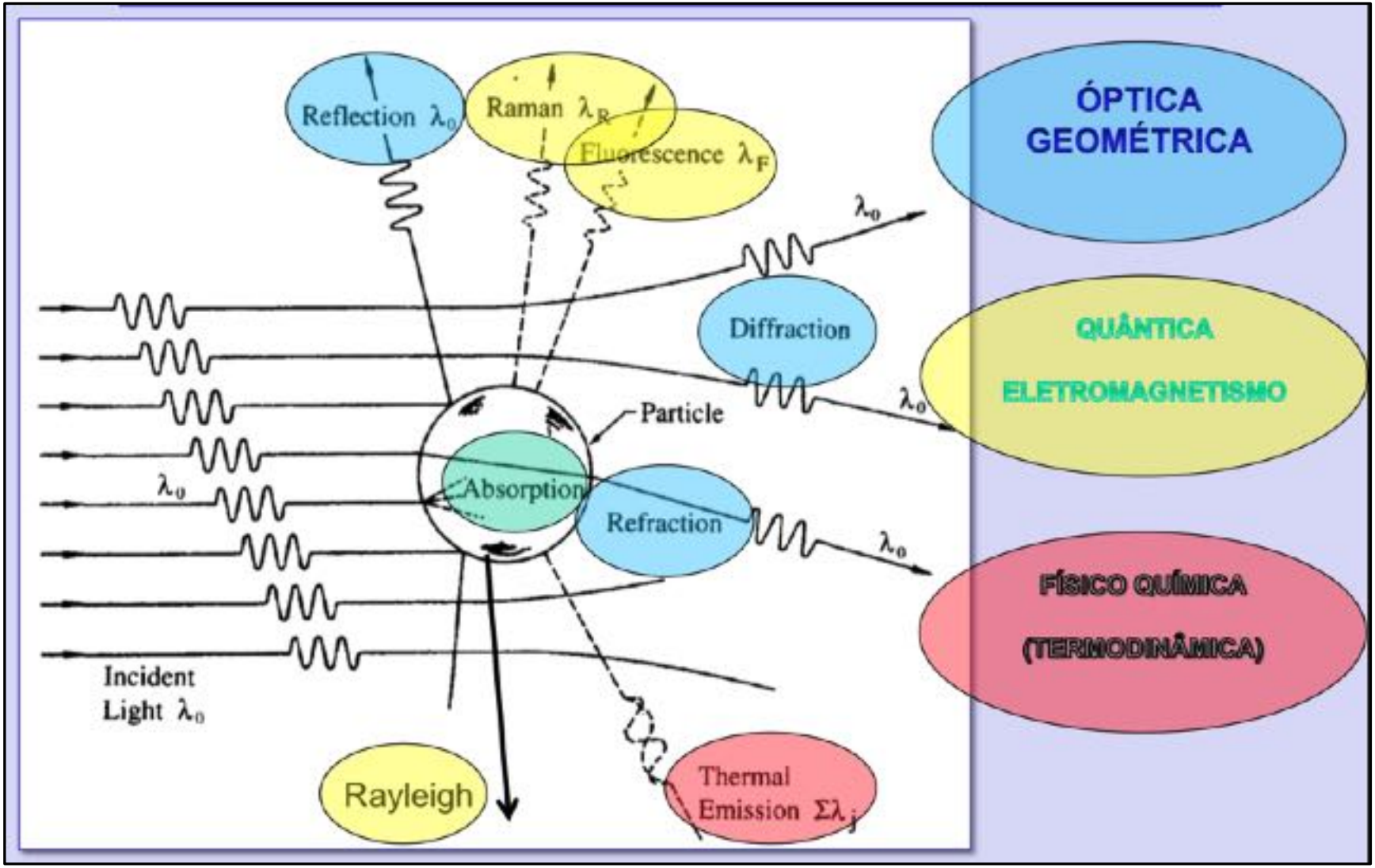
Reflection λ_0
Raman λ_R
Fluorescence λ_F
λ_0
Diffraction
λ_0
Particle
λ_0
Absorption
Refraction
λ_0
Incident
Light λ_0
Rayleigh
Thermal
Emission $\Sigma\lambda_j$
ÓPTICA
GEOMÉTRICA
QUÂNTICA
ELETROMAGNETISMO
FÍSICO QUÍMICA
(TERMODINÂMICA)

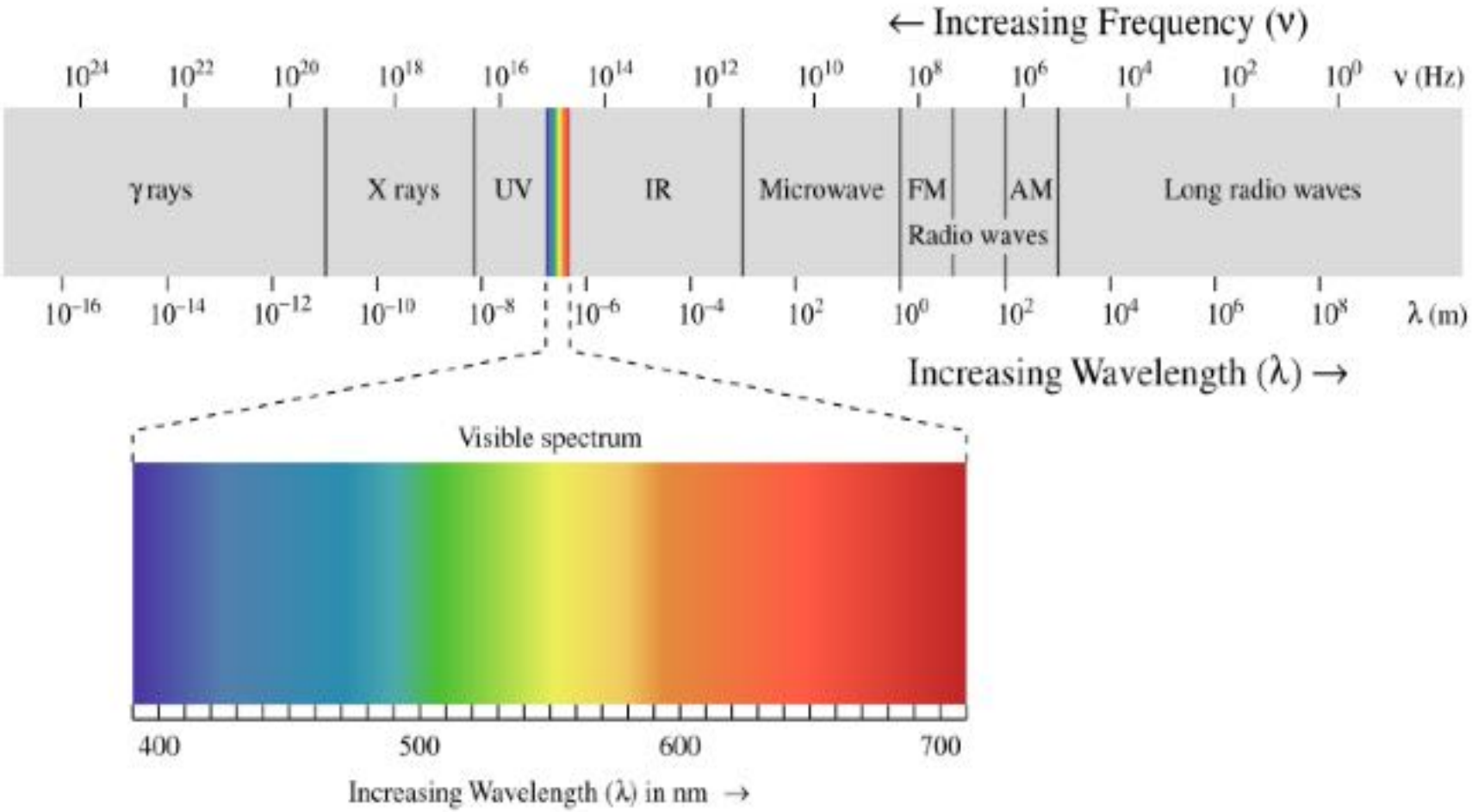
← Increasing Frequency (ν)
10^{24} 10^{22} 10^{20} 10^{18} 10^{16} 10^{14} 10^{12} 10^{10} 10^{8} 10^{6} 10^{4} 10^{2} 10^{0} ν (Hz)
γ rays
X rays
UV
IR
Microwave
FM
AM
Radio waves
Long radio waves
10^{-16} 10^{-14} 10^{-12} 10^{-10} 10^{-8} 10^{-6} 10^{-4} 10^{2} 10^{0} 10^{2} 10^{4} 10^{6} 10^{8} λ (m)
Increasing Wavelength (λ) →
Visible spectrum
400
500
600
700
Increasing Wavelength (λ) in nm →

$$C = \lambda . f$$

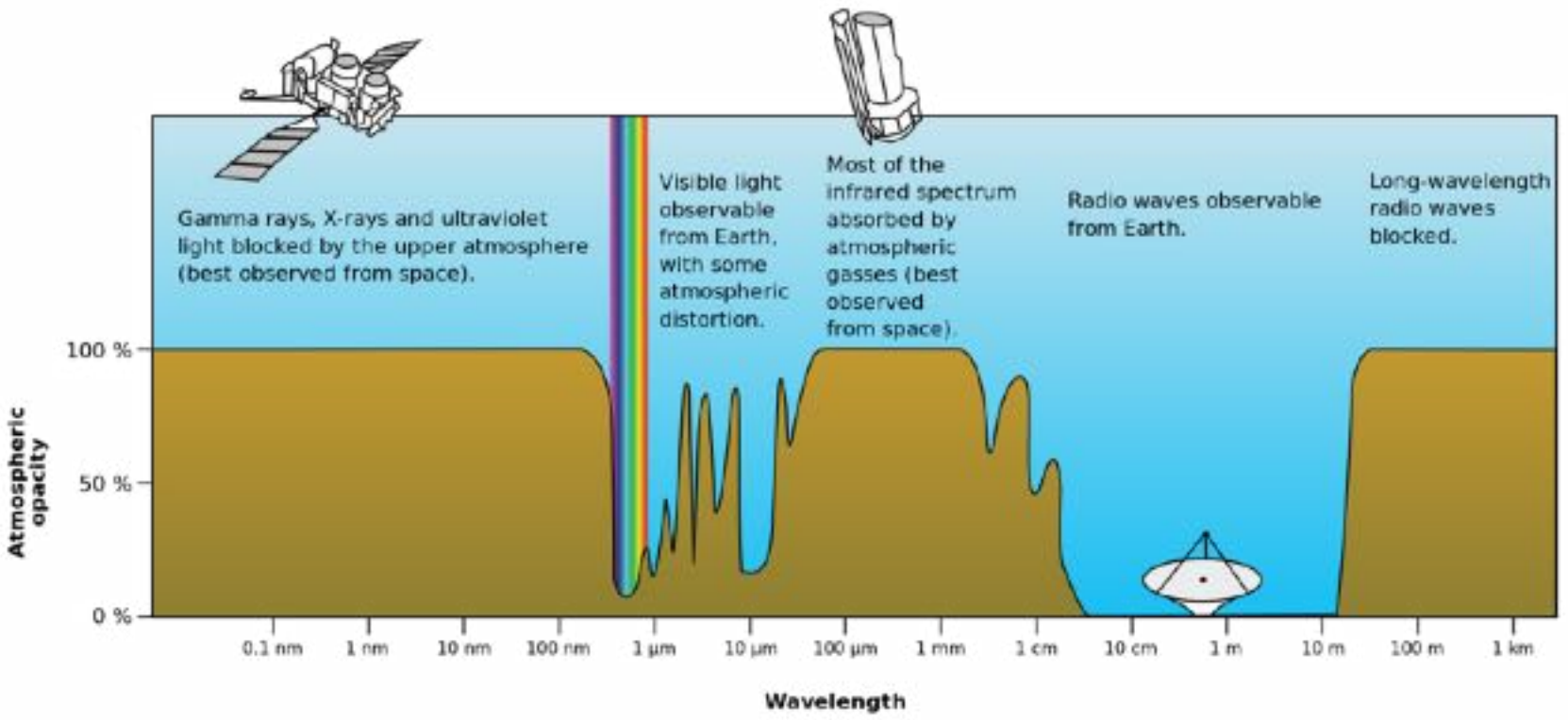
Gamma rays, X-rays and ultraviolet light blocked by the upper atmosphere (best observed from space).
Visible light observable from Earth, with some atmospheric distortion.
Most of the infrared spectrum absorbed by atmospheric gasses (best observed from space).
Radio waves observable from Earth.
Long-wavelength radio waves blocked.
Atmospheric opacity
100 %
50 %
0 %
0.1 nm
1 nm
10 nm
100 nm
1 µm
10 µm
100 µm
1 mm
1 cm
10 cm
1 m
10 m
100 m
1 km
Wavelength

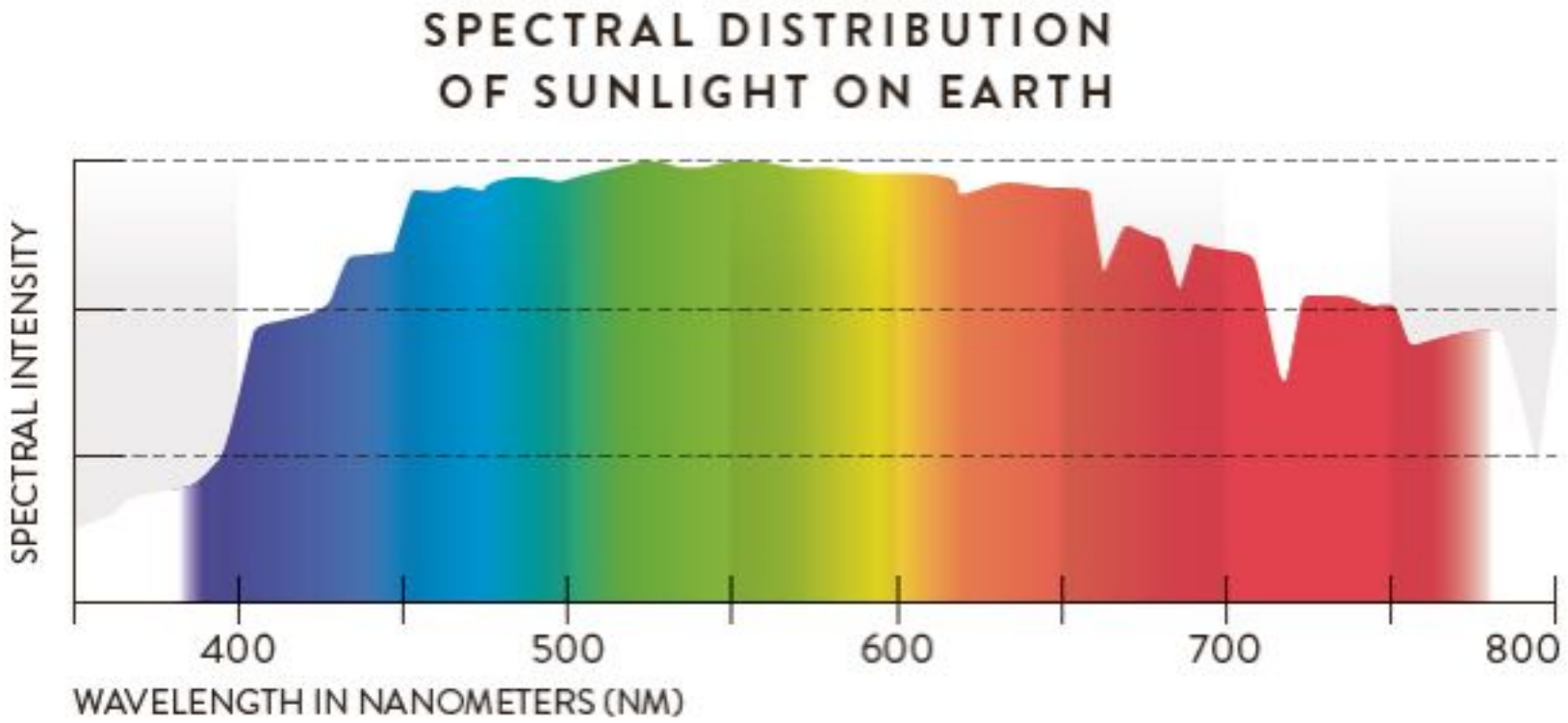
SPECTRAL DISTRIBUTION
OF SUNLIGHT ON EARTH
SPECTRAL INTENSITY
400
500
600
700
800
WAVELENGTH IN NANOMETERS (NM)

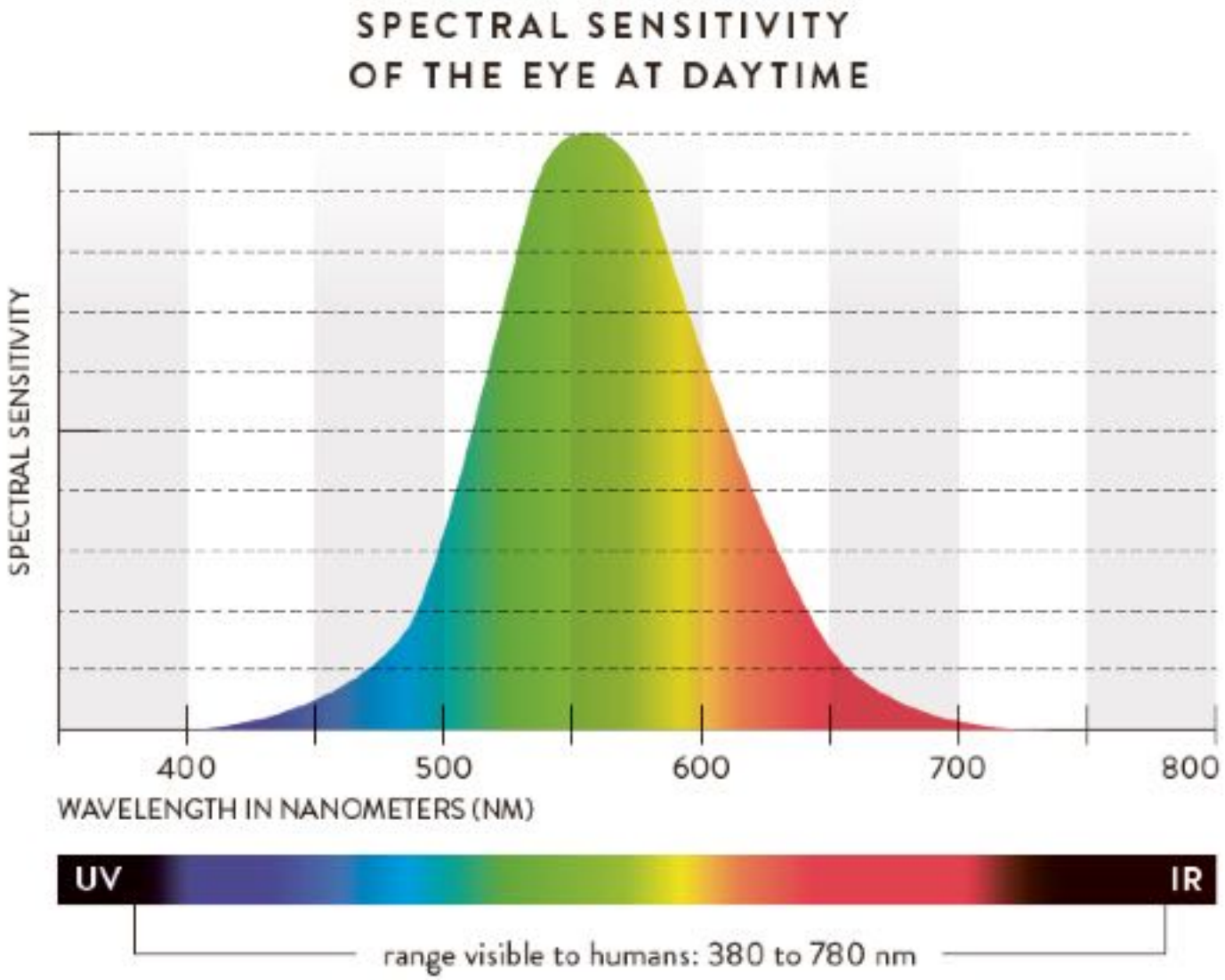
SPECTRAL SENSITIVITY
OF THE EYE AT DAYTIME
SPECTRAL SENSITIVITY
400
500
600
700
800
WAVELENGTH IN NANOMETERS (NM)
UV
IR
range visible to humans: 380 to 780 nm

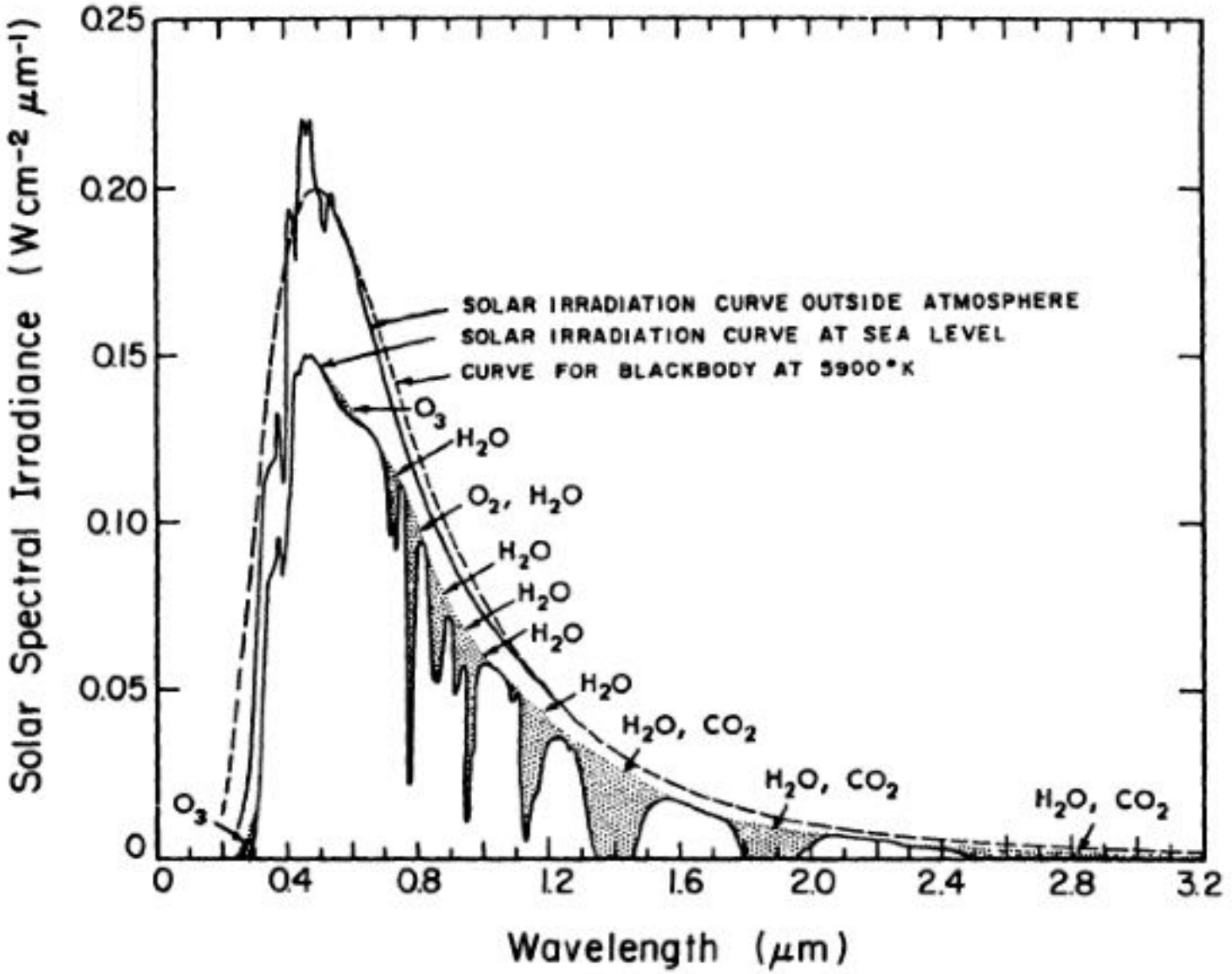
Solar Spectral Irradiance ($W cm^{-2} \mu m^{-1}$)
0.25
0.20
0.15
0.10
0.05
0
0
0.4
0.8
1.2
1.6
2.0
2.4
2.8
3.2
Wavelength (μm)
SOLAR IRRADIATION CURVE OUTSIDE ATMOSPHERE
SOLAR IRRADIATION CURVE AT SEA LEVEL
CURVE FOR BLACKBODY AT 5900°K
O_3
H_2O
O_2, H_2O
H_2O
H_2O
H_2O
H_2O
H_2O, CO_2
H_2O, CO_2
H_2O, CO_2
O_3

QUANTO DA RADIAÇÃO A TERRA EMITE PARA O ESPAÇO?

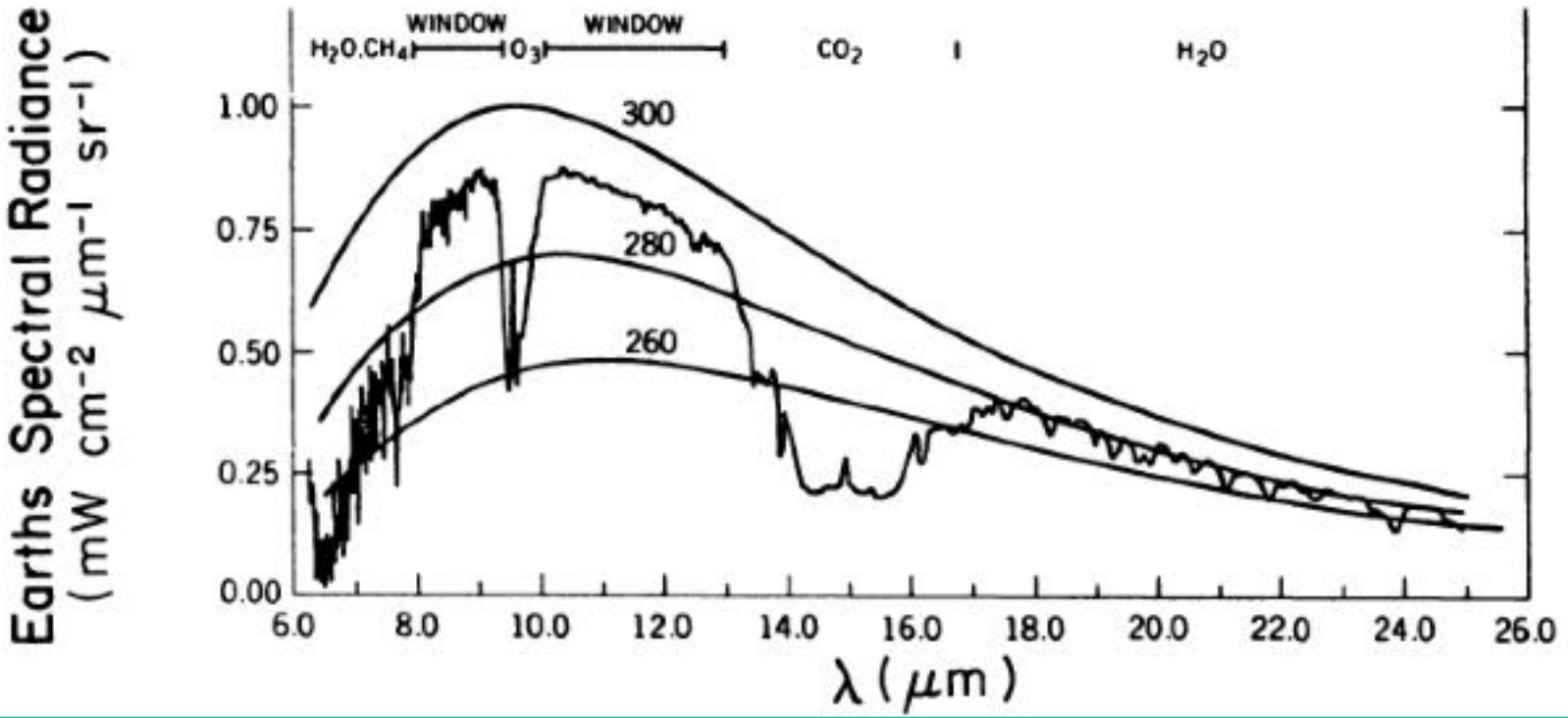

RADIAÇÃO DE UM CORPO NEGRO

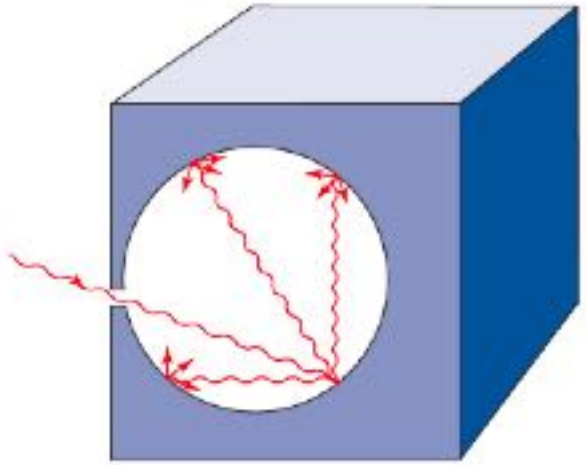

$$B_\lambda(T) = \frac{c_1 \lambda^{-5}}{\pi \left(e^{c_2/\lambda T} - 1\right)}$$

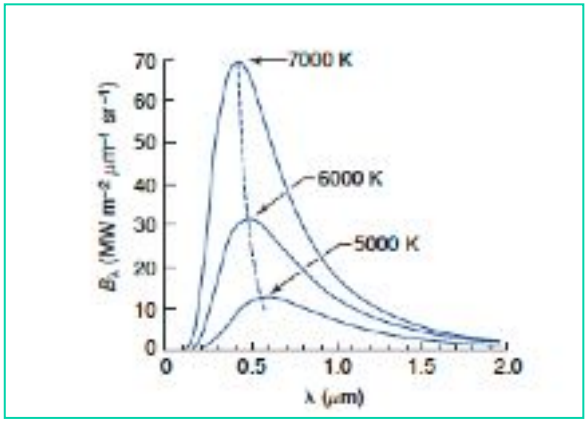

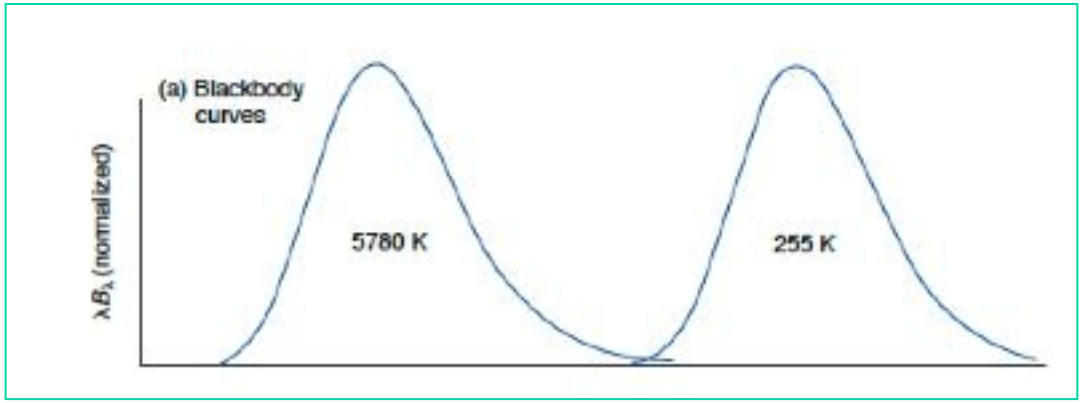

A LUZ INTERAGINDO COM A MATÉRIA

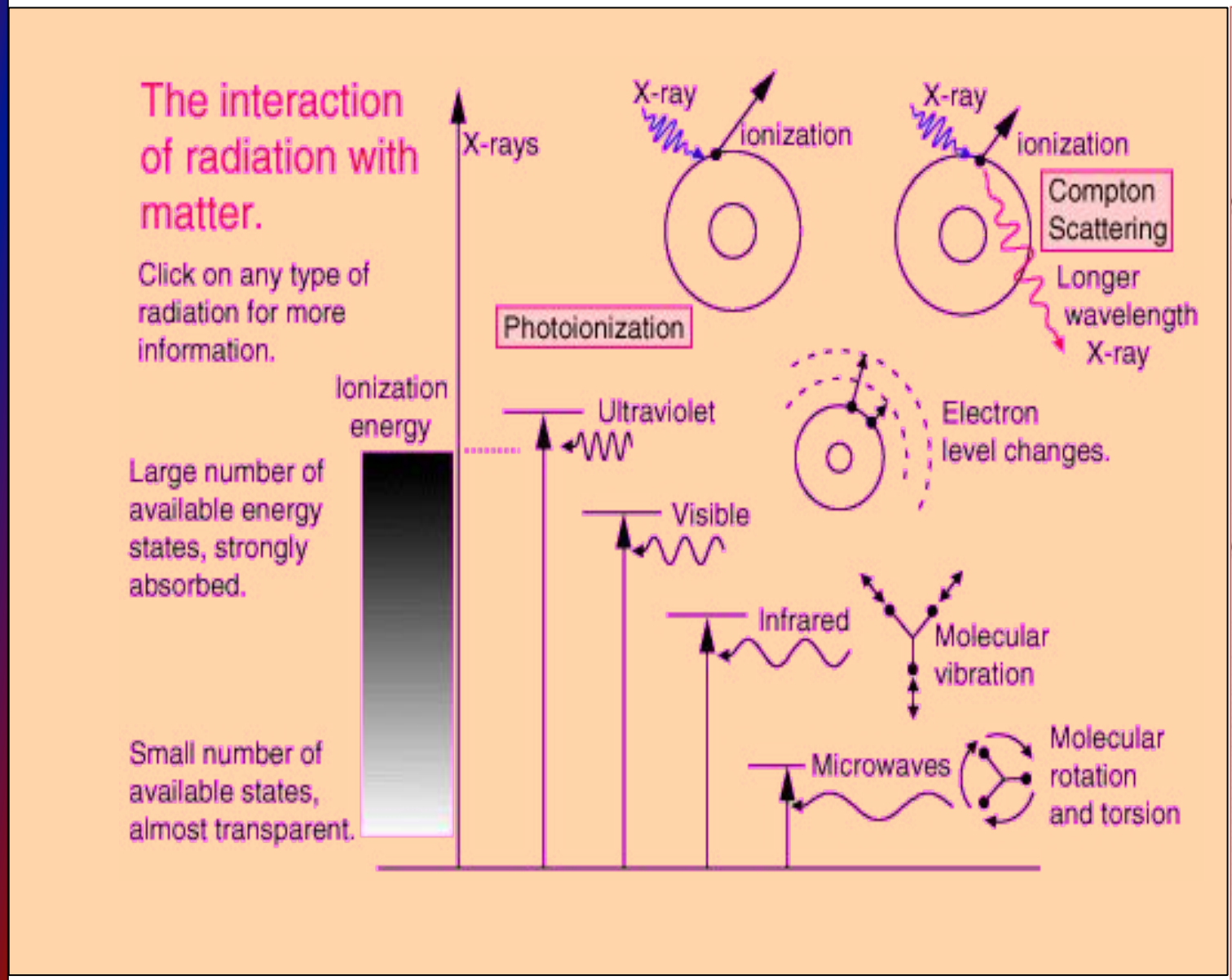

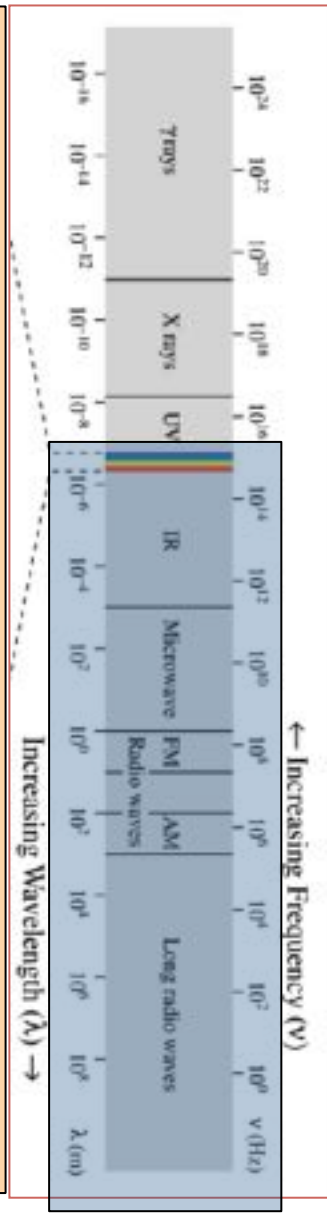

A LUZ INTERAGINDO COM A MATÉRIA

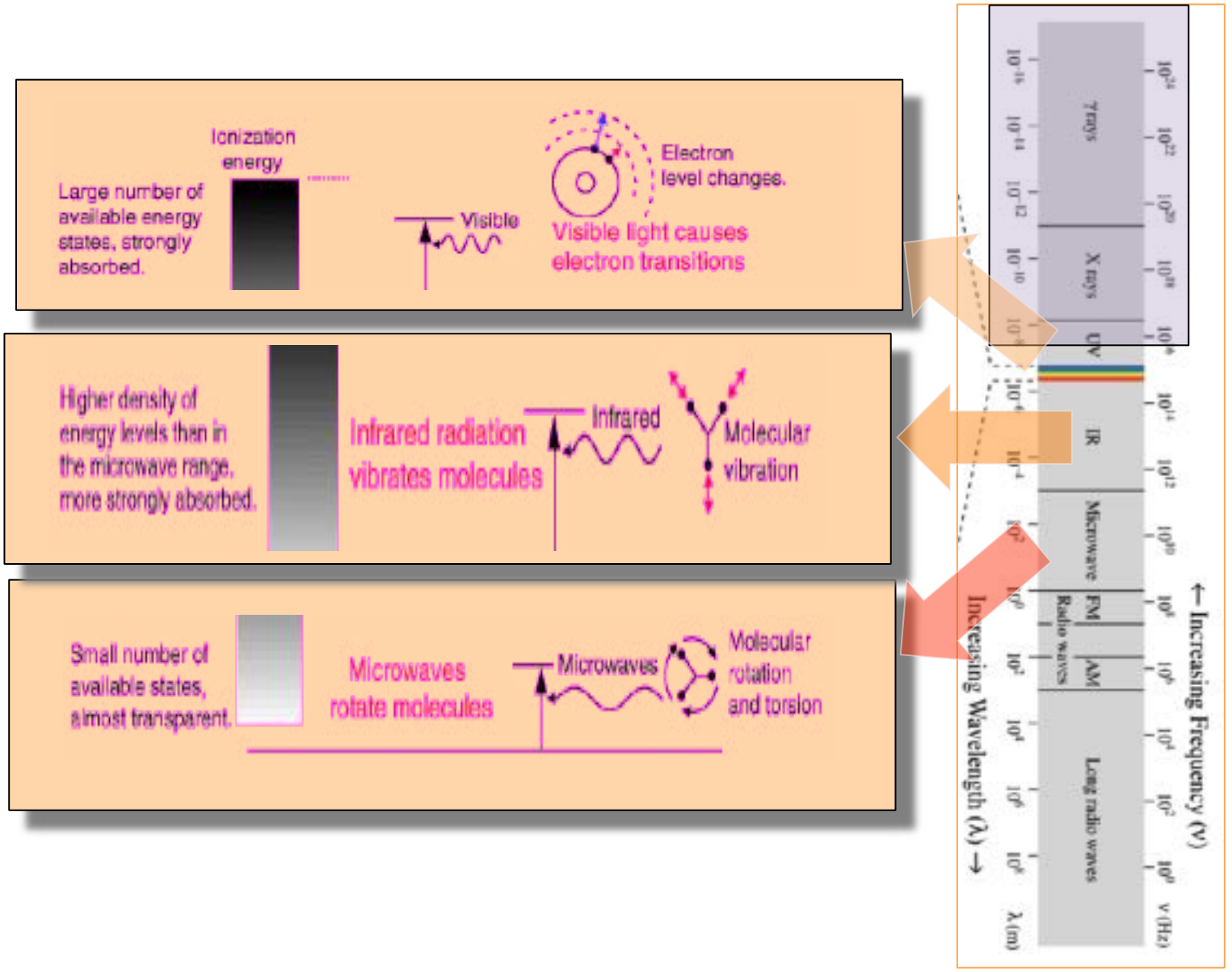

Sensoriamento Remoto da Atmosfera com Lasers

A LUZ NA ATMOSFERA

Scattering type	Cross section (cm^2)	Ratio (%)
Rayleigh	1.156×10^{-27}	100
O_2 RRS	7.10×10^{-29}	6.1
N_2 RRS	2.94×10^{-29}	2.5
Air RRS	3.82×10^{-29}	3.3
VRS	–	0.1

λ_o= 700 nm

ESPALHAMENTO RAYLEIGH – POR QUÊ O CÉU É AZUL ?

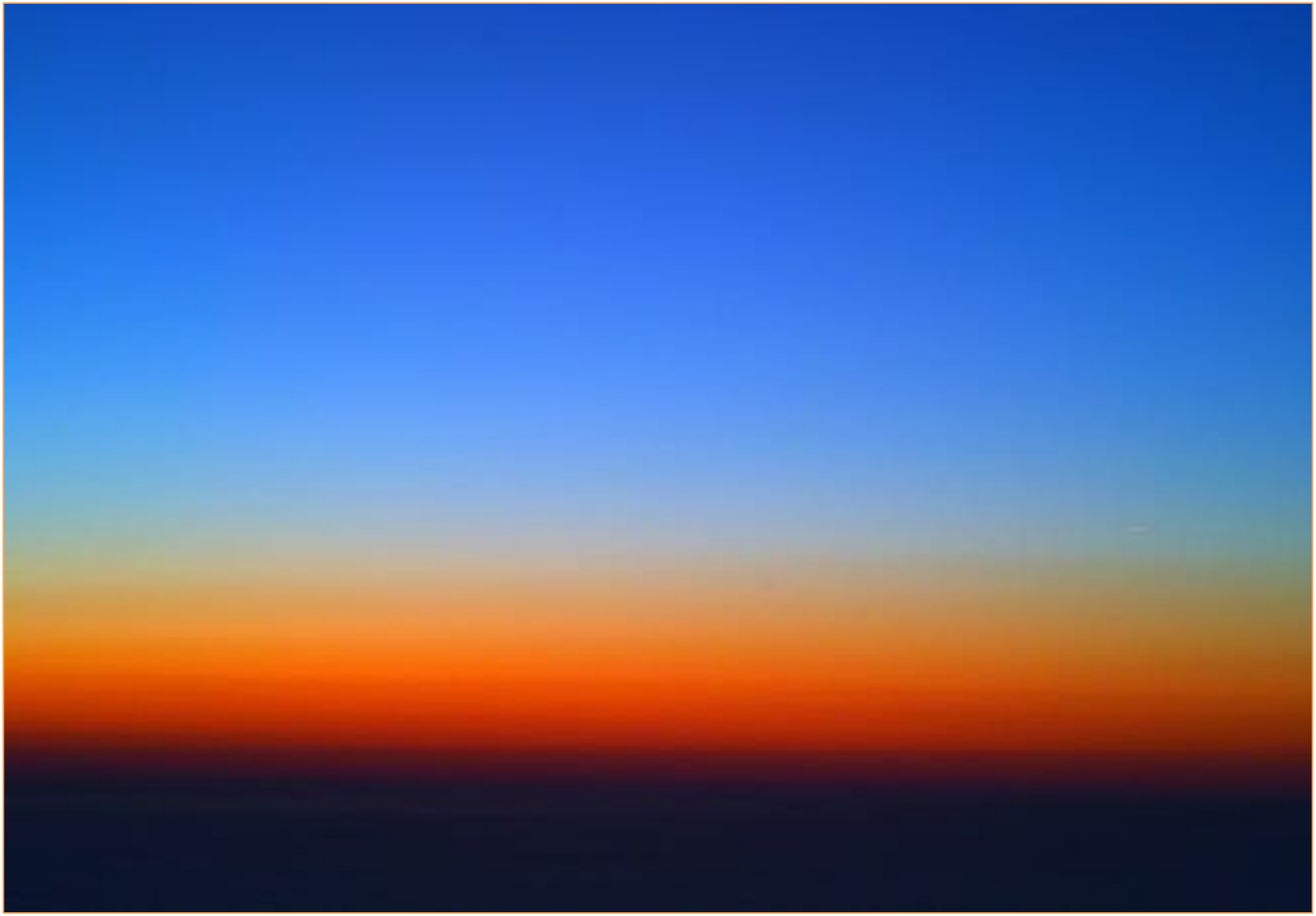

RAYLEIGH SCATTERING – HISTORICAL BACKGROUND

Leonardo da Vinci (~1500)

Francois Arago (1809)

John Tyndall (1859)

John William Strutt – Lord Rayleigh (1871)

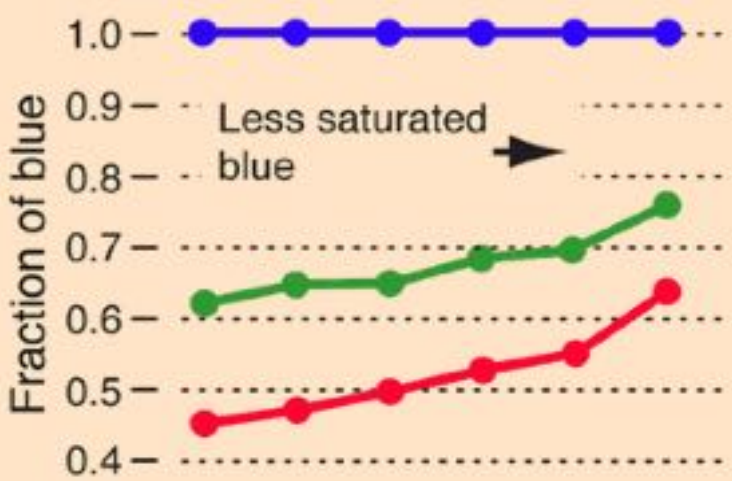

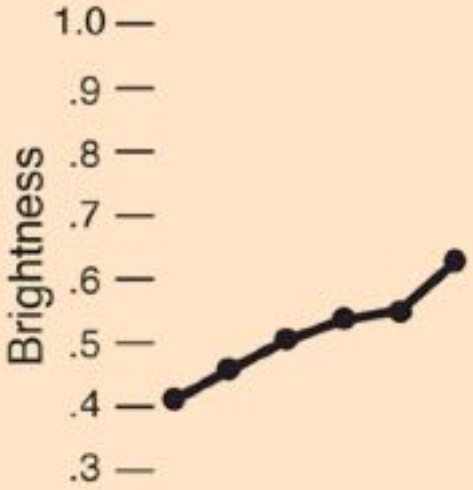

An informal measurement of sky brightness and saturation

The points chosen approach the sun direction and avoid obvious clouds.

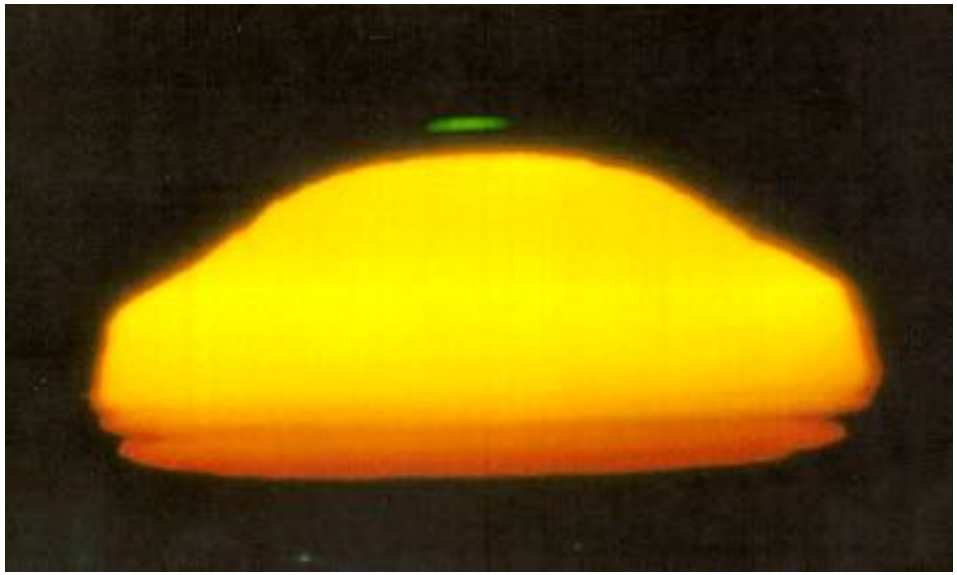

Green Flash

The famous but seldom seen "green flash" or "emerald flash" which occurs just before the last part of the sun disappears from view at sunset is caused by the same atmospheric refraction and scattering effects which produce the red sunset.

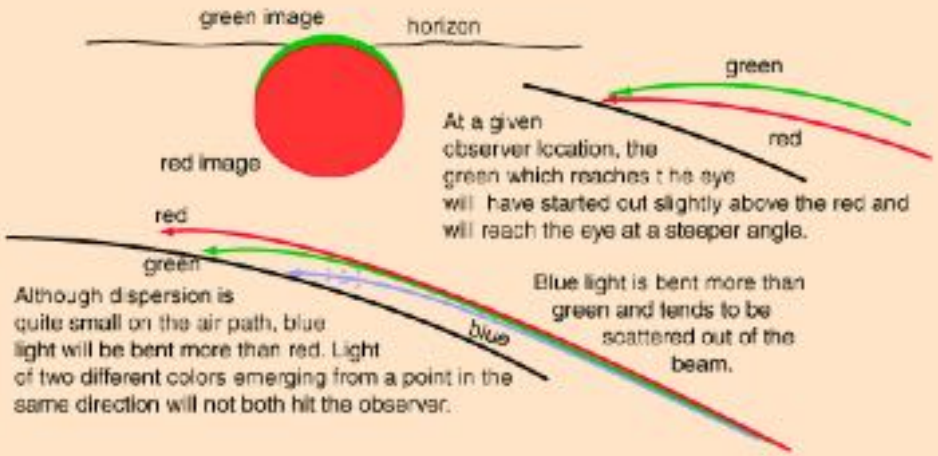

RAYLEIGH SCATTERING – INTENSITY

The Intensity of the scattered light is proportional to the inverse of the fourth power of the EM wavelength.

$$I_\lambda \sim 1/\lambda^4.$$

$$\frac{\lambda_1}{\lambda_2} = (440 / 550)^4$$

$$\frac{256}{625}$$

```
% // N
```

```
0.4096
```

RAYLEIGH SCATTERING – DIMENSION ANALYSIS

$$E_s \propto \frac{E_i V}{r.k}$$

$$[k] = \frac{[E_i][V]}{[r][E_s]}$$

$$[k] = [L]^2 \quad \Rightarrow \quad k = [\lambda]^2$$

RAYLEIGH SCATTERING – DIMENSION ANALYSIS

SCATTERED INTENSITY (POWER)

$$I_s \propto E_s^2$$

$$I_s \propto \frac{E_i^2 V^2}{r^2 \lambda^4}$$

WHY DON'T WE SEE THE SKY AS VIOLET THEN ?

" The wonders of Photoshop and Gimp "

RAYLEIGH SCATTERING – POLARIZATION

IN SOME DIRECTIONS THE INTENSITY IS LARGER THAN OTHERS

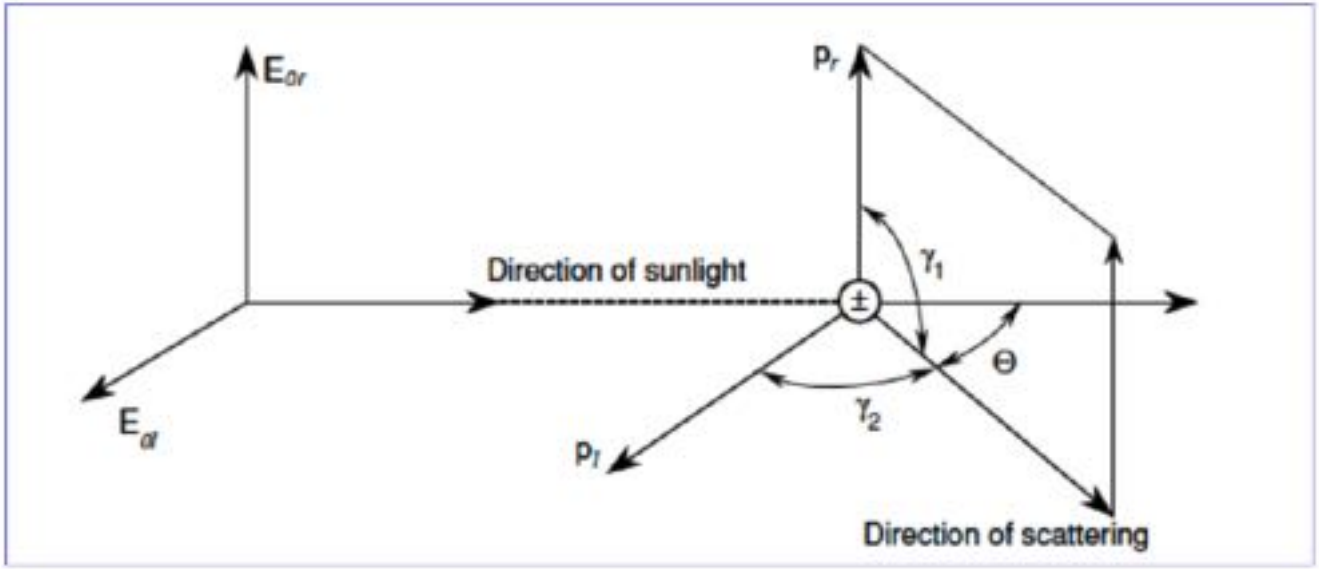

RAYLEIGH SCATTERING – POLARIZATION

UNPOLARIZED

$$I = \frac{I_0}{r^2}\alpha^2\left(\frac{2\pi}{\lambda}\right)^4 \frac{1+\cos^2\Theta}{2}.$$

LIOU 3.3.9

POLARIZED

$$I_r = I_{0r}k^4\alpha^2/r^2,$$

$$I_l = I_{0l}k^4\alpha^2\cos^2\Theta/r^2,$$

$$I = I_r + I_l = (I_{0r} + I_{0l}\cos^2\Theta)k^4\alpha^2/r^2.$$

$$k = \frac{2\pi}{\lambda} \qquad \frac{\omega}{k} = c$$

$$\omega = 2\pi.\nu$$

RAYLEIGH SCATTERING – POLARIZATION

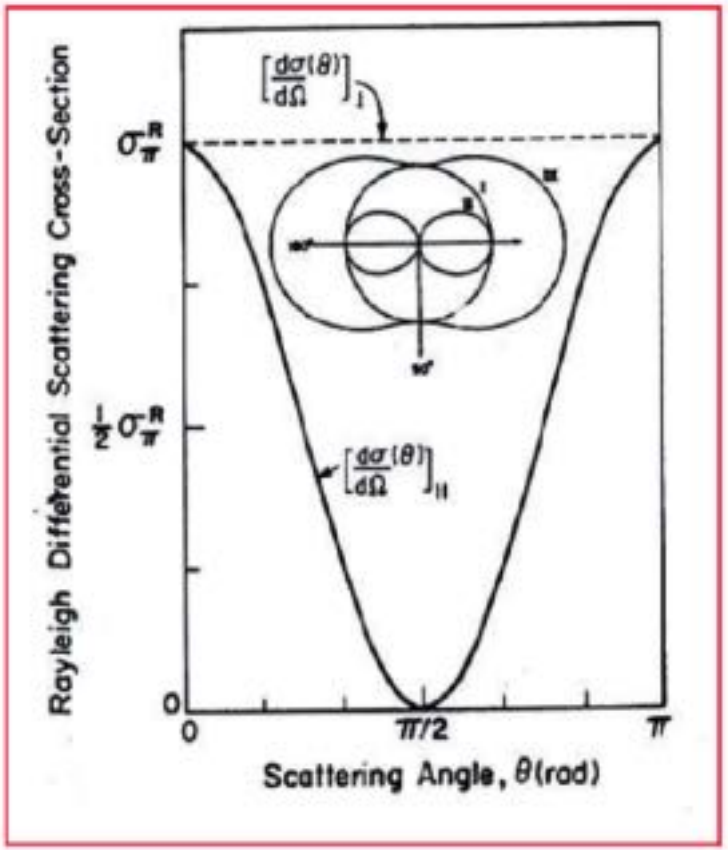

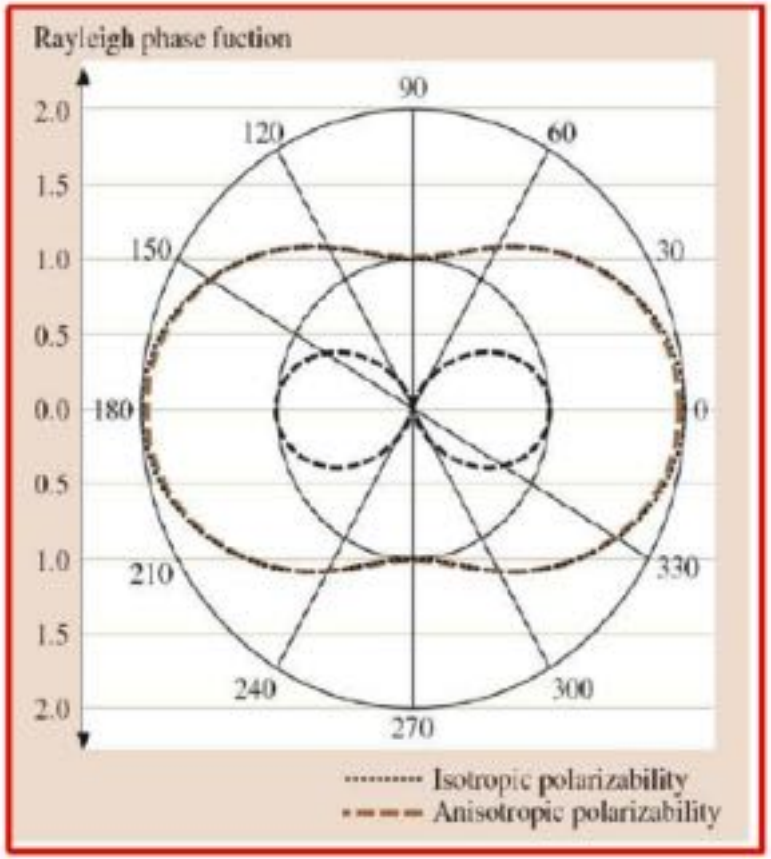

RAYLEIGH SCATTERING CROSS SECTION

$$\sigma_s = \frac{8\pi^3 (m_r^2 - 1)^2}{3\lambda^4 N_s^2} \left(\frac{6 + 3\delta_p}{6 - 7\delta_p} \right)$$

RAYLEIGH SCATTERING CROSS SECTION

Rayleigh-scattering calculations for the terrestrial atmosphere

Anthony Bucholtz

20 May 1995 / Vol. 34, No. 15 / APPLIED OPTICS 2765

Planet. Space Sci., Vol. 32, No. 6, pp. 785-790, 1984
Printed in Great Britain

SHORT PAPER

RAYLEIGH SCATTERING BY AIR

D. R. Bates

JOURNAL OF ATMOSPHERIC AND OCEANIC TECHNOLOGY

On Rayleigh Optical Depth Calculations

BARRY A. BODHAINE
NOAA/Climate Monitoring and Diagnostics Laboratory, Boulder, Colorado

Correct equations and common approximations for calculating Rayleigh scatter in pure gases and mixtures and evaluation of differences

Wynn L. Eberhard

$$\sigma(\lambda) = \frac{24\pi^3(n_s^2 - 1)^2}{\lambda^4 N_s^2 (n_s^2 + 2)^2} \left(\frac{6 + 3\rho_n}{6 - 7\rho_n}\right),$$

Which units ?

λ is wavelength (in cm)

$N_s = 2.54743 \times 10^{?}$ cm^{-3}

n_s = refractive index

ρ_n = depolarization factor

IN SEARCH OF ACCURACY

Here we suggest a method for calculation of Rayleigh optical depth that goes back to first principles as suggested by Penndorf (1957) rather than using curve-fitting techniques, although it is true that the refractive index of air is still derived from a curve fit to experimental data. We suggest using all of the latest values of the physical constants of nature, and we suggest including the variability in refractive index, and also the mean molecular weight of air, due to CO_2 even though these effects are in the range of 0.1%–0.01%. It should be noted that aerosol optical depths are often as low as 0.01 at Mauna Loa. Since Rayleigh optical depth is of the order of 1 at 300 nm, it is seen that a 0.1% error in Rayleigh optical depth translates into a 10% error in aerosol optical depth. Furthermore, it simply makes sense to perform the calculations as accurately as possible.

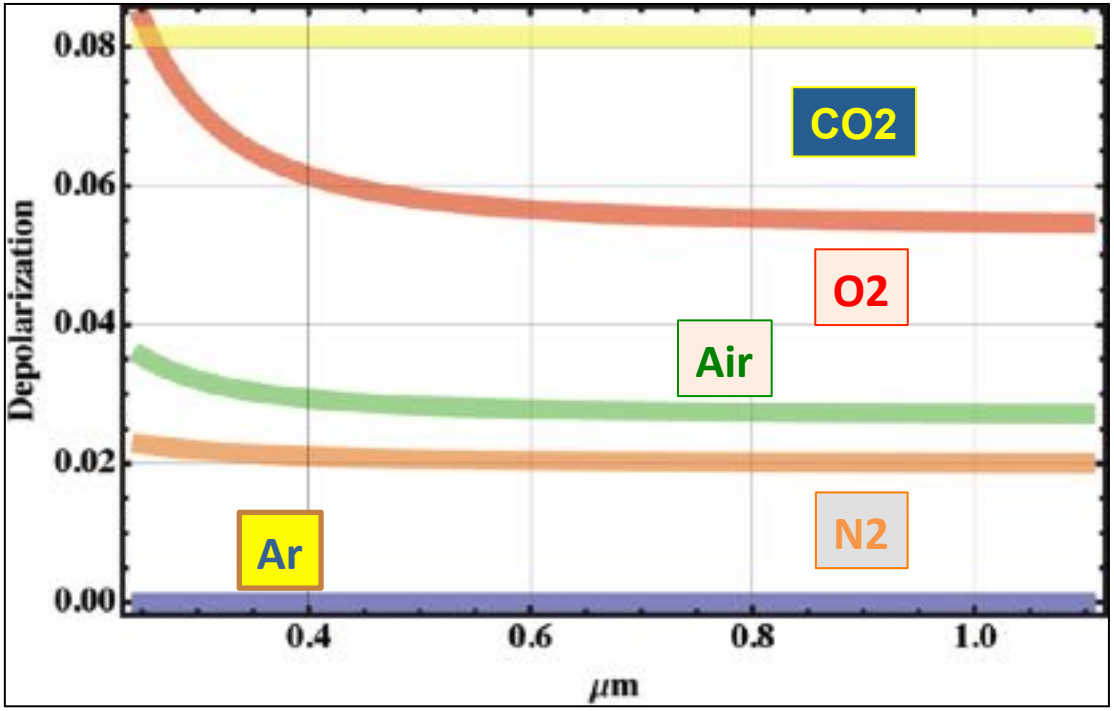
0.08
0.06
0.04
0.02
0.00
Depolarization
0.4
0.6
0.8
1.0
μm
CO2
O2
Air
N2
Ar

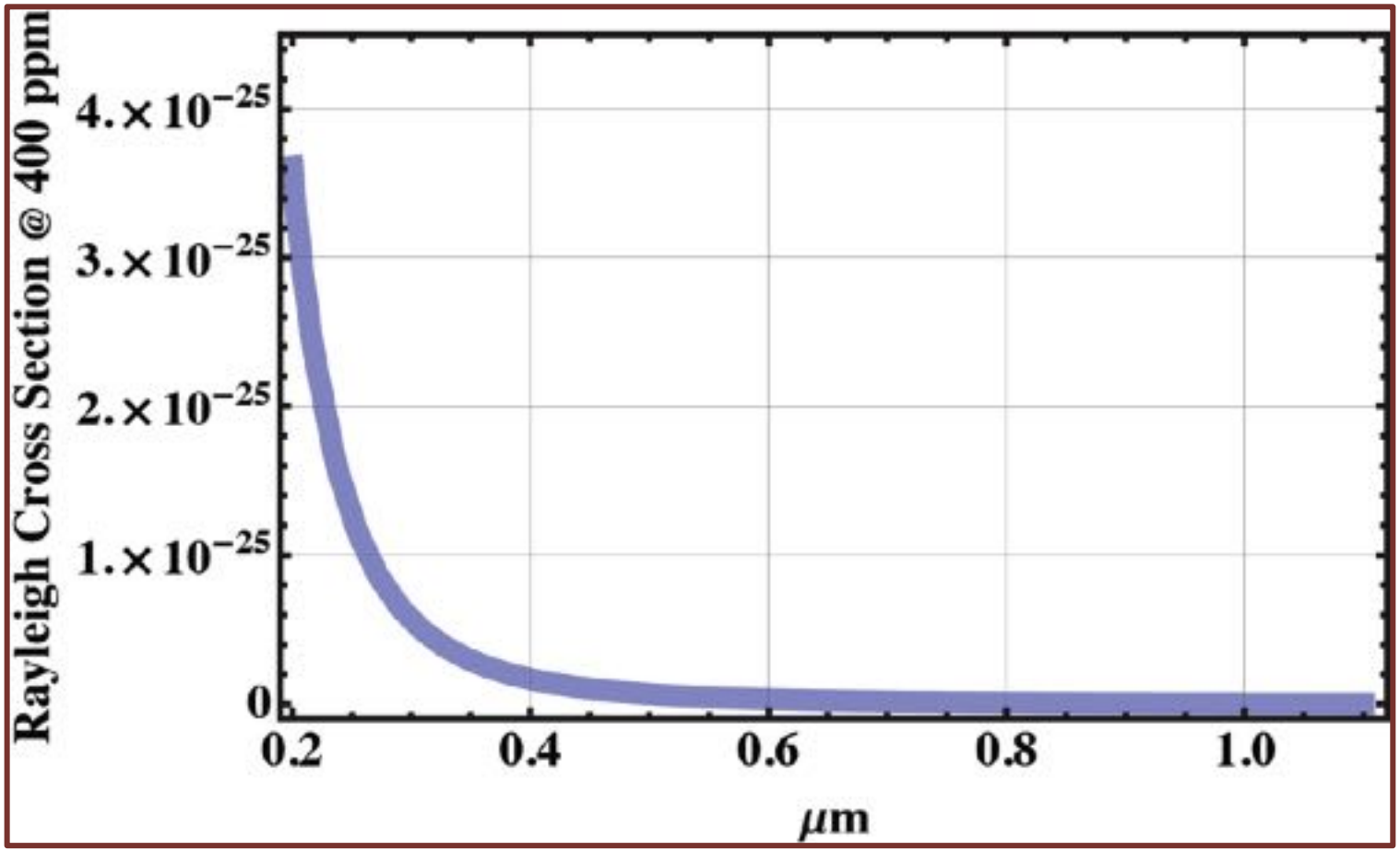
Rayleigh Cross Section @ 400 ppm
4.×10^−25
3.×10^−25
2.×10^−25
1.×10^−25
0
0.2
0.4
0.6
0.8
1.0
μm

TOTAL RAYLEIGH VOLUME-SCATTERING

P_S & T_S are standard (reference) pressure and temperature and are available from atmospheric models or radiossondes.

Table 2. Total Rayleigh-Scattering Cross Section σ and Total Rayleigh Volume-Scattering Coefficient β_s for Standard Air (P_s = 1013.25 mbars, T_s = 288.15 K)

Wavelength (μm)	Rayleigh-Scattering Cross Section σ (cm^2)	Rayleigh Volume-Scattering Coefficient β_s (km^{-1})
0.20	3.612 ($\times 10^{-25}$)	9.202 ($\times 10^{-1}$)
0.21	2.836	7.225
0.22	2.269	5.781
0.23	1.841	4.691
0.24	1.515	3.859
0.25	1.259	3.208
0.26	1.056	2.690
0.27	8.939 ($\times 10^{-26}$)	2.277
0.28	7.614	1.940
0.29	6.534	1.665
0.30	5.642	1.437
0.31	4.903	1.249
0.32	4.279	1.090
0.33	3.752	9.557 ($\times 10^{-2}$)

RADIOSSONDE DATA RETRIEVAL

83779 SBMT Marte Civ Observations at 00Z 10 Sep 2012

PRES hPa	HGHT m	TEMP C	DWPT C	RELH %	MIXR g/kg	DRCT deg	SKNT knot	THTA K	THTE K	THTV K
1000.0	176									
938.0	733	20.8	17.5	80	13.60	180	6	298.6	338.3	301.0
928.0	811	12.4	10.8	90	8.84	161	10	291.7	317.1	293.3
925.0	838	11.8	10.4	91	8.63	155	11	291.4	316.1	292.9
923.0	856	11.6	10.1	91	8.48	155	11	291.3	315.6	292.8
884.0	1215	7.0	4.5	84	6.01	164	10	290.2	307.6	291.2
878.0	1272	17.4	6.4	48	6.91	165	10	301.6	322.4	302.8
873.0	1321	20.8	8.8	46	8.20	150	10	305.6	330.6	307.1
858.0	1473	23.6	11.6	47	10.09	105	10	310.0	341.2	311.9
853.0	1523	23.6	11.0	45	9.74	110	12	310.5	340.7	312.4
850.0	1554	23.6	10.6	44	9.53	105	12	310.9	340.4	312.6
839.0	1668	23.2	9.2	41	8.78	33	4	311.6	339.0	313.2
834.0	1719	22.7	9.1	42	8.74	0	0	311.6	338.9	313.3
747.0	2657	13.8	6.4	61	8.12	30	10	311.9	337.4	313.5
730.0	3211	8.6	4.8	77	7.76	10	6	312.0	336.3	313.4
675.0	3518	4.6	3.2	91	7.19	36	8	310.8	333.2	312.1
658.0	3717	3.4	1.2	85	6.38	55	10	311.7	331.8	312.9
649.0	3828	2.8	0.1	82	5.98	66	10	312.2	331.2	313.4
635.0	4006	3.8	-4.2	56	4.43	85	10	315.3	329.8	316.2
608.0	4359	3.0	-8.0	44	3.46	121	10	316.3	329.9	319.0
594.0	4546	1.5	-7.8	50	3.61	140	10	318.7	330.7	319.4
575.0	4807	-0.6	-7.6	60	3.83	135	15	319.2	332.0	319.9
569.0	4891	-1.1	-7.3	64	3.90	125	14	319.4	332.4	320.1
554.0	5104	-1.8	-9.5	56	3.39	100	11	321.2	332.6	321.9
551.0	5147	-1.9	-9.9	54	3.29	103	11	321.6	332.7	322.2
537.0	5350	-3.7	-10.8	58	3.14	120	13	321.8	332.5	322.4
513.0	5705	-7.0	-12.4	66	2.90	115	10	322.1	332.0	322.6
508.0	5786	-7.7	-12.7	67	2.85	92	7	322.1	331.9	322.7
500.0	5918	-6.9	-18.9	38	1.73	55	2	324.6	330.7	324.9
495.0	5989	-6.5	-26.5	19	0.89	354	2	326.0	329.3	326.2
493.0	6020	-6.6	-26.9	18	0.86	330	3	326.2	329.4	326.4
460.0	6561	-9.1	-33.9	11	0.47	250	11	329.7	331.5	329.8
452.0	6698	-9.7	-35.7	10	0.41	250	13	330.5	332.1	330.6
400.0	7630	-17.9	-39.9	13	0.30	250	27	331.6	332.8	331.7
376.0	8088	-22.1	-42.6	14	0.24	250	29	332.1	333.0	332.1
368.0	8247	-23.5	-43.5	14	0.22	248	25	332.2	333.1	332.2
358.0	8448	-24.3	-45.3	13	0.19	244	20	333.7	334.5	333.8
345.0	8715	-26.7	-44.2	18	0.22	240	11	334.1	335.0	334.1
331.0	9014	-29.1	-43.9	26	0.26	225	11	334.4	335.5	334.5
329.0	9058	-29.7	-43.7	27	0.27	223	12	334.5	335.6	334.5
323.0	9188	-30.6	-42.0	32	0.30	215	16	335.0	336.2	335.1
300.0	9710	-34.1	-39.1	60	0.43	230	35	337.2	338.9	337.3
293.0	10113	-37.9	-41.5	69	0.36	230	43	337.4	338.9	337.5

RADIOSSONDE DATA RETRIEVAL

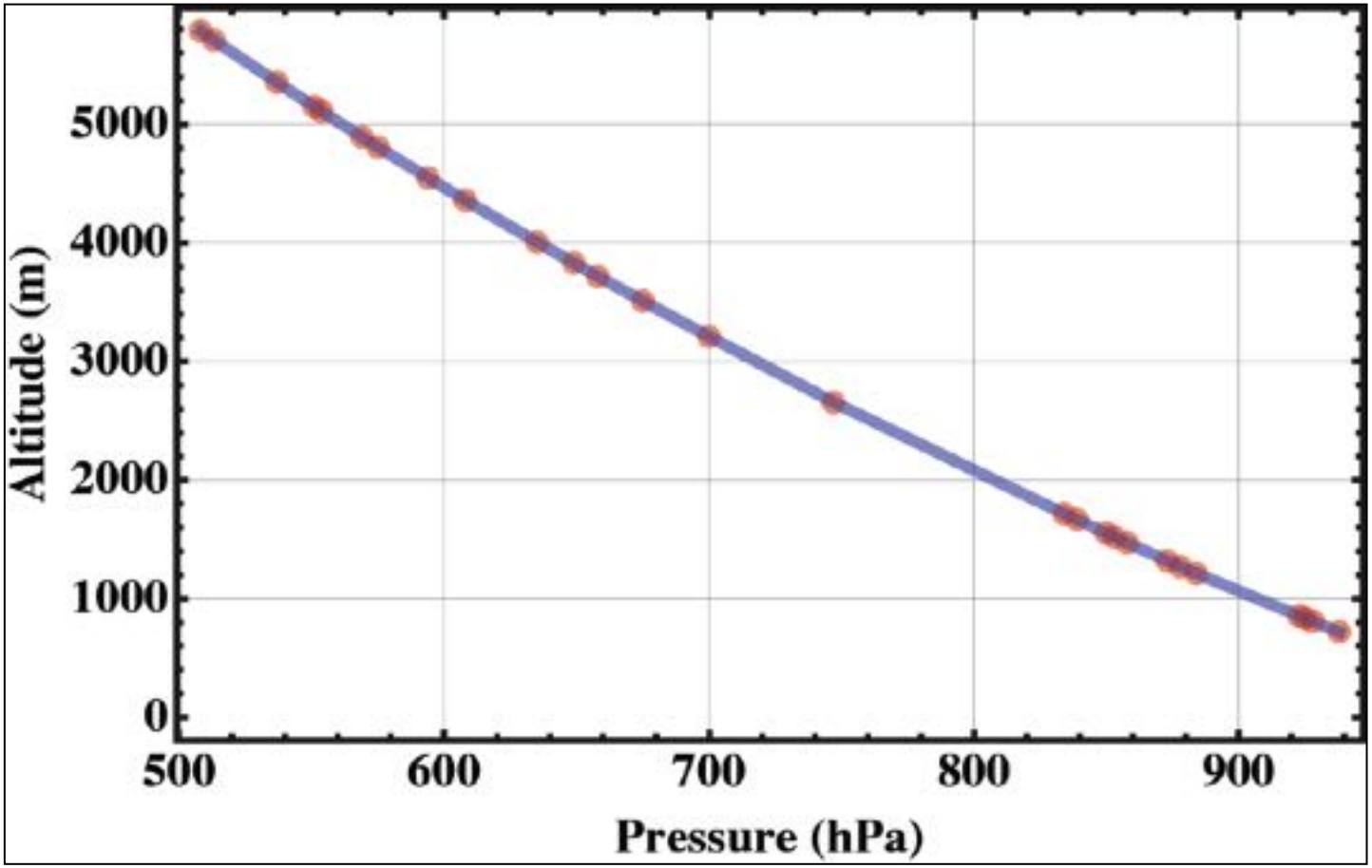

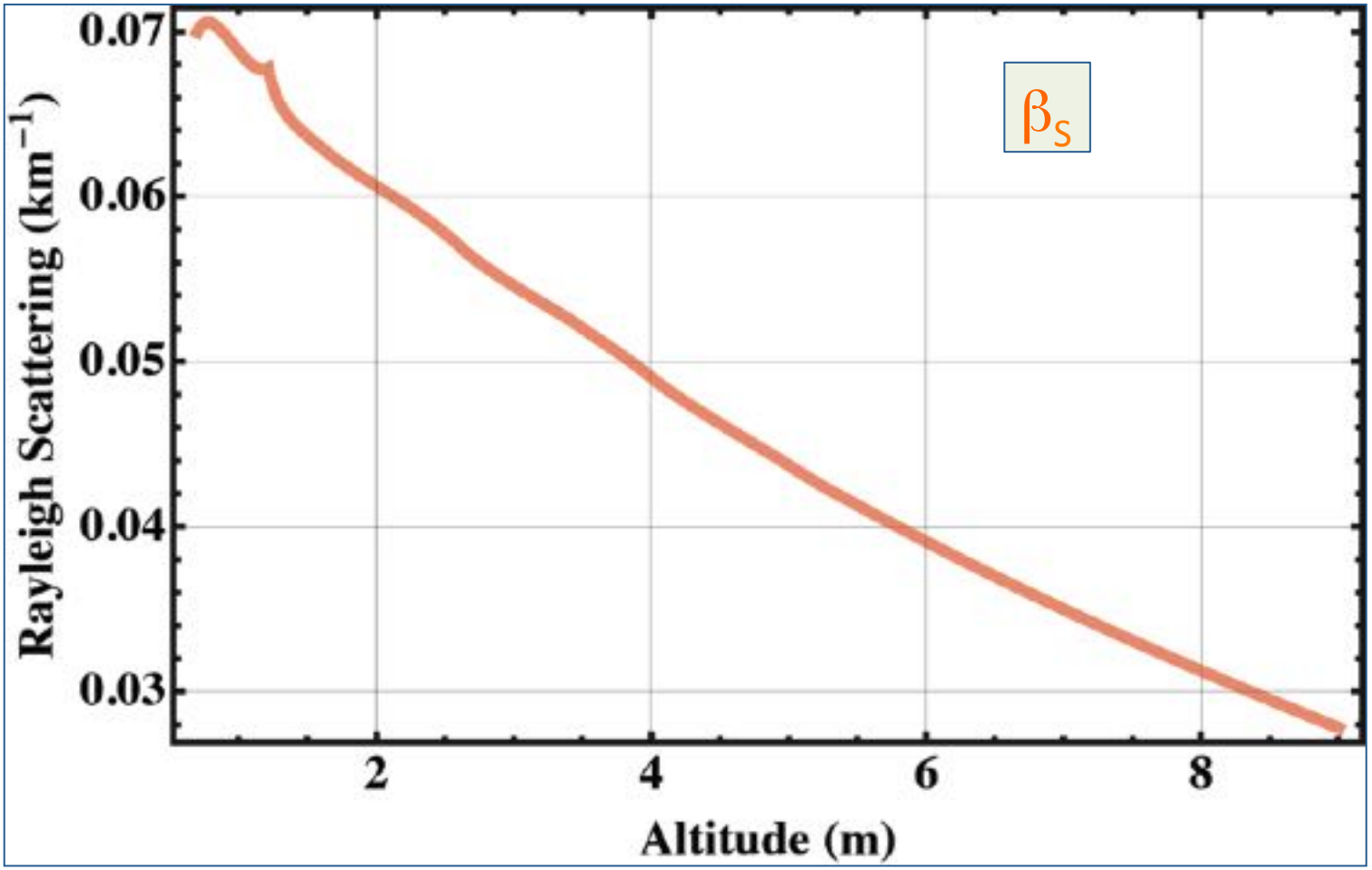
0.07
0.06
0.05
0.04
0.03
Rayleigh Scattering (km^{-1})
2
4
6
8
Altitude (m)
β_S

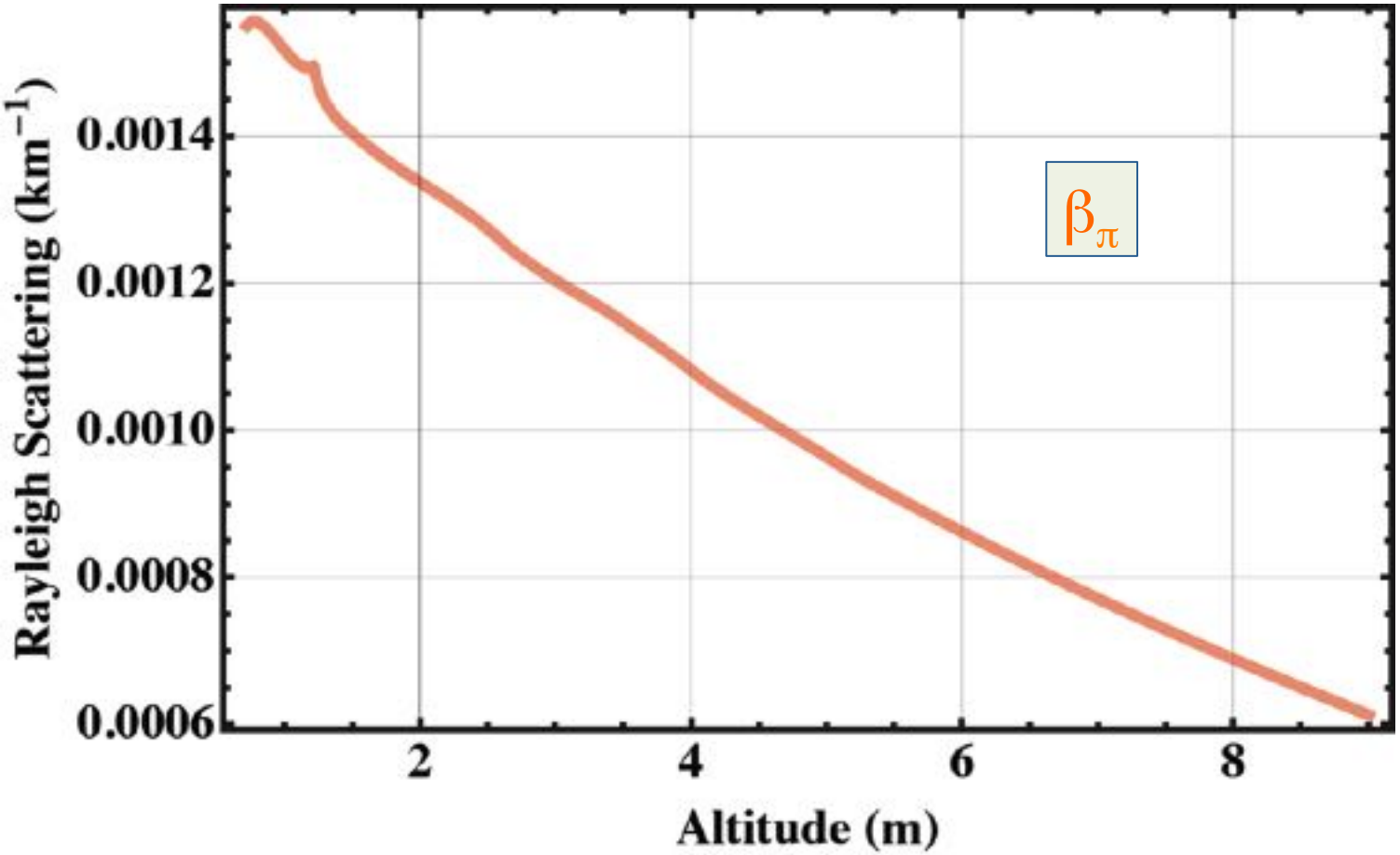
Rayleigh Scattering (km^{-1})
0.0014
0.0012
0.0010
0.0008
0.0006
2
4
6
8
Altitude (m)
β_π

MIE SCATTERING – TOWARDS A BIGGER SCATTERER

RAYLEIGH → **MIE**

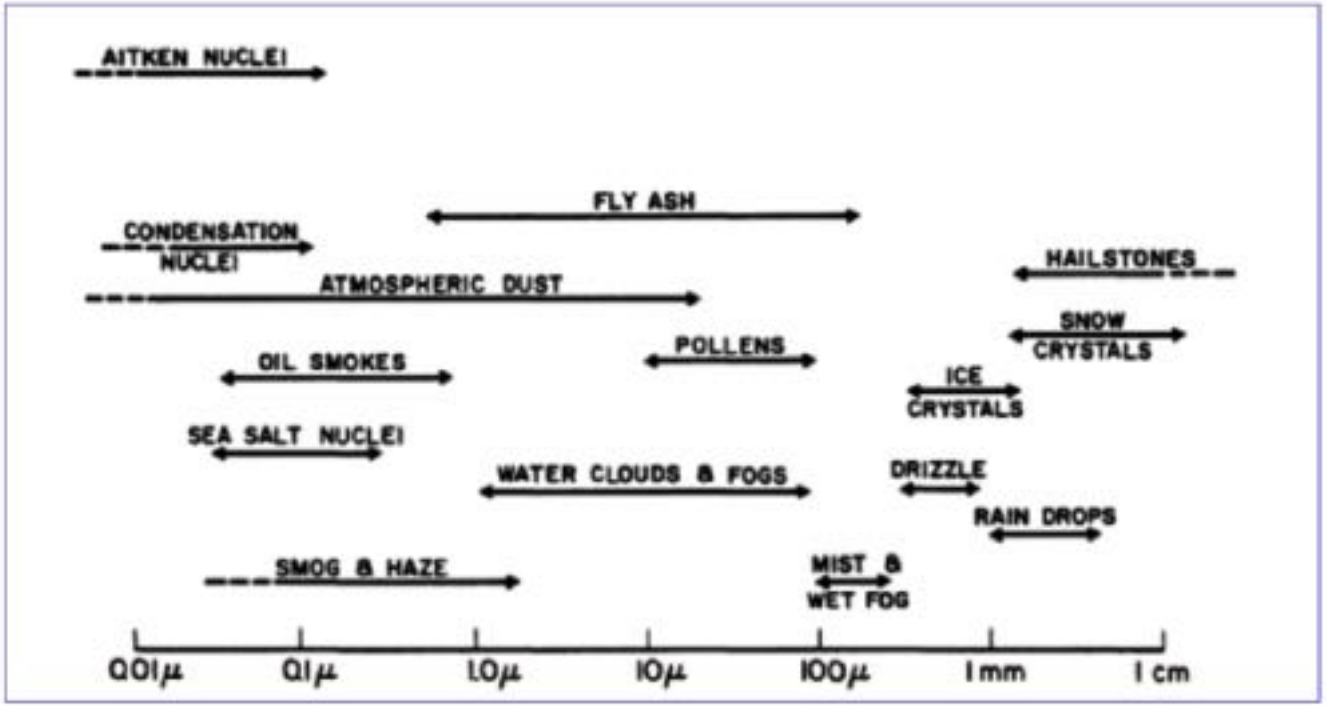

MIE SCATTERING - BUILDING CONCEPTS

SIZE PARAMETER

$$x = \frac{2\pi a}{\lambda}$$

SCATTERING EFFICIENCY

$$Q_s = \frac{\sigma_s}{\pi . a^2}$$

BOTH ADIMENSIONAL QUANTITIES

MIE SCATTERING – TOWARDS A BIGGER SCATTERER

$$x \ll 1$$

RAYLEIGH SCATTERING

$$x \gtrsim 1$$

MIE SCATTERING

MIE SCATTERING – TOWARDS A BIGGER SCATTERER

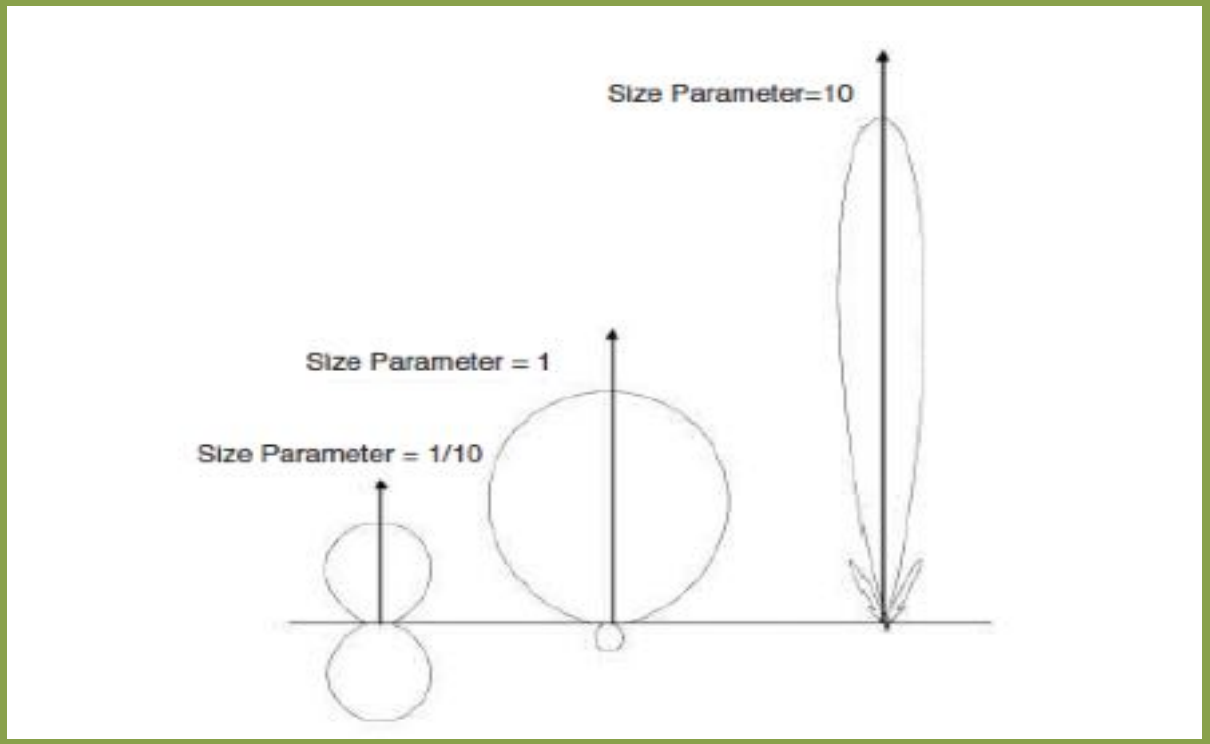

MIE SCATTERING – TOWARDS A BIGGER SCATTERER

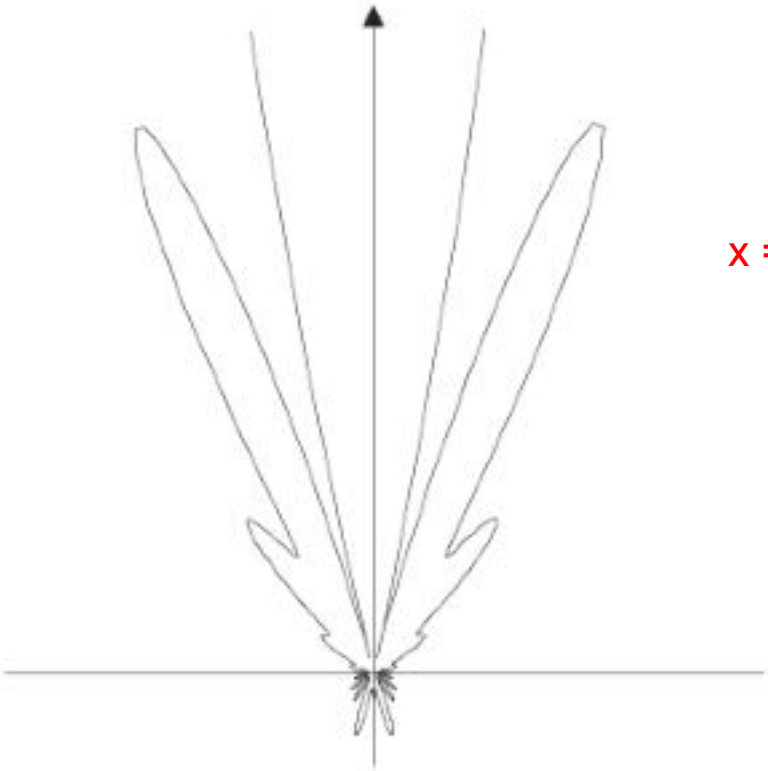

x = 10

MIE SCATTERING – TOWARDS A BIGGER SCATTERER

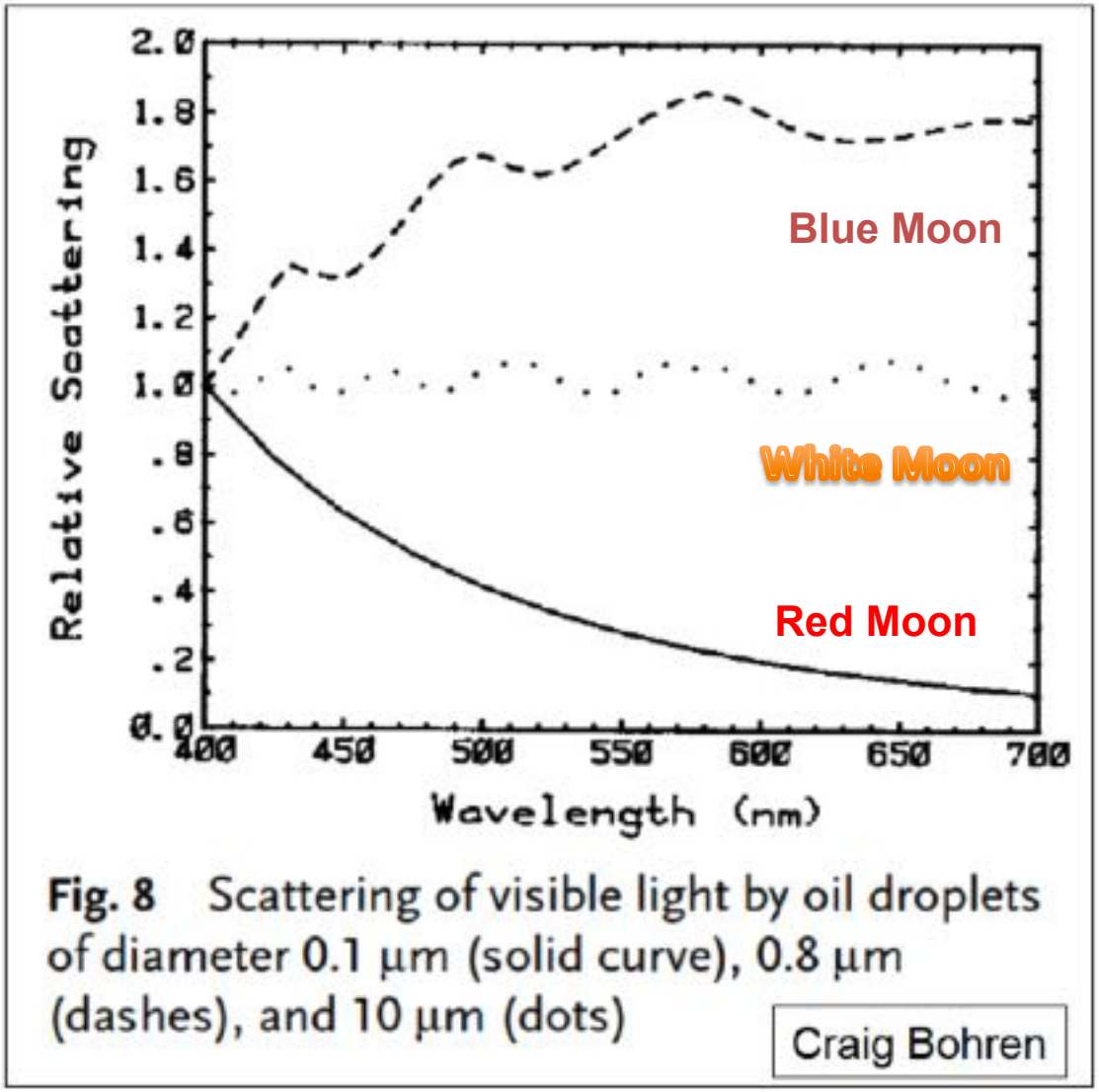

Fig. 8 Scattering of visible light by oil droplets of diameter 0.1 μm (solid curve), 0.8 μm (dashes), and 10 μm (dots)

Craig Bohren

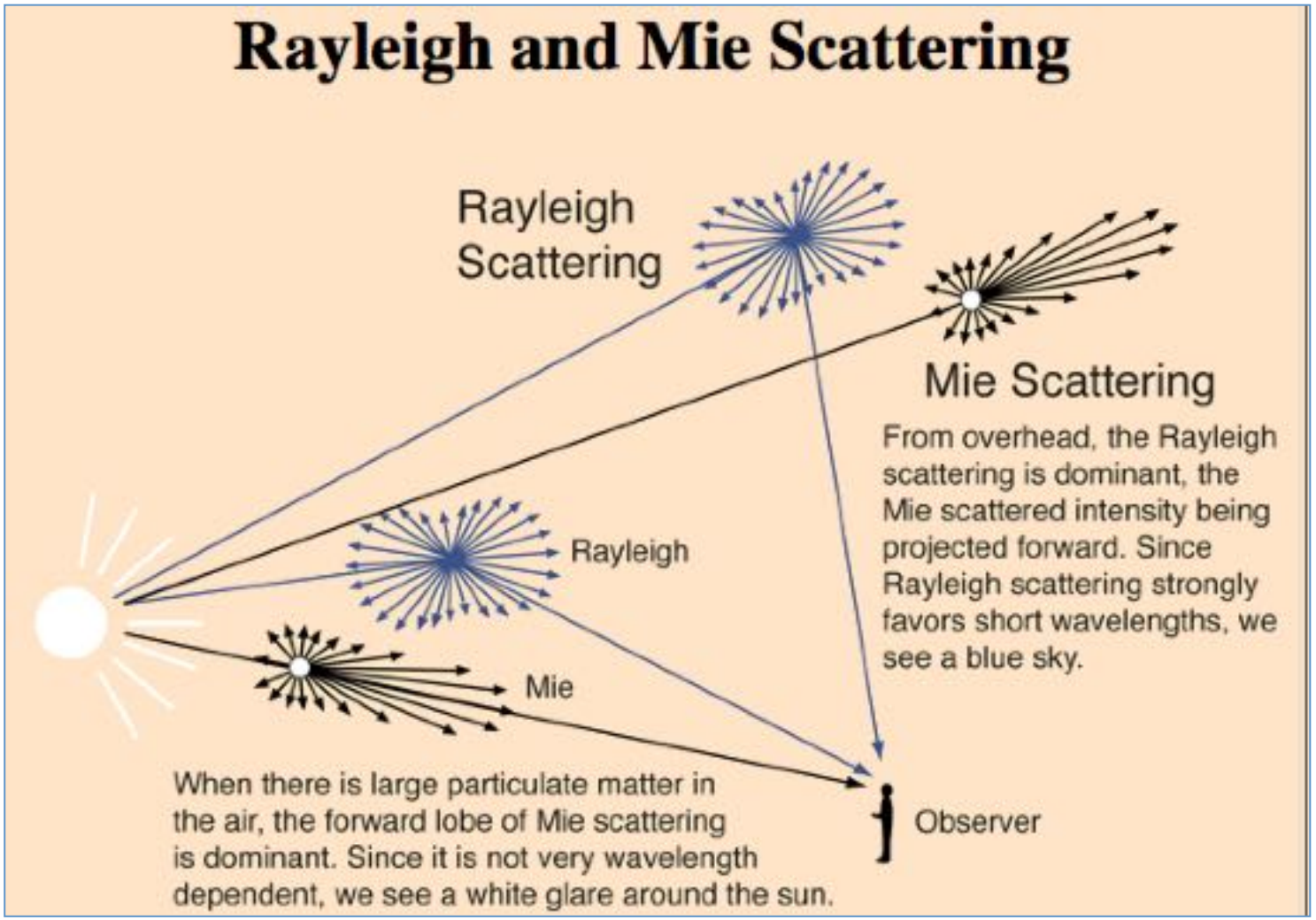
Rayleigh and Mie Scattering
Rayleigh Scattering
Mie Scattering
From overhead, the Rayleigh scattering is dominant, the Mie scattered intensity being projected forward. Since Rayleigh scattering strongly favors short wavelengths, we see a blue sky.
Rayleigh
Mie
When there is large particulate matter in the air, the forward lobe of Mie scattering is dominant. Since it is not very wavelength dependent, we see a white glare around the sun.
Observer

MIE SCATTERING – AROUND A BIGGER SCATTERER

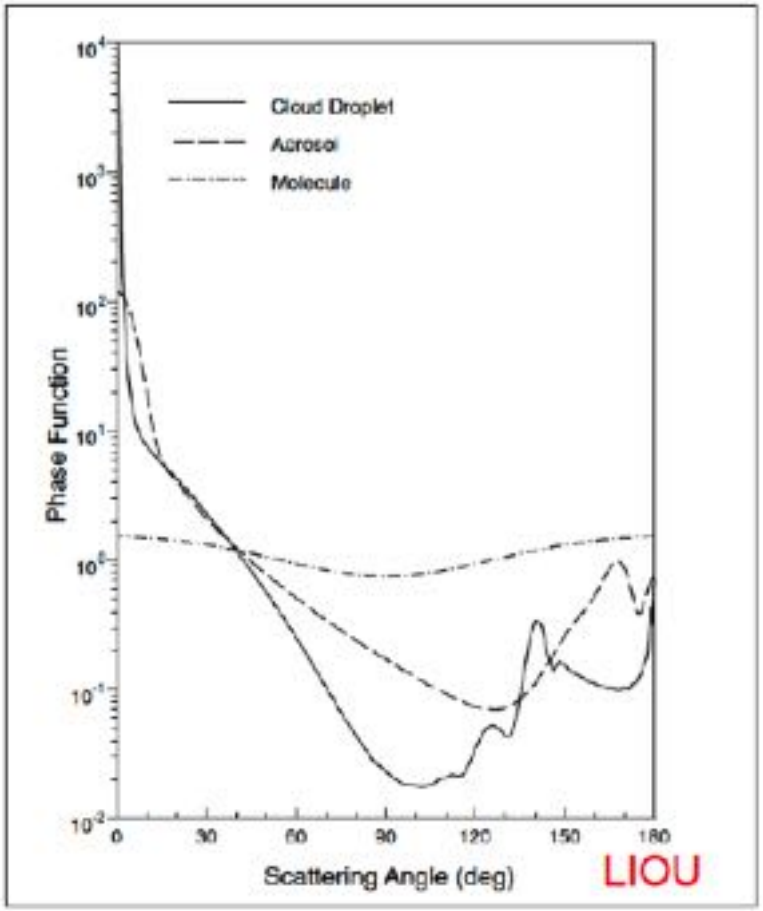

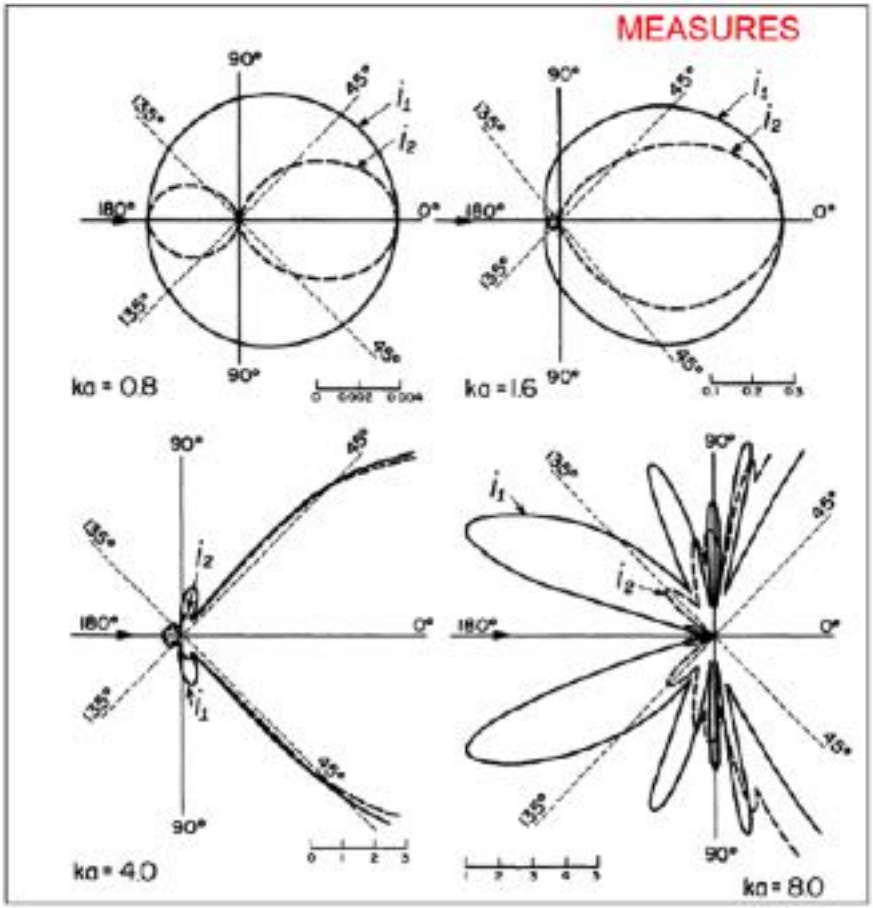

ka=x

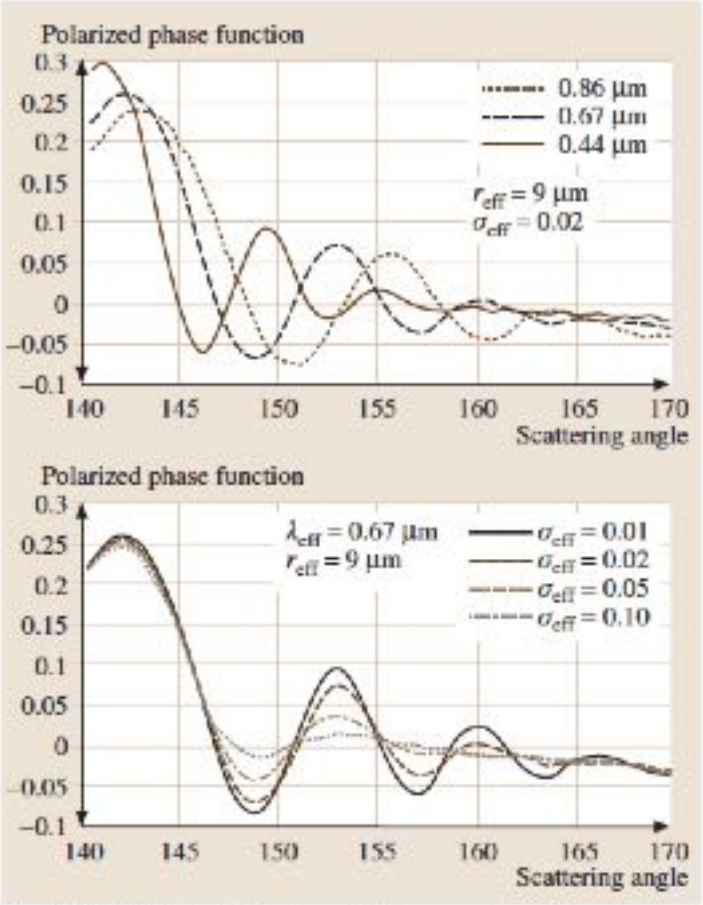

Fig. 19.2 Polarized Mie scattering phase function as a function of scattering angle for cloud droplet having a lognormal particle size distribution with an effective radius $r_{eff} = 9\,\mu m$. *Upper panel*: phase function as a function of wavelength with fixed $\sigma_{eff} = 0.02$ effective size variance; *lower panel*: as a function of effective size variance (courtesy of *Bréon* and *Goloub*, 2003)

MIE SCATTERING – SOME RESULTS

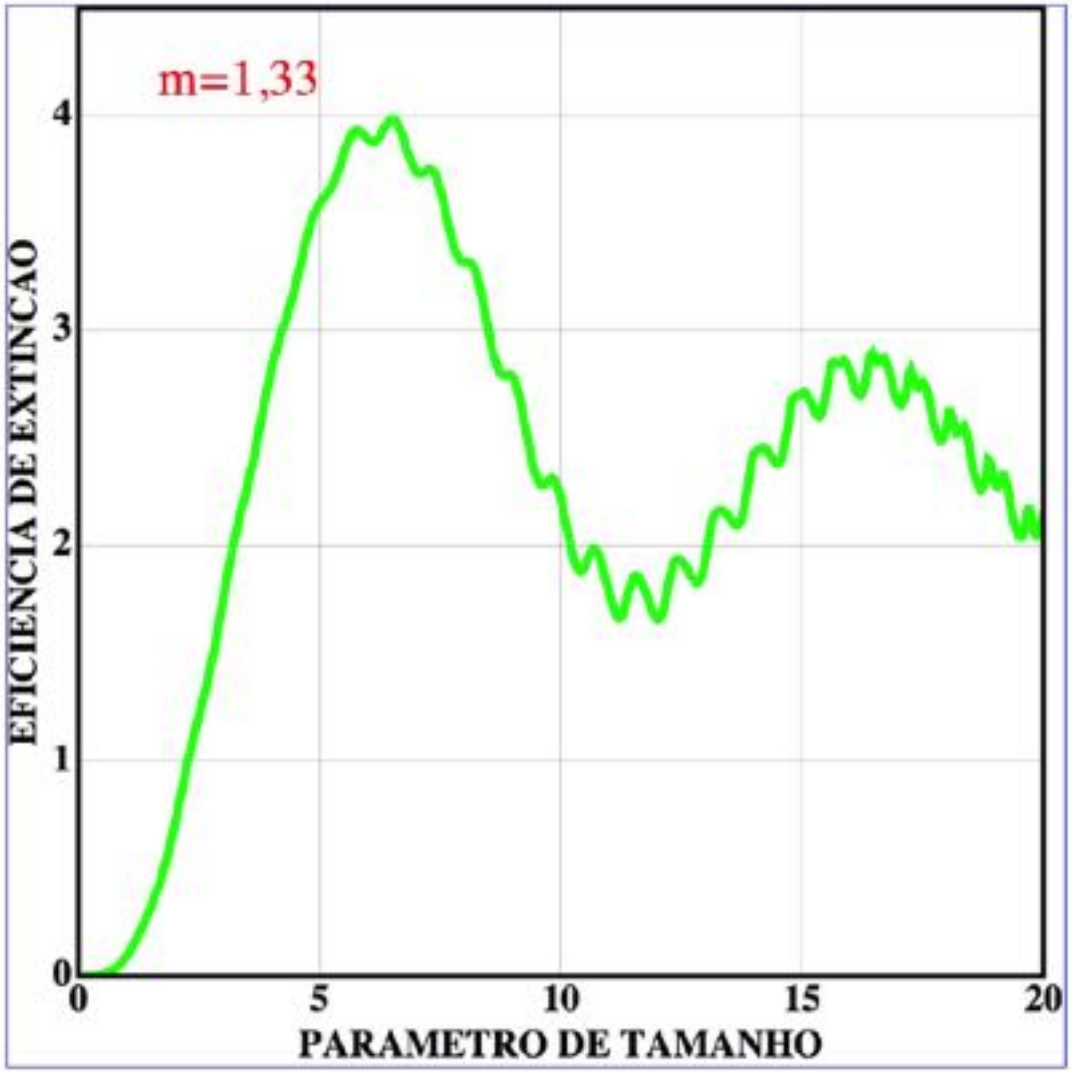

MIE SCATTERING – SOME RESULTS

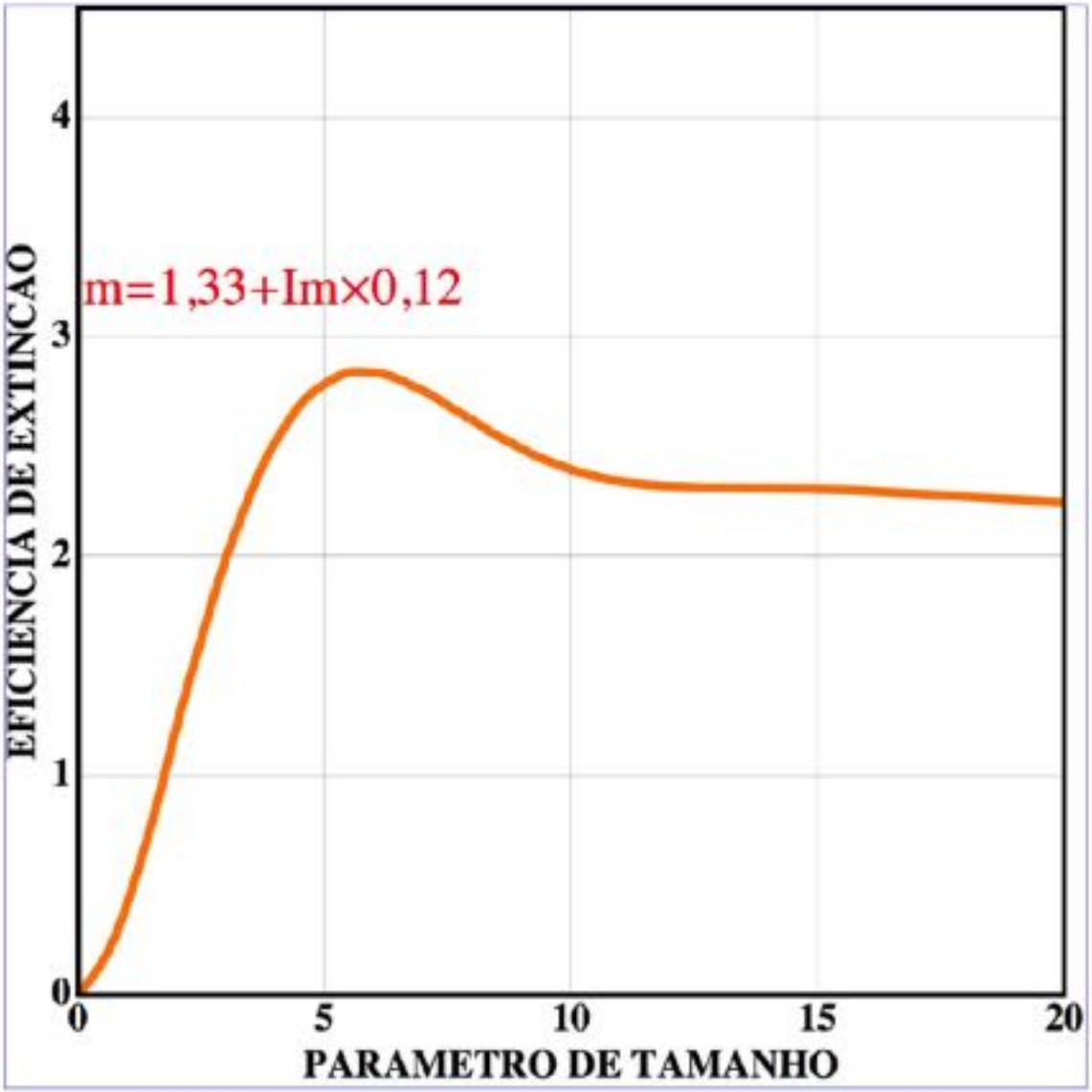

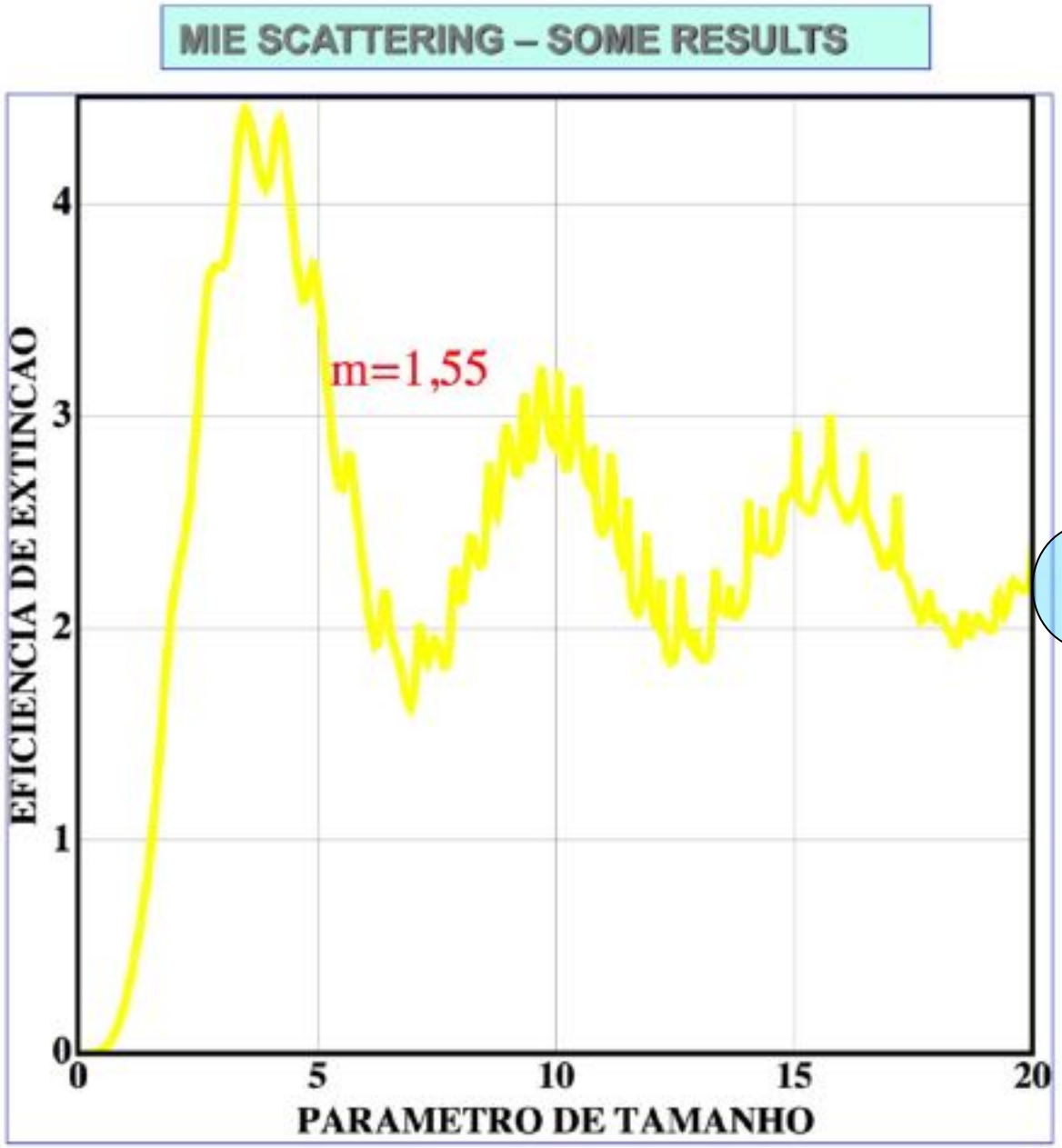
MIE SCATTERING – SOME RESULTS
EFICIENCIA DE EXTINCAO
PARAMETRO DE TAMANHO
m=1,55
0
1
2
3
4
0
5
10
15
20
2

MIE SCATTERING - BUILDING CONCEPTS

Qual é o espalhamento ???

Passive remote sensing	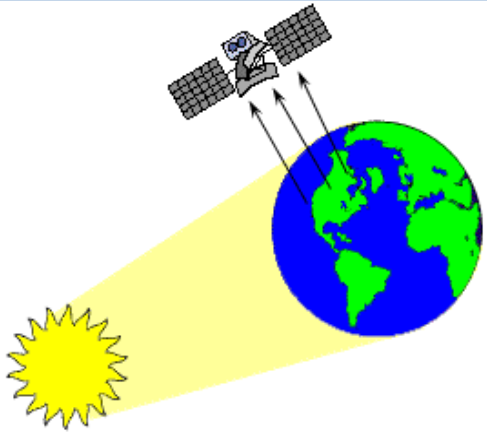	Based on "uncontroled illumination": - Sun - terrestrial emission	Passive methods: - extinction - scattering - longwave emission
Active remote sensing	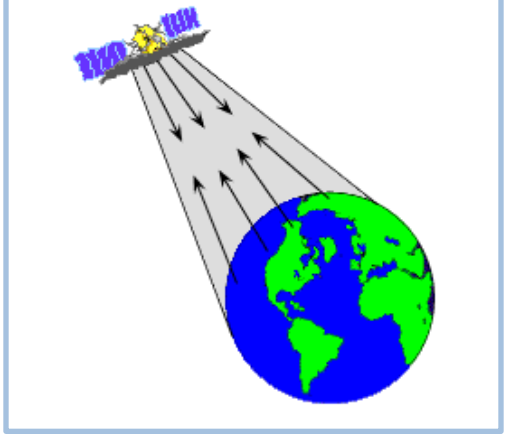	Based on "controled illumination" and measurement of backscattering	Active methods: - lidar - radar

Lidar (light detection and ranging) is an active remote sensing technology that measures distance by illuminating a target with a laser and analyzing the reflected light

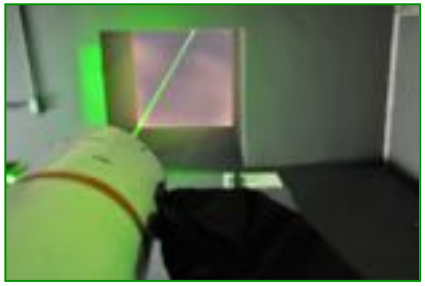

LIDAR-RABILIA

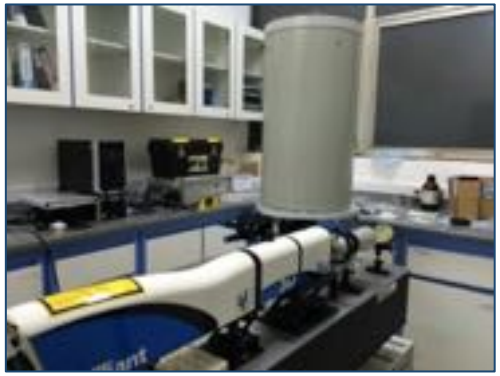

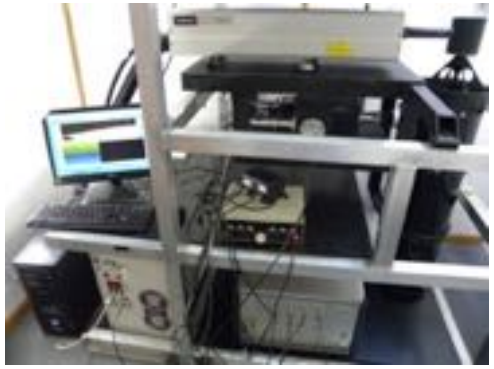

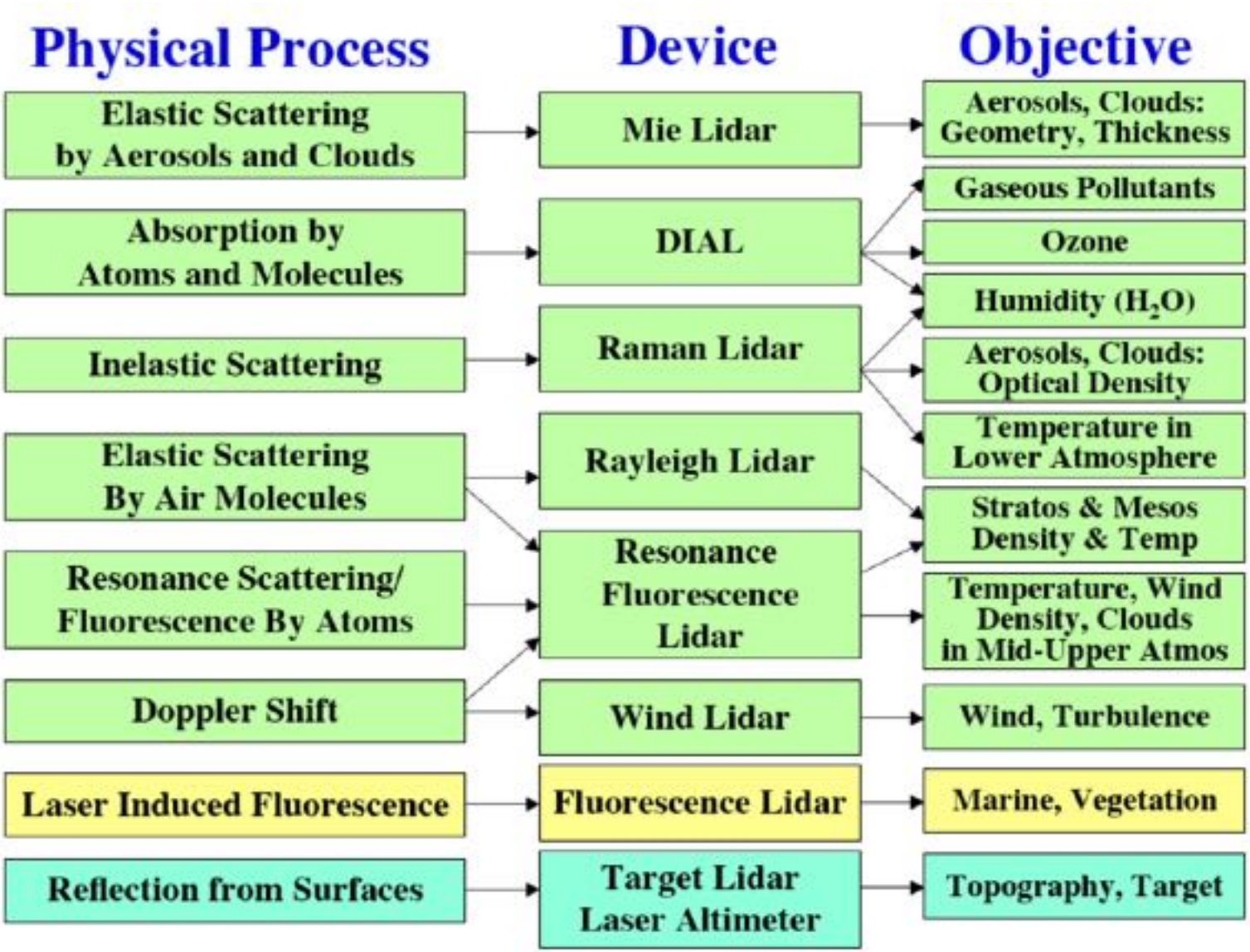
Physical Process
Device
Objective
Elastic Scattering by Aerosols and Clouds
Absorption by Atoms and Molecules
Inelastic Scattering
Elastic Scattering By Air Molecules
Resonance Scattering/ Fluorescence By Atoms
Doppler Shift
Laser Induced Fluorescence
Reflection from Surfaces
Mie Lidar
DIAL
Raman Lidar
Rayleigh Lidar
Resonance Fluorescence Lidar
Wind Lidar
Fluorescence Lidar
Target Lidar Laser Altimeter
Aerosols, Clouds: Geometry, Thickness
Gaseous Pollutants
Ozone
Humidity (H_2O)
Aerosols, Clouds: Optical Density
Temperature in Lower Atmosphere
Stratos & Mesos Density & Temp
Temperature, Wind Density, Clouds in Mid-Upper Atmos
Wind, Turbulence
Marine, Vegetation
Topography, Target

Laser-atmosphere interactions…

Laser – Atmosphere Interaction	Atmospheric Parameter-Species
Elastic Scattering ($\lambda_1 = \lambda_2$)	Aerosols (PMs), clouds, atmospheric density, atmospheric structure, temperature…
Inelastic Scattering (Raman Scattering) ($\lambda_1 = \lambda_2 + \Delta\lambda_R$)	Water vapor, RH, O_3, temperature, Aerosols (extinction, backscatter coefficients)
Differential Absorption DIAL (λ_1, λ_2)	SO_2, O_3, NO_2, NO, CO_2, Hg, HF, HCl, NH_3, HCs, CO, H_2O
Resonance Scattering	K, Na, Li, Ca, Fe
Doppler shift	Wind measurements
Laser Induced Fluorescence (LIF)	OH^-

Search Lights (~1940)

tp://www.skylighters.org/howalightworks/

LIght Detection And Ranging

551.501.71 : 551.508.93 : 538.8

Lidar : a new atmospheric probe

By R. T. H. COLLIS
Stanford Research Institute, Menlo Park, California

(Manuscript received 26 July 1965; in revised form 6 December 1965)

Summary

Pulsed-light techniques of probing the atmosphere have been greatly extended by employing lasers as energy sources in instruments called 'lidars.' Because of the nature of laser energy and the manner in which it is used in current and proposed systems, lidar is best discussed in terms of radar. Apart from the basic capabilities of lidar for detecting backscattering from atmospheric constituents, possibilities exist for more sophisticated techniques based on the wave nature of the energy. The basic capabilities of lidar, however, make it possible to observe the atmosphere with previously unknown resolution and sensitivity. Apart from providing new information about clouds, lidar has shown that the concentration of the particulate matter content of clear air is highly variable and that such variations can indicate the structure and motion of the clear atmosphere. These capabilities have applications in atmospheric and meteorological research and various operational activities.

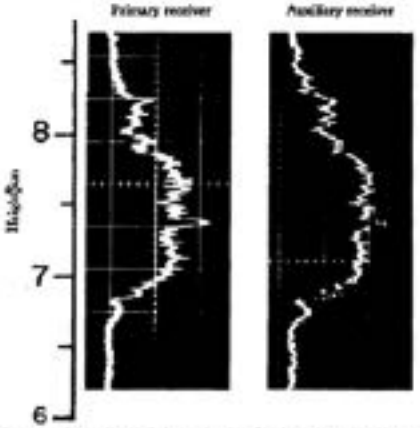

Figure 1. Simultaneous observations of cirrus cloud 4 October 1965. The two traces show the returns (relative intensity vs height) from cirrus cloud as observed simultaneously by the SRI Mark II 1965 lidar and an auxiliary receiver located at a distance of 17 m.

R.T. H. Collins, Lidar: A new atmospheric probe, Quart. J. Royal Meteor. Society, 220-230, 1966

1930 Synge proposed a method to determine the atmospheric density with an anti-aircraft searchlight and a telescope (bistatic configuration)

1936 First reported results of density profiles: **Duclaux** (3.4 km), **Hulbert** (28 km)

1938 First reported use of **a monostatic configuration for cloud base height, using a pulsed light source** (Bureau)

1953 First retrieval of temperature profiles from density profiles (**Elterman**)

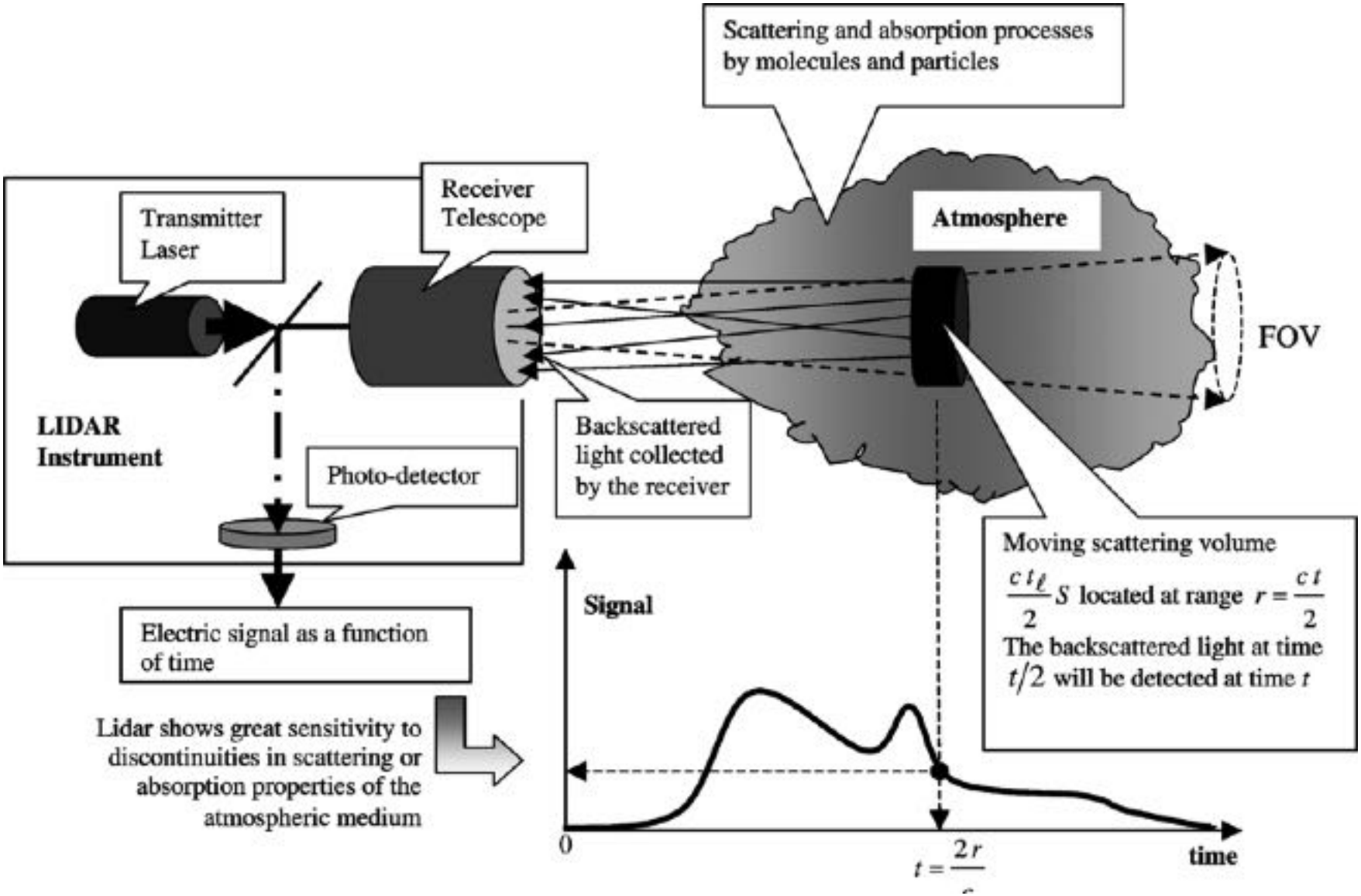
Scattering and absorption processes by molecules and particles
Transmitter Laser
Receiver Telescope
Atmosphere
FOV
LIDAR Instrument
Photo-detector
Backscattered light collected by the receiver
Moving scattering volume
$\frac{c\,t_\ell}{2} S$ located at range $r = \frac{c\,t}{2}$
The backscattered light at time $t/2$ will be detected at time t
Electric signal as a function of time
Signal
Lidar shows great sensitivity to discontinuities in scattering or absorption properties of the atmospheric medium
0
$t = \frac{2r}{c}$
time

AULA VI

LIDAR EQUATION- BUILDING CONCEPTS

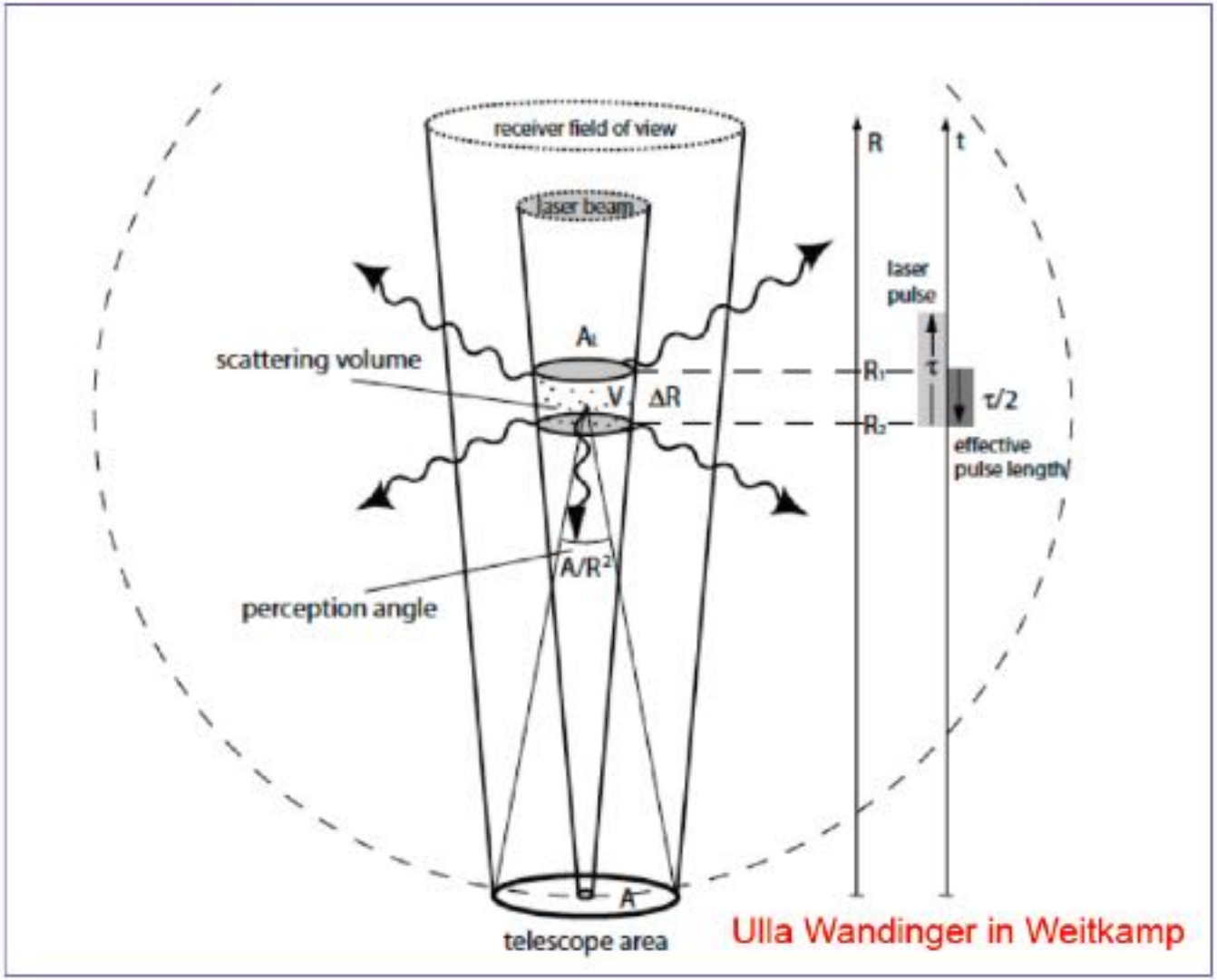

LIDAR EQUATION- BUILDING CONCEPTS

At a given Range (R) and Wavelength (λ) :

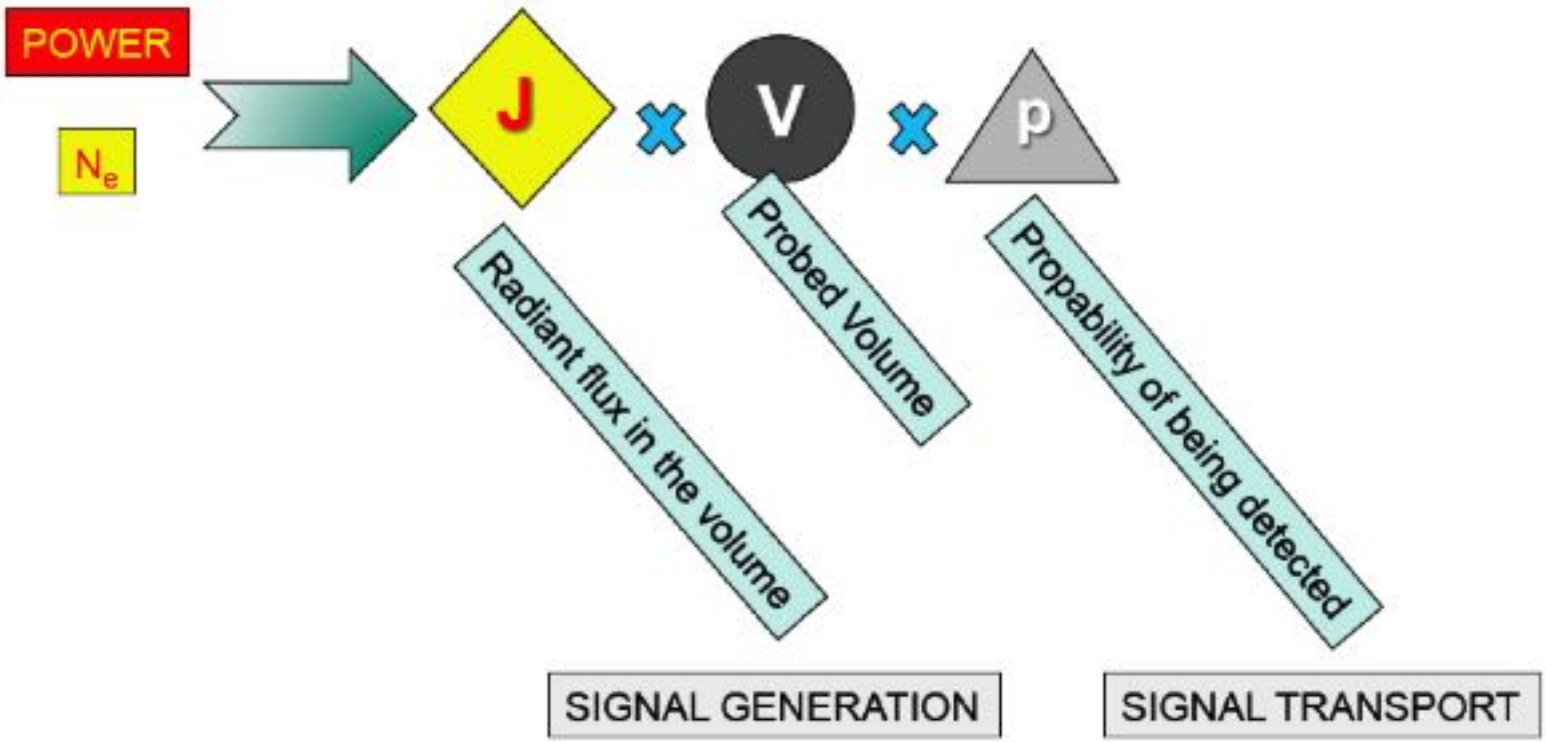

LIDAR EQUATION- BUILDING CONCEPTS

At a given Range (R) and Wavelength (λ) :

SIGNAL GENERATION

NATURE OF INTERACTION

$$J(\lambda,R,r) = \beta_\pi(\lambda,R,r)I(R,r)$$

BACKSCATTERING

IRRADIANCE AT TARGET

SIGNAL TRANSPORT

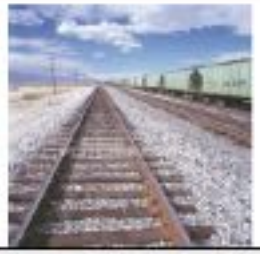

INSTRUMENT + ATMOSPHERE

$$p(\lambda,R,r) = \frac{A_o}{R^2} \times T(\lambda,R) \times \varepsilon(\lambda) \times \zeta(R,r)$$

ATMOSPHERIC TRANSMISSION

ACCEPTANCE SOLID ANGLE

SPECTRAL EFFICIENCY

GEOMETRIC FACTOR

LIDAR EQUATION - BUILDING CONCEPTS

AULA VI

SIGNAL GENERATION

SIGNAL TRANSPORT

$$J(\lambda,R,r) = \beta_\pi(\lambda,R,r) I(R,r)$$

$$p(\lambda,R,r) = \frac{A_0}{R^2} \times T(\lambda,R) \times \varepsilon(\lambda) \times \zeta(R,r)$$

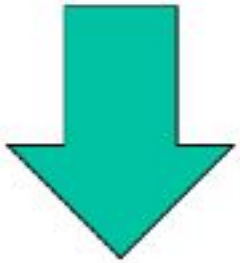

RANGING + PULSE DURATION

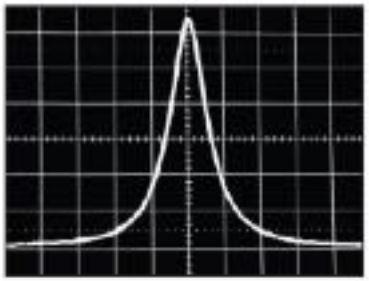

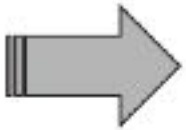

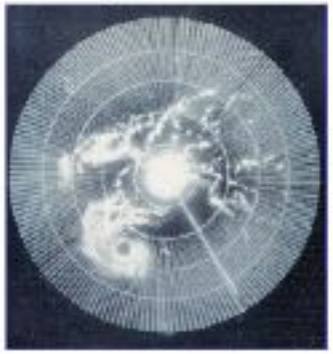

AULA VI

LIDAR EQUATION - RANGING

$$L_1 = \frac{c \times \Delta t}{2}$$

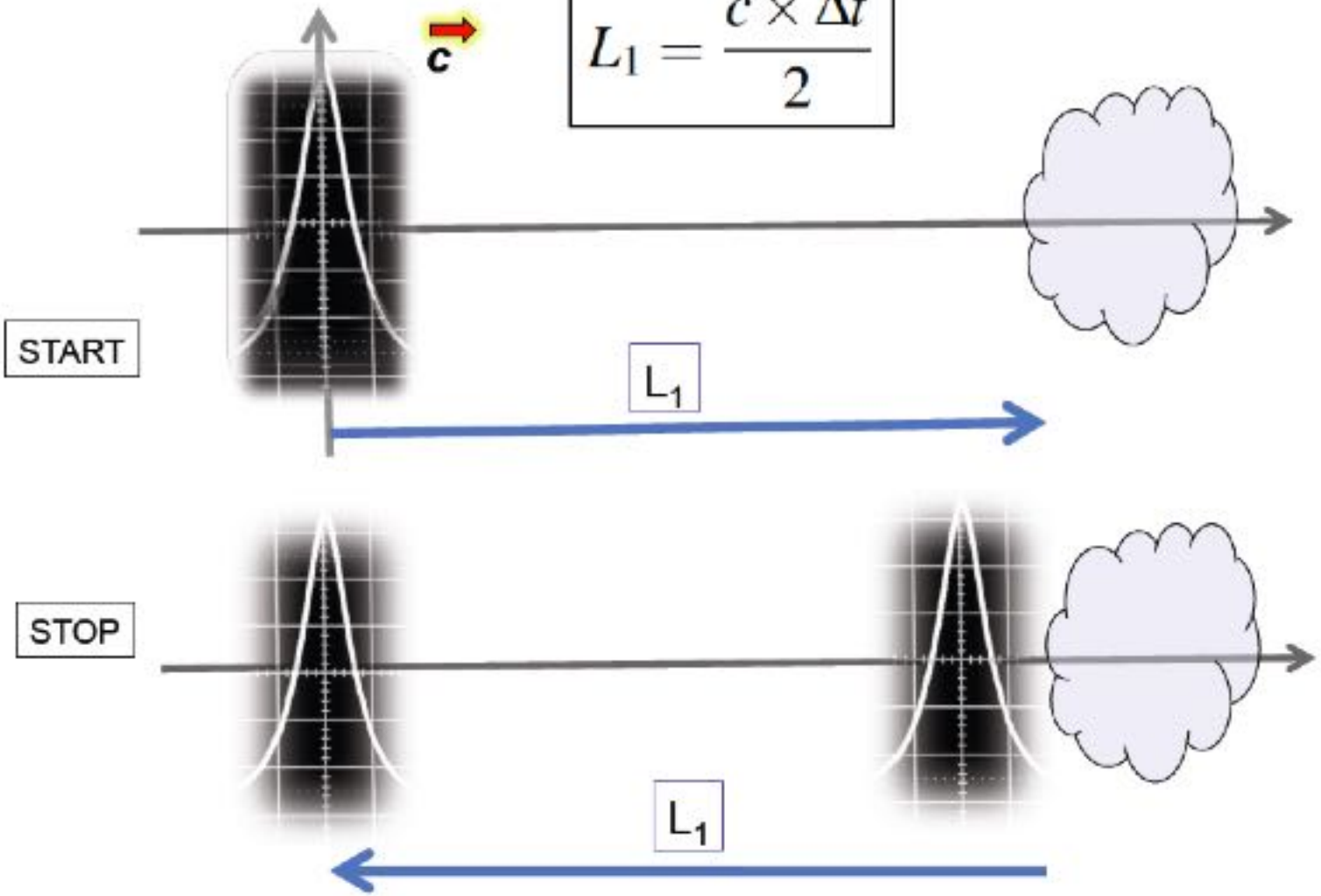

LIDAR EQUATION – PROBED VOLUME

$$V_P = A_L . \Delta R$$

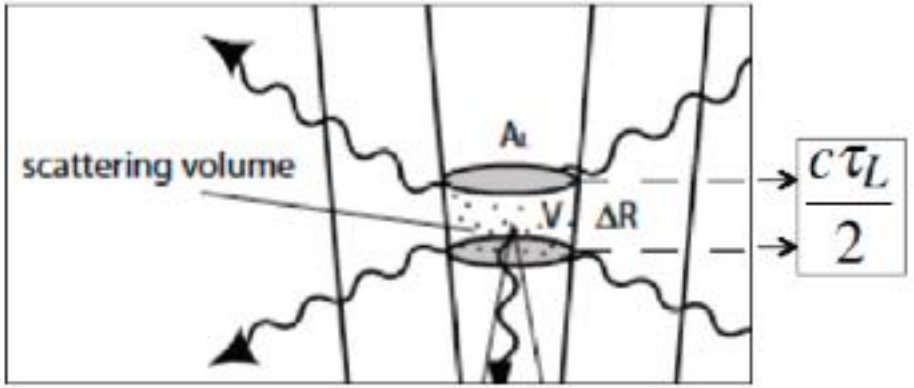

$$V_P = A_L . \frac{c\tau_L}{2}$$

LIDAR EQUATION- TRANSMISSION IN THE ATMOSPHERE

$$T(\lambda, r) \equiv e^{-2\int_0^R \alpha(\lambda, r)dr}$$

EXTINCTION COEFFICIENT

LIDAR EQUATION – THE FINAL CUT

$$J(\lambda,R,r)=\beta_\pi(\lambda,R,r)I(R,r)$$

$$V_P=A_L.\frac{c\tau_L}{2}$$

$$p(\lambda,R,r)=\frac{A_o}{R^2}\times T(\lambda,R)\times e(\lambda)\times\zeta(R,r)$$

$$P_o=I(R,r).A_L$$

$$T(\lambda,r)\equiv e^{-2\int_0^R\alpha(\lambda,r)dr}$$

$$P(\lambda,R)=P_o\frac{A_o}{R^2}\beta_\pi(\lambda,R)\varepsilon(\lambda)\zeta(R).\left(\frac{c\tau_L}{2}\right)e^{-2\int_0^R\alpha(\lambda,r)dR}$$

ELASTIC LIDAR EQUATION

LIDAR EQUATION – OVERLAP FUNCTION

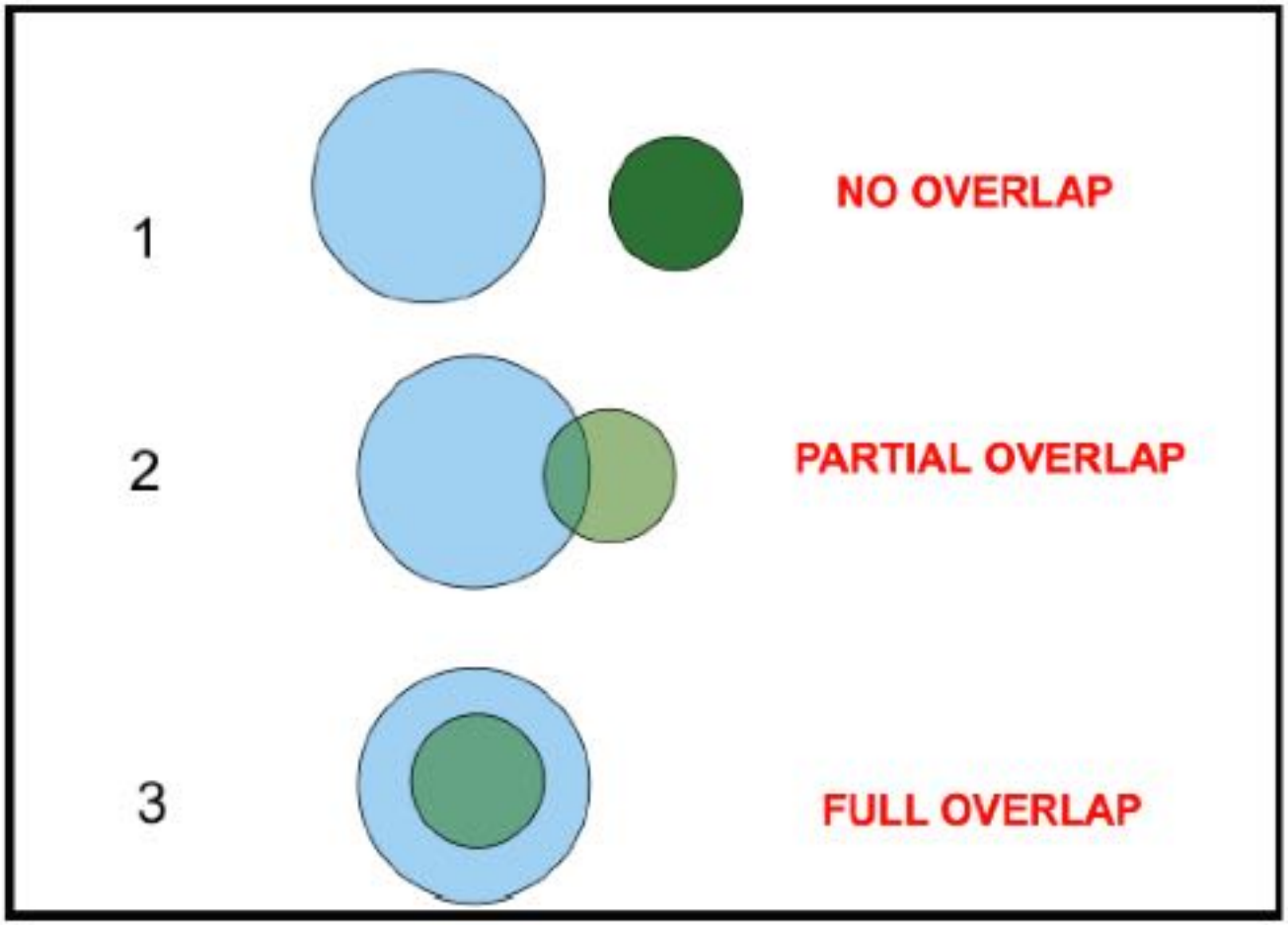

AULA VI

LIDAR EQUATION – SYSTEM EFFICIENCY

$$P(\lambda,R) = P_o \frac{A_o}{R^2} \beta_\pi(\lambda,R) \varepsilon(\lambda) \zeta(R). \left(\frac{c\tau_L}{2}\right) e^{-2\int_0^R \alpha(\lambda,r)dR}$$

SYSTEM EFFICIENCY = SPECTRAL RESPONSE

LIDAR EQUATION – SPECTRAL RESPONSE

SPECTRAL RESPONSE

$$\varepsilon(\lambda) = \prod_{0 \le i \le n} \varepsilon_i(\lambda)$$

MIRRORS, FILTERS, DETECTORS

LIDAR EQUATION – SPECTRAL DETECTORS

AULA VI

SPECTRAL RESPONSE

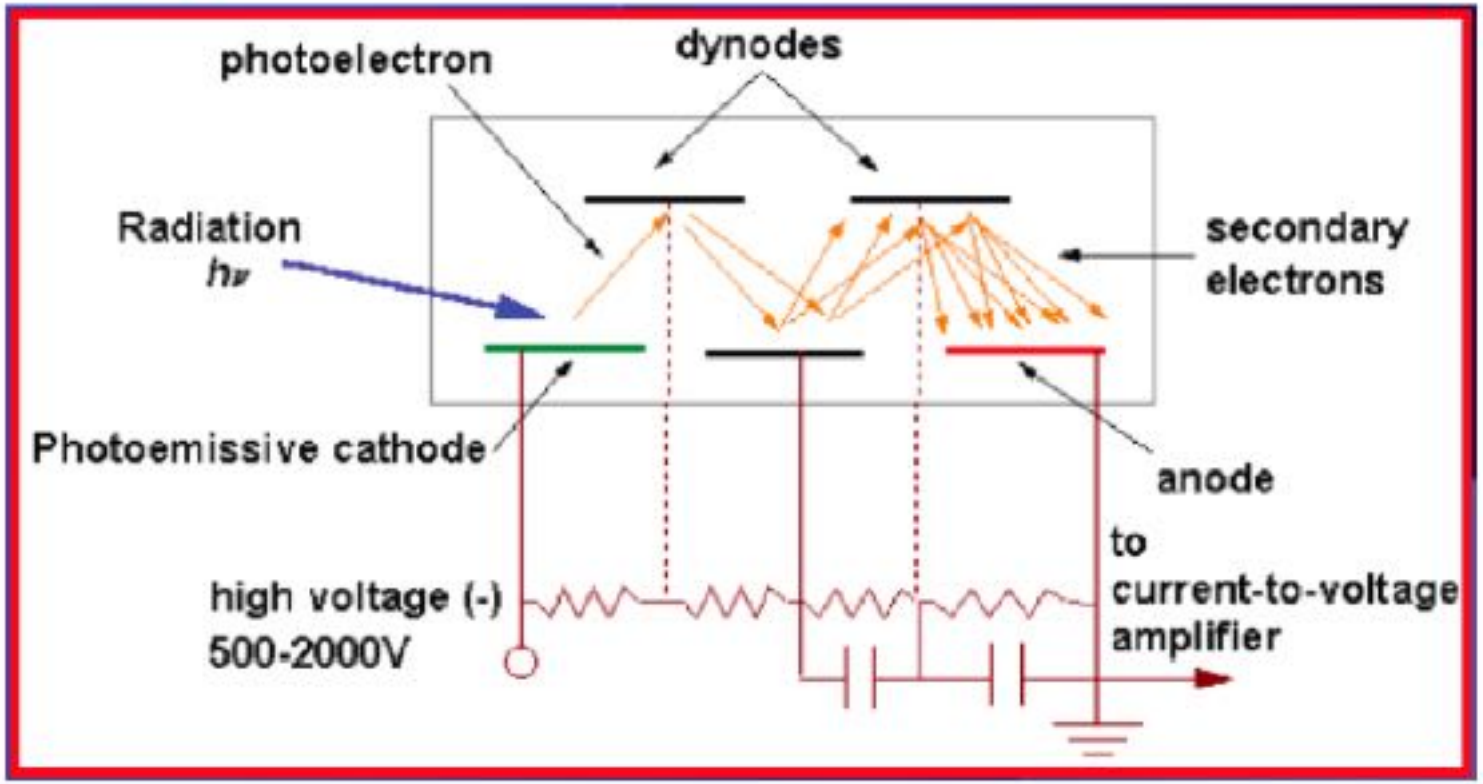

AULA VI

LIDAR EQUATION – SOLUTIONS

ATMOSPHERIC OPTICAL PARAMETERS

$$P(\lambda,R) = P_o \frac{A_o}{R^2} \beta_\pi(\lambda,R)\varepsilon(\lambda)\zeta(R).\left(\frac{c\tau_L}{2}\right) e^{-2\int_0^R \alpha(\lambda,r)dR}$$

BACKSCATTERING COEFFICIENT

$$[\beta(R)] = km^{-1}.sr^{-1}$$

EXTINCTION COEFFICIENT

$$[\alpha(R)] = km^{-1}$$

AEROSOL STUDIES WITH LIDARS – SOLUTIONS

ATMOSPHERIC OPTICAL PARAMETERS

$$\beta(R) = \beta_{aer}(R) + \beta_{mol}(R)$$

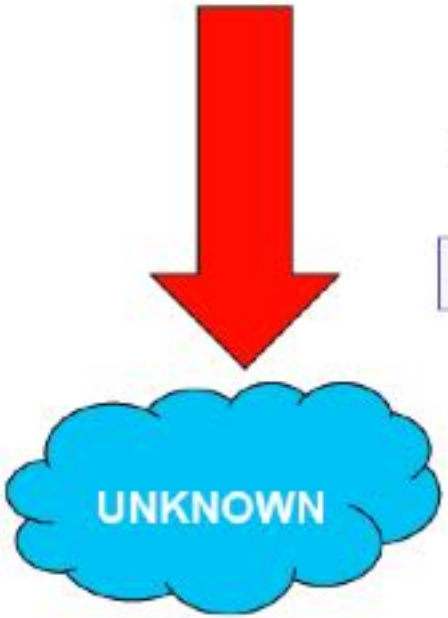

$$\alpha(R) = \alpha_{aer}(R) + \alpha_{mol}(R)$$

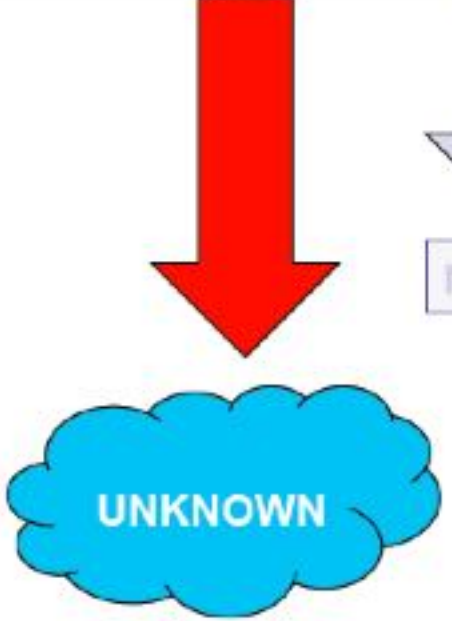

AEROSOL STUDIES WITH LIDARS – SOLUTIONS

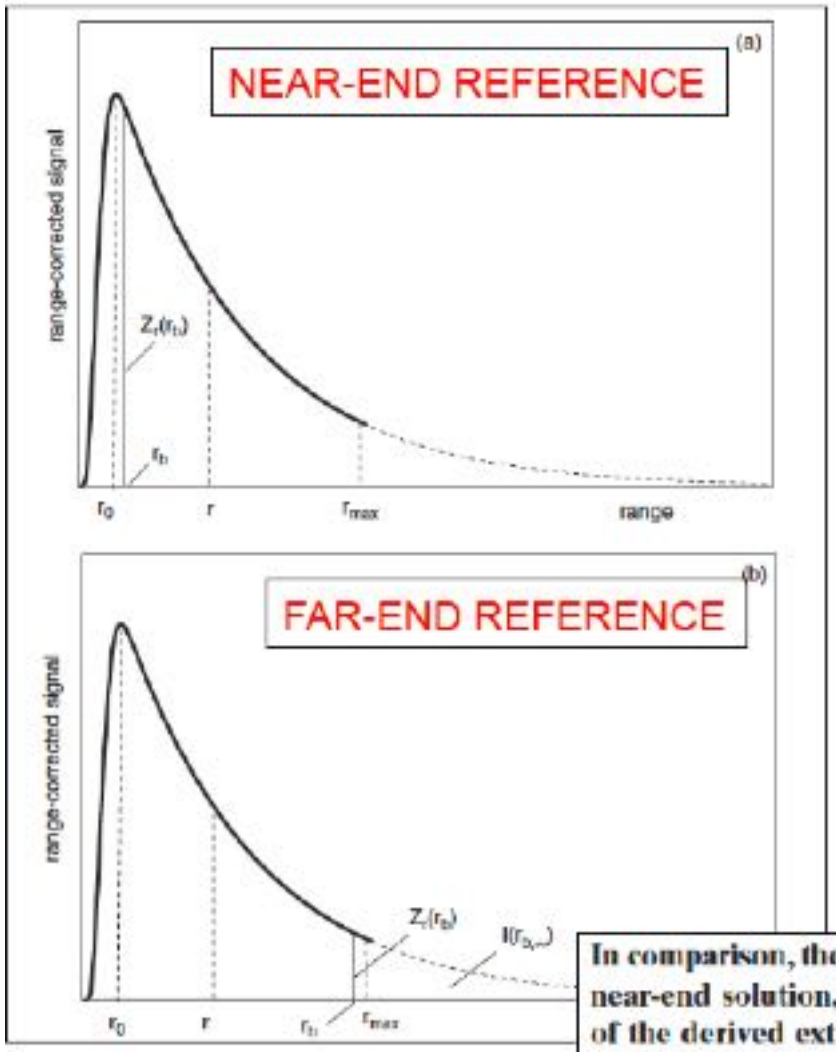

In comparison, the far-end boundary point solution is much more stable than the near-end solution, at least, in turbid atmospheres. It yields only positive values of the derived extinction coefficient, κ_t, even if the signal-to-noise ratio is poor. However in clear atmospheres, it has no significant advantages as compared to the near-end solution.

KOVALEV & EICHINGER

AEROSOL STUDIES WITH LIDARS – SOLUTIONS

LIDAR RATIO

$$P(\lambda,R) = P_o \frac{A_o}{R^2} \beta_\pi(\lambda,R) \varepsilon(\lambda) \zeta(R). \left(\frac{c\tau_L}{2}\right) e^{-2\int_0^R \alpha(\lambda,r)dR}$$

$$L_{aer}(R) = \frac{\alpha_{mol}(R)}{\beta_{mol}(R)} = \frac{8\pi}{3} sr$$

LIDAR RATIO (MOLECULAR)

$$L_{aer}(R) = \frac{\alpha_{aer}(R)}{\beta_{aer}(R)}$$

LIDAR RATIO (AEROSOL)

AEROSOL STUDIES WITH LIDARS - LIDAR EQUATION SOLUTIONS

$$\frac{d\chi(R)}{dR} = \frac{1}{\chi(R)}\frac{d\chi(R)}{dR} - 2\chi(R)$$

BERNOUILLI EQUATION

$$\chi(R) = L_{aer}[\beta_{aer}(R) + \beta_{mol}(R)]$$

1. KOVALEV & EICHINGER
2. WEITKAMP
3. MEASURES

AEROSOL STUDIES WITH LIDARS – EXAMPLE

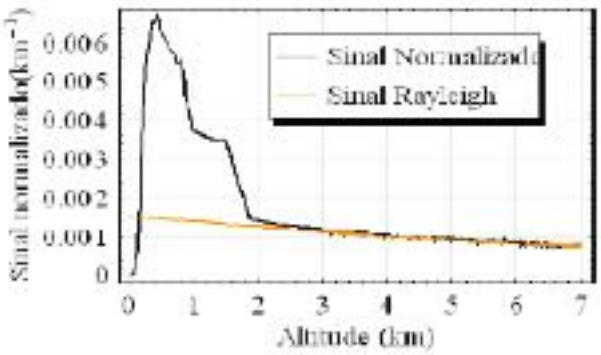

Figura 4.8: Exemplo de calibração do sinal lidar

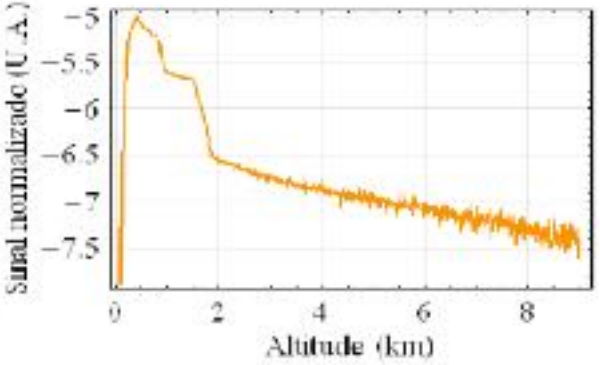

Figura 4.9: Sinal identificado como o vetor de medidas y no algoritmo

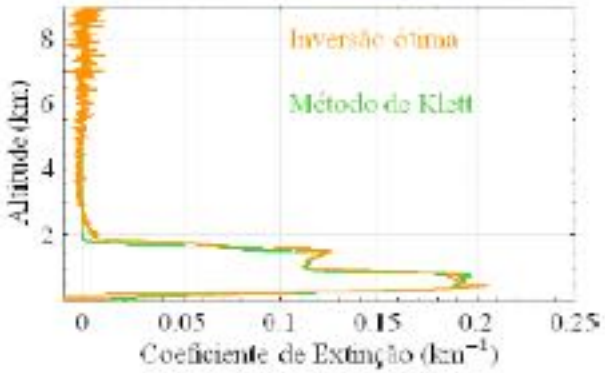

Figura 4.10: Estimativa do coeficiente de extinção.

AEROSOL STUDIES WITH LIDARS – AERONET CLOSURE

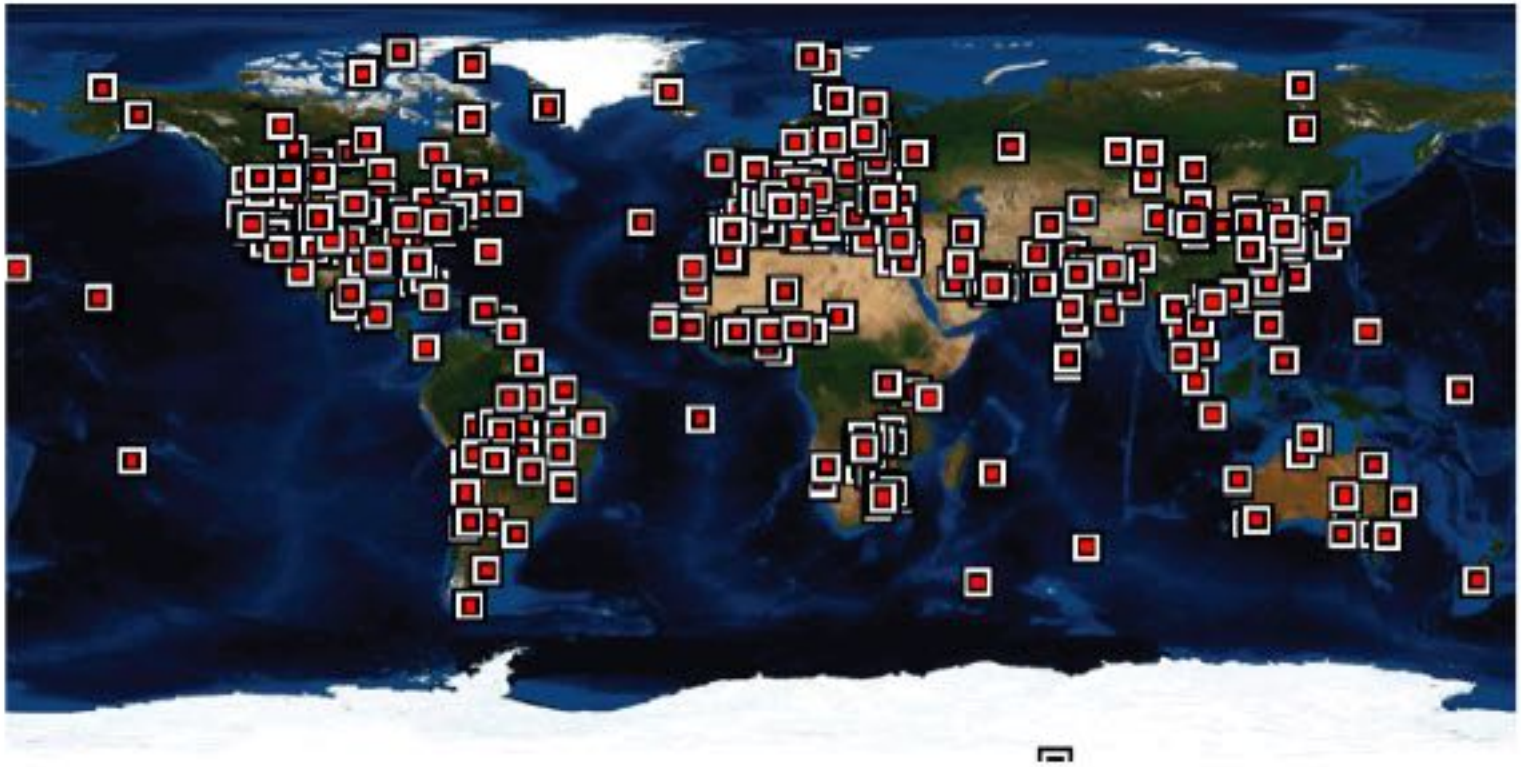

AEROSOL STUDIES WITH LIDARS – AERONET CLOSURE

AOT(λ)

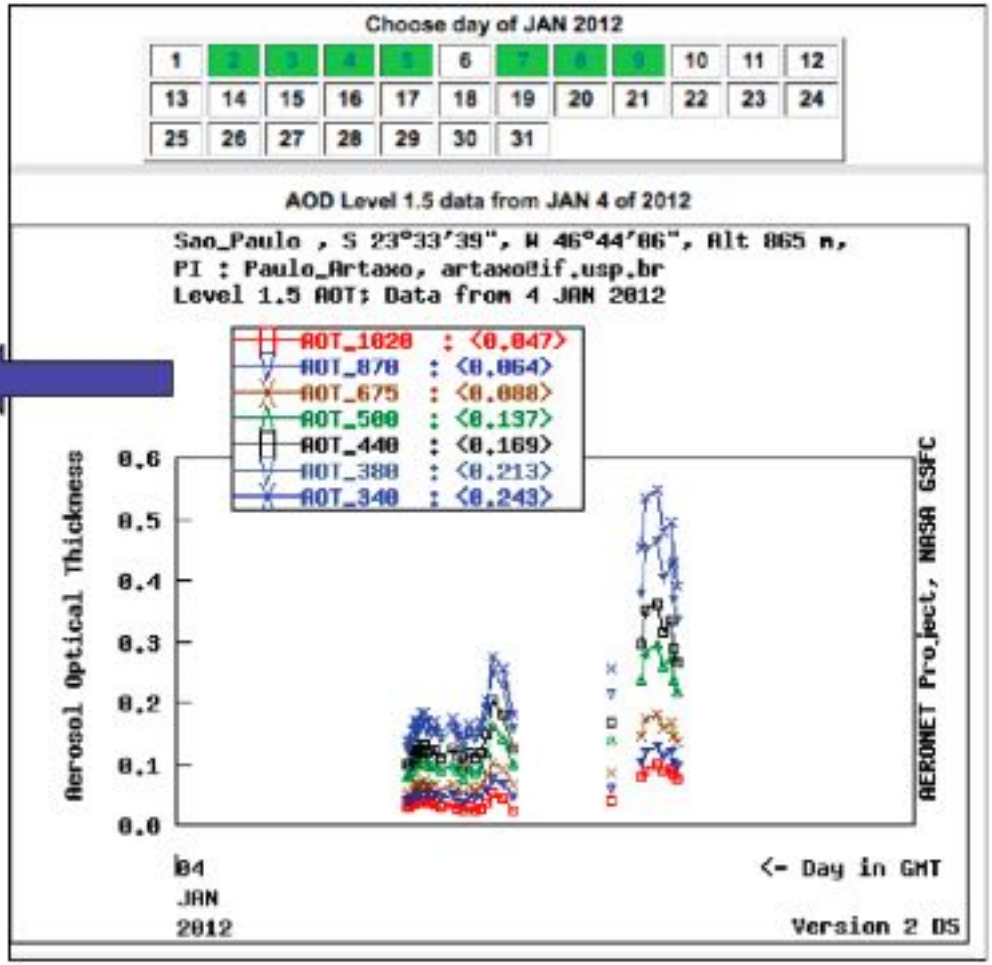

AEROSOL STUDIES WITH LIDARS – AERONET CLOSURE

$$AOT_{aeronet}(\lambda) \equiv \tau(\lambda, z) = \int_o^{\infty} \alpha(\lambda, z) dz$$

$$AOT_{aeronet} \equiv AOT_{lidar}(\lambda) = \int_o^{\infty} \alpha_{aer}(\lambda, z) dz$$

$$AOT_{lidar}(\lambda) = L_{aer} \times \sum \beta_{aer}(\lambda, z) \Delta z$$

AEROSOL STUDIES WITH LIDARS – RAMAN LIDARS

$$P(\lambda,R) = P_o \frac{A_o}{R^2} \beta_\pi(\lambda_L,\lambda_R,R)\varepsilon(\lambda)\zeta(R).\left(\frac{c\tau_L}{2}\right) e^{-\int_0^R \alpha(\lambda_L,r)+\alpha(\lambda_R,r)dR}$$

RAMAN SCATTERING CROSS SECTION

DIFFERENTIAL TRANSMISSION

AEROSOL STUDIES WITH LIDARS – RAMAN LIDARS

$$\alpha(355,z) = \frac{\frac{d}{dz}\left[ln\frac{N(z)}{z^2P(z)}\right] - \alpha_{mol}(355,z) - \alpha_{mol}(387,z)}{1+\frac{355}{387}}$$

λ_L = 355 nm

λ_R = 387 nm

NITROGEN RAMAN SCATTERING

λ_L = 355 nm

AEROSOL STUDIES WITH LIDARS – HRSL LIDARS

HIGH RESOLUTION SPECTRAL LIDARS

AEROSOL DOPPLER BROADENING

MOLECULAR DOPPLER BROADENING

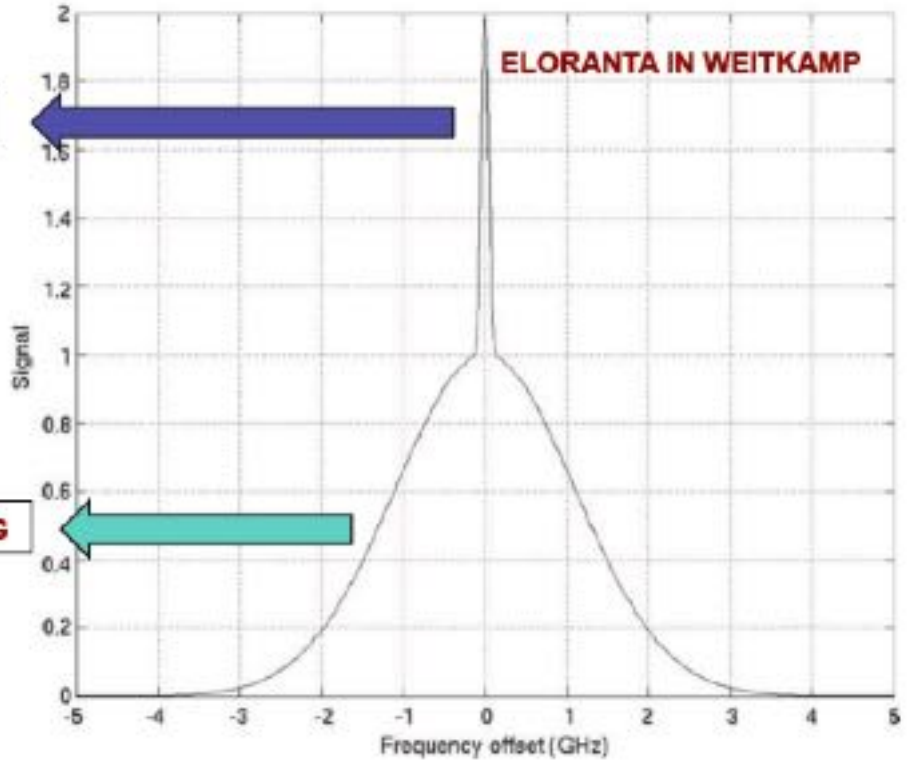

AEROSOL STUDIES WITH LIDARS – HRSL LIDARS

HIGH RESOLUTION SPECTRAL LIDARS

$$P_{\mathrm{mol}}(r) = K_{\mathrm{mol}} r^{-2} O(r) \beta_{\mathrm{mol}}(r) \exp\left(-2\int_0^r \alpha(r')\mathrm{d}r'\right)$$

$$P_{\mathrm{aer}}(r) = K_{\mathrm{aer}} r^{-2} O(r) \beta_{\mathrm{aer}}(r) \exp\left(-2\int_0^r \alpha(r')\mathrm{d}r'\right)$$

$$\Re(r) = \frac{\beta_{\mathrm{aer}}(r)}{\beta_{\mathrm{mol}}(r)} = \frac{K\,P_{\mathrm{aer}}(r)}{P_{\mathrm{mol}}(r)}.$$

The problem of the analysis of lidar data is related to problems of lidar signal interpretation. Despite the wide variety of the lidar systems developed for periodical and routine atmospheric measurements, no widely accepted method of lidar data inversion or analysis has been developed or adopted. A researcher interested in the practical application of lidars soon learns the following: (1) no standard analysis method exists that can be used even for the simplest lidar measurements; (2) in the technical literature, only scattered practical recommendations can be found concerning the derivation of useful information from lidar measurements; (3) lidar data processing is, generally, considered an art rather than a routine procedure; and (4) the quality of the inverted lidar data depends dramatically on the experience and skill of the researcher.

Kovalev & Eichinger – Elastic Lidar

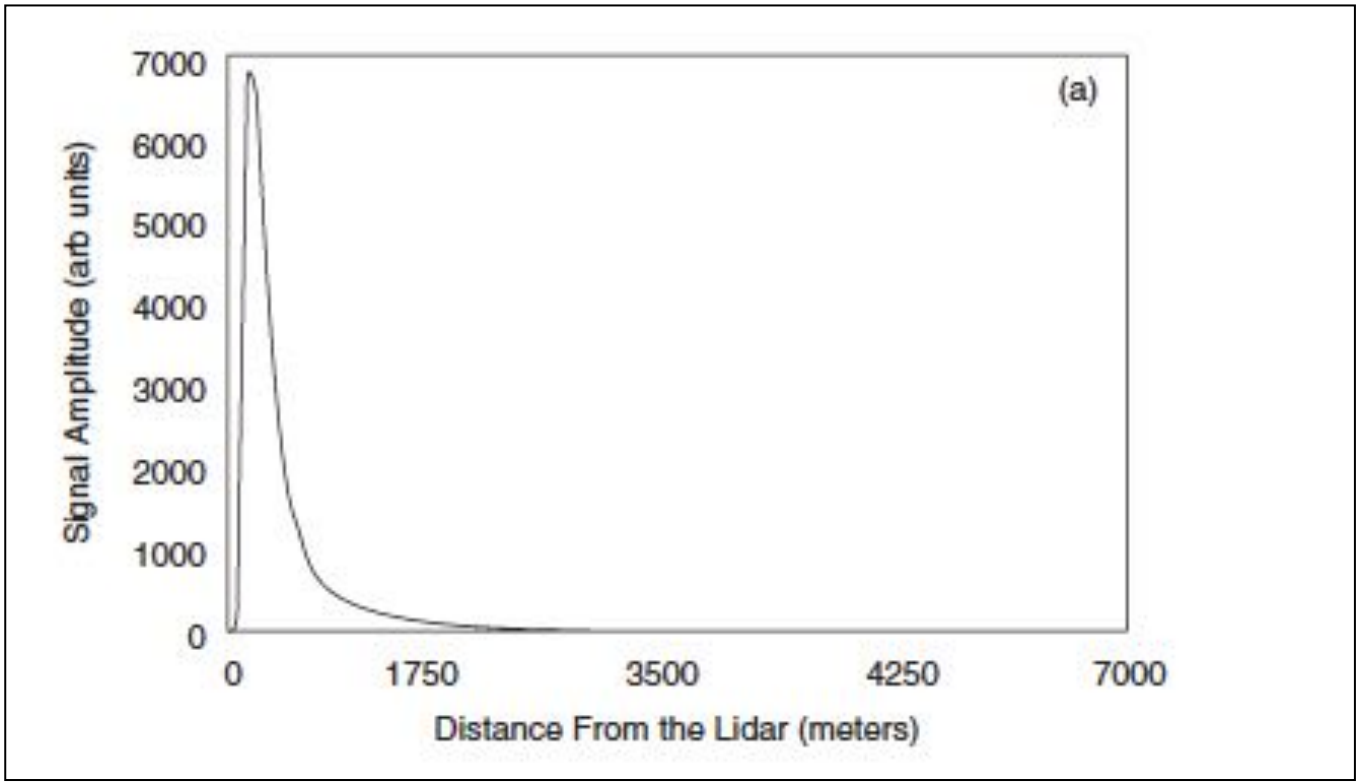

The “non-exciting” typical lidar retrieval

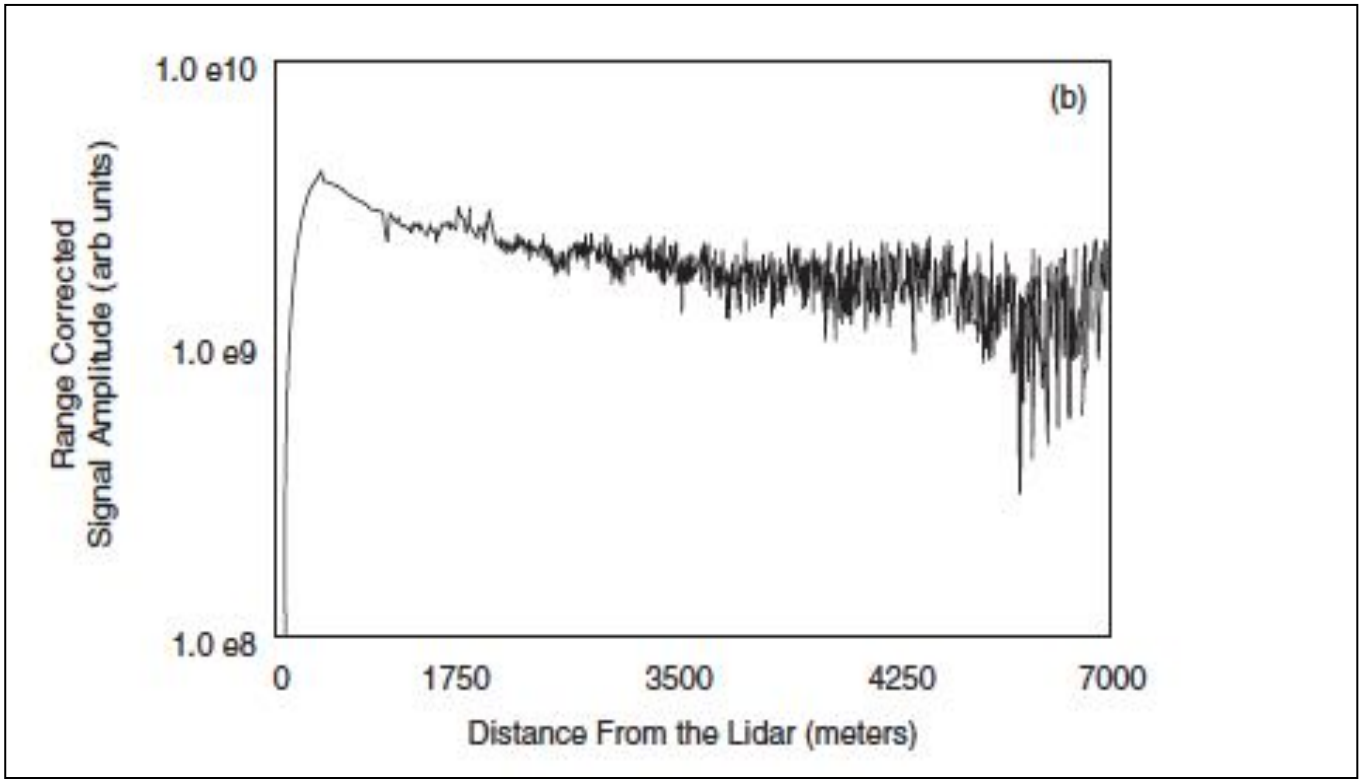

The “somehow-exciting” typical lidar retrieval

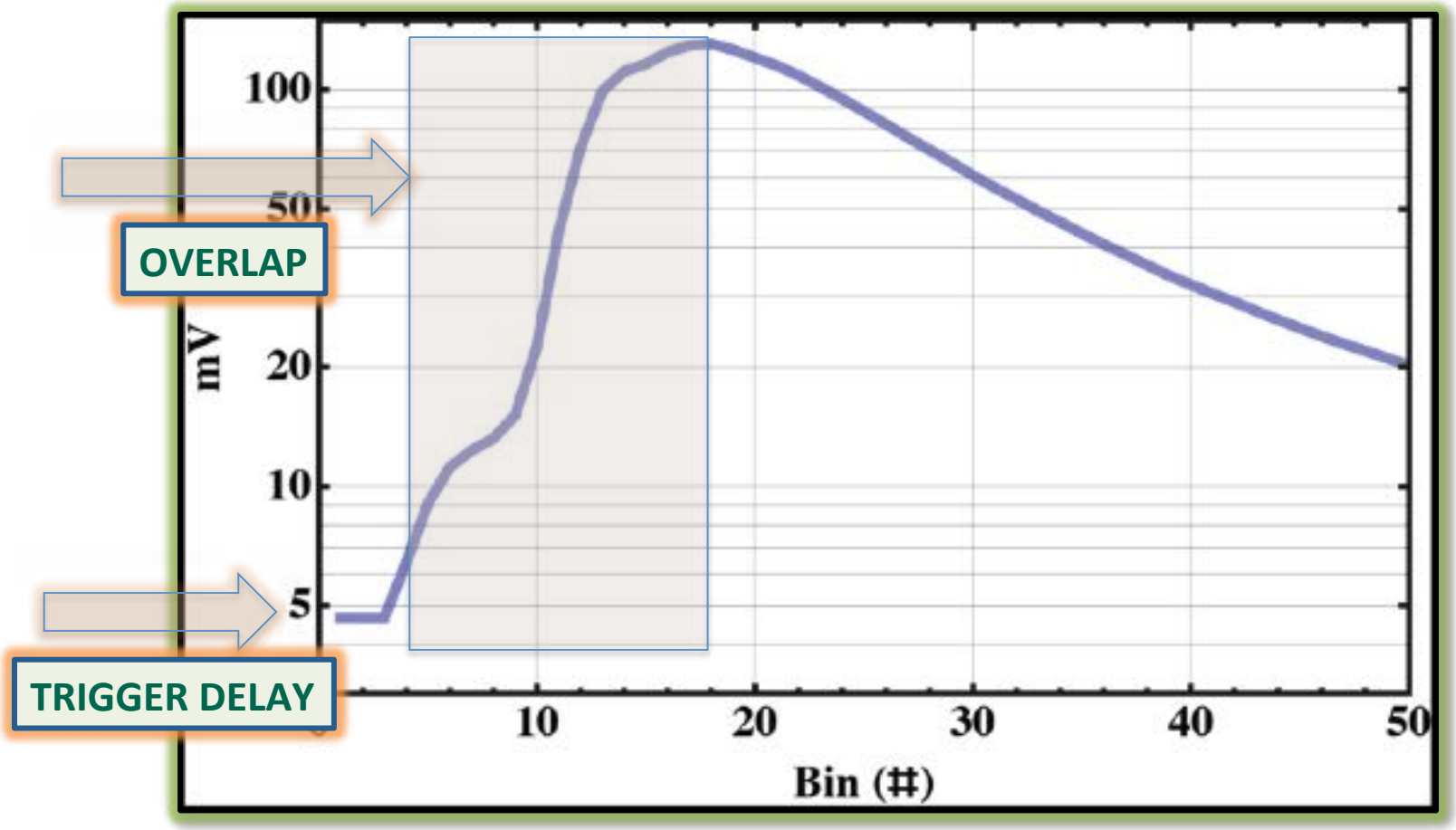

LIDAR ANALOGIC SIGNAL “CLOSE-LOOK”

Solving the Lidar Equation

As clarified in Elastic Lidar by Kovalev and Hooper, the general solution technique that we will use here was first developed by Barrett and Ben-Dov, 1967. The first study of the stability of the solution and use of the backward integration to improve the stability occurred in the Soviet Union by Kaul in 1977 and Zuev in 1978. These efforts were not known in the west so it is the well-known paper by Klett, 1981 that is most often cited as the source of this technique.

Aerosol Scattering Ratio

$$\mathcal{R}(\lambda_L, r) = \frac{\beta_\pi^{mol}(\lambda_L, r) + \beta_\pi^{aer}(\lambda_L, r)}{\beta_\pi^{mol}(\lambda_L, r)} = 1 + \frac{\beta_\pi^{aer}(\lambda_L, r)}{\beta_\pi^{mol}(\lambda_L, r)}$$

Aerosol Scattering Ratio

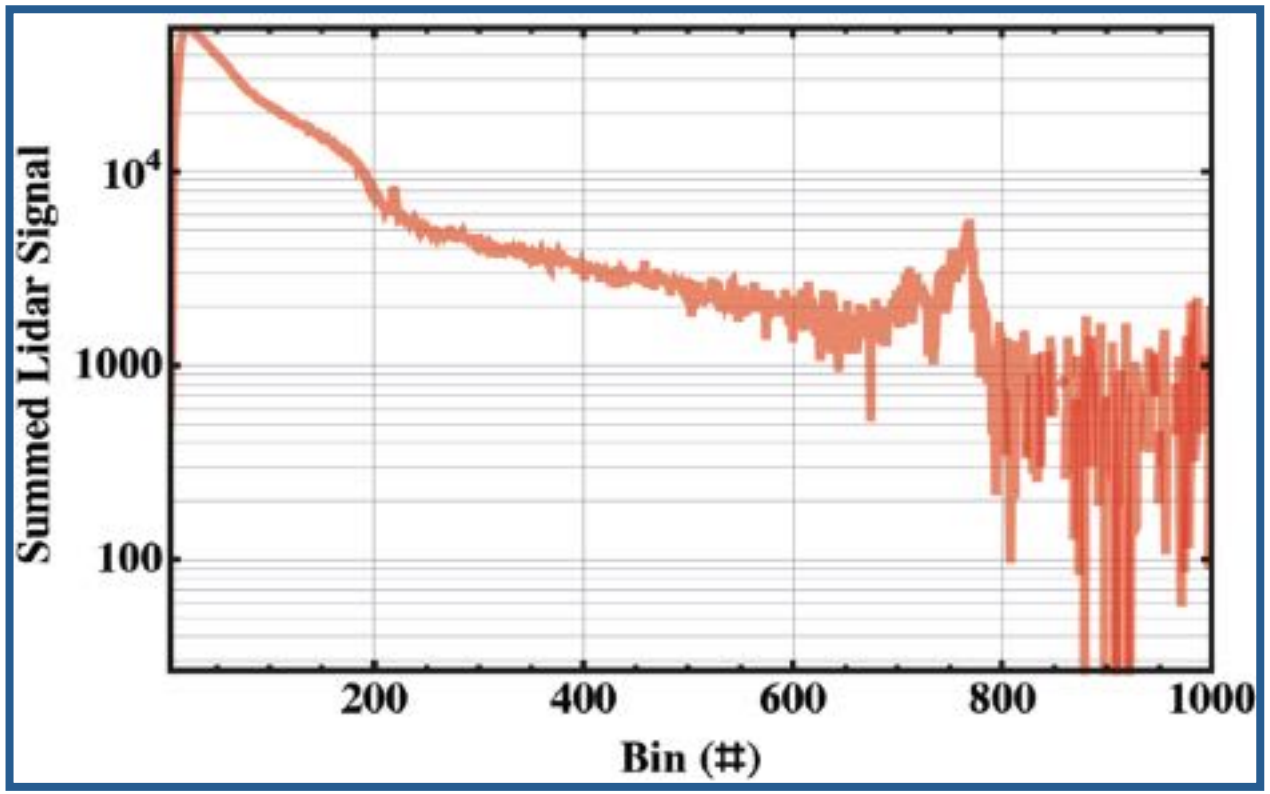

Aerosol Scattering Ratio

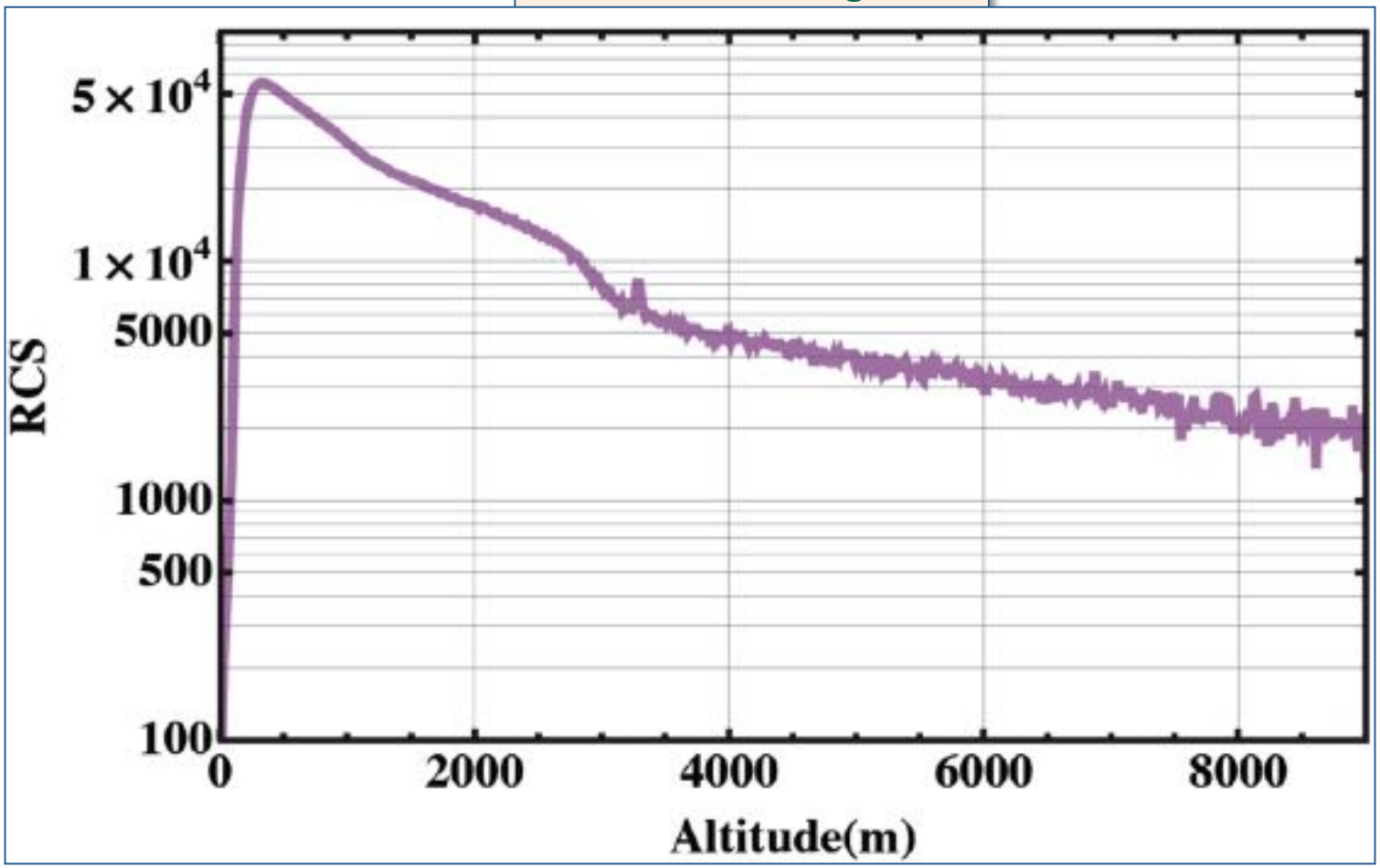

Aerosol Scattering Ratio

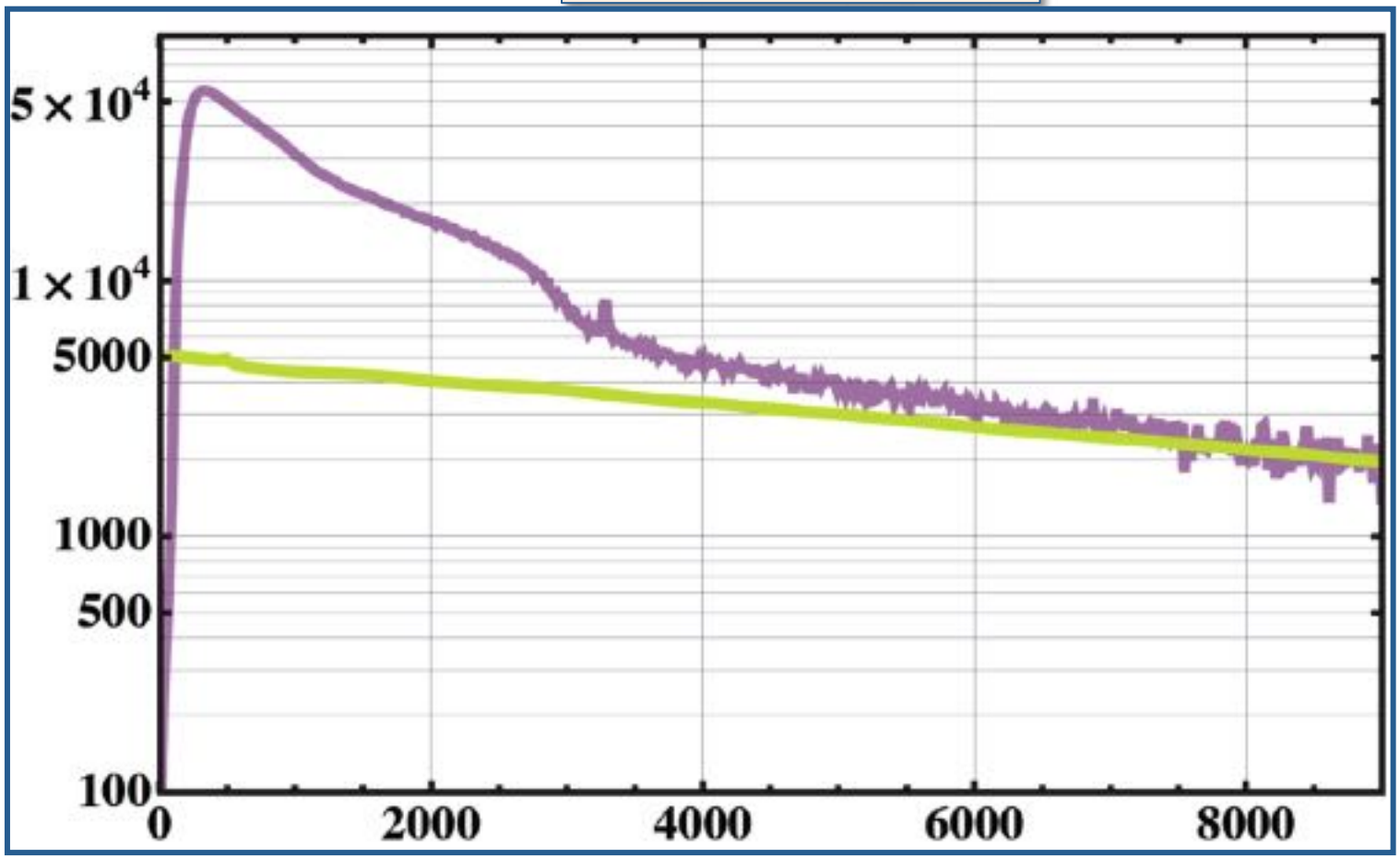

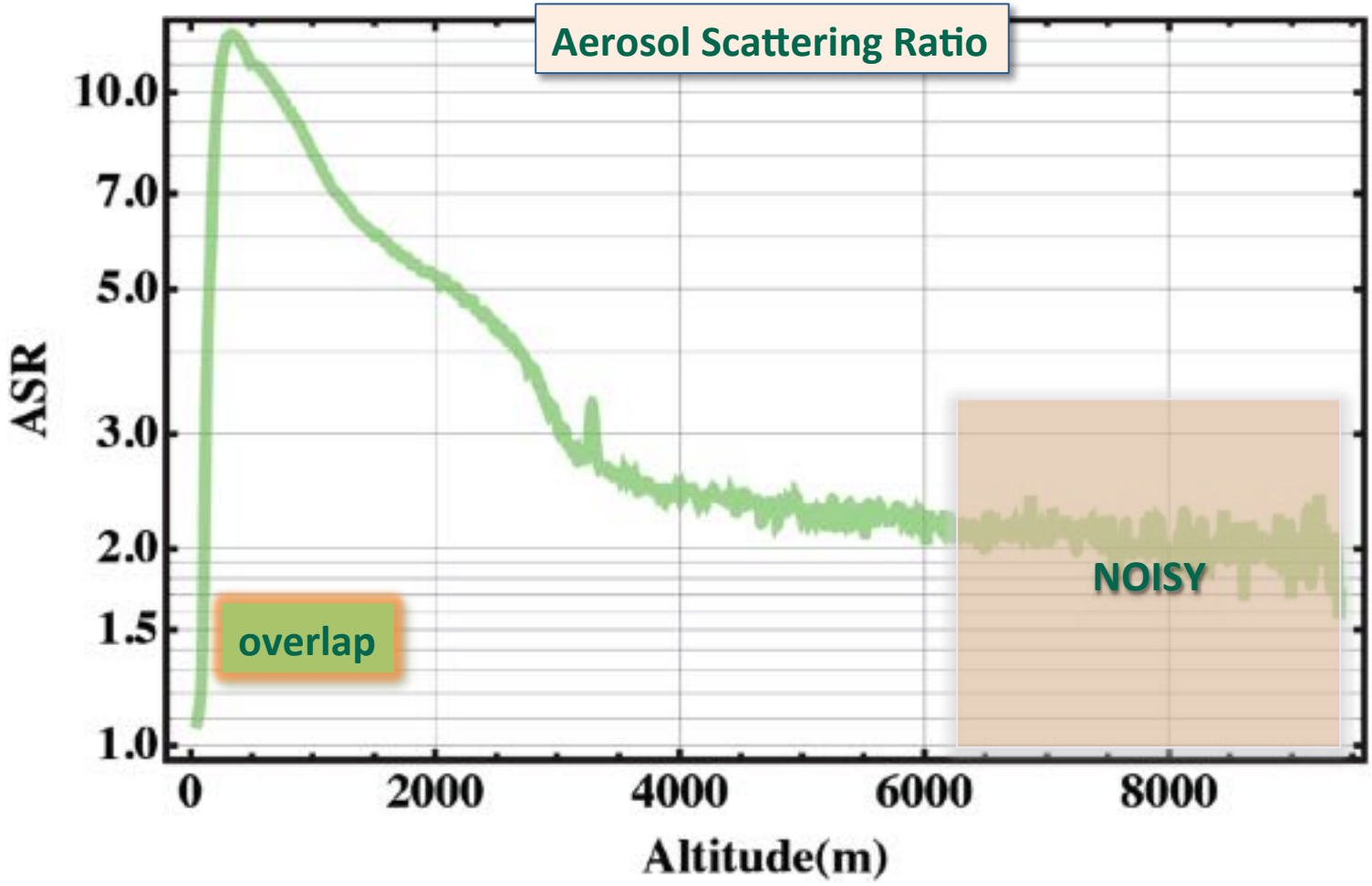
Aerosol Scattering Ratio
ASR
10.0
7.0
5.0
3.0
2.0
1.5
1.0
overlap
NOISY
0
2000
4000
6000
8000
Altitude(m)

Aerosol Scattering Ratio

$$\mathscr{R} = 1 + \frac{\beta_\pi^{aer}(\lambda, r)}{\beta_\pi^{mol}(\lambda, r)}$$

$$\beta_\pi^{aer}(\lambda, r) = (\mathscr{R} - 1) \times \beta_\pi^{mol}(\lambda, r)$$

Aerosol Backscattering Coefficient

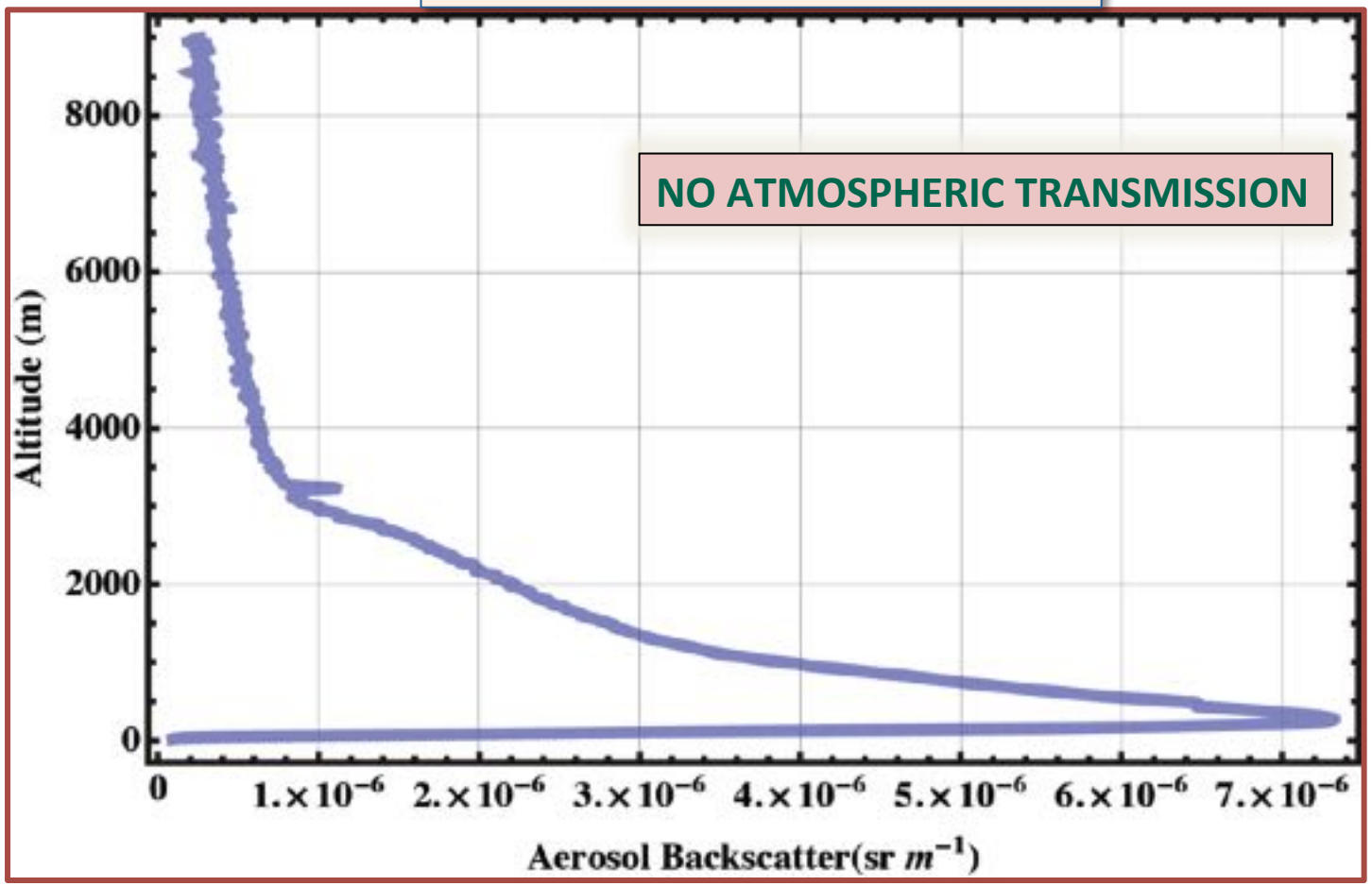

Aerosol Backscattering Coefficient

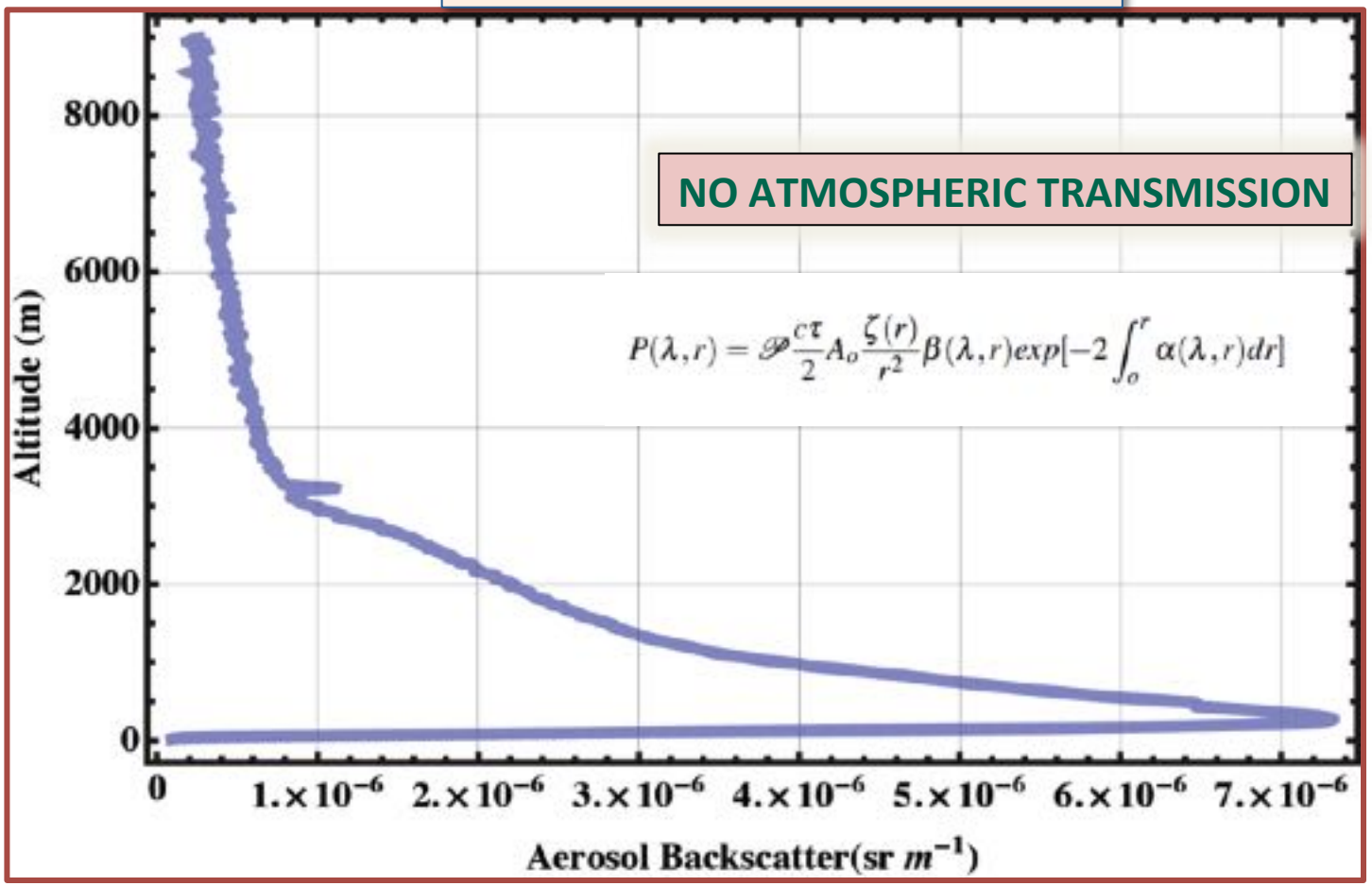

Satélite CALIPSO e Aplicações

Evolução do lidar

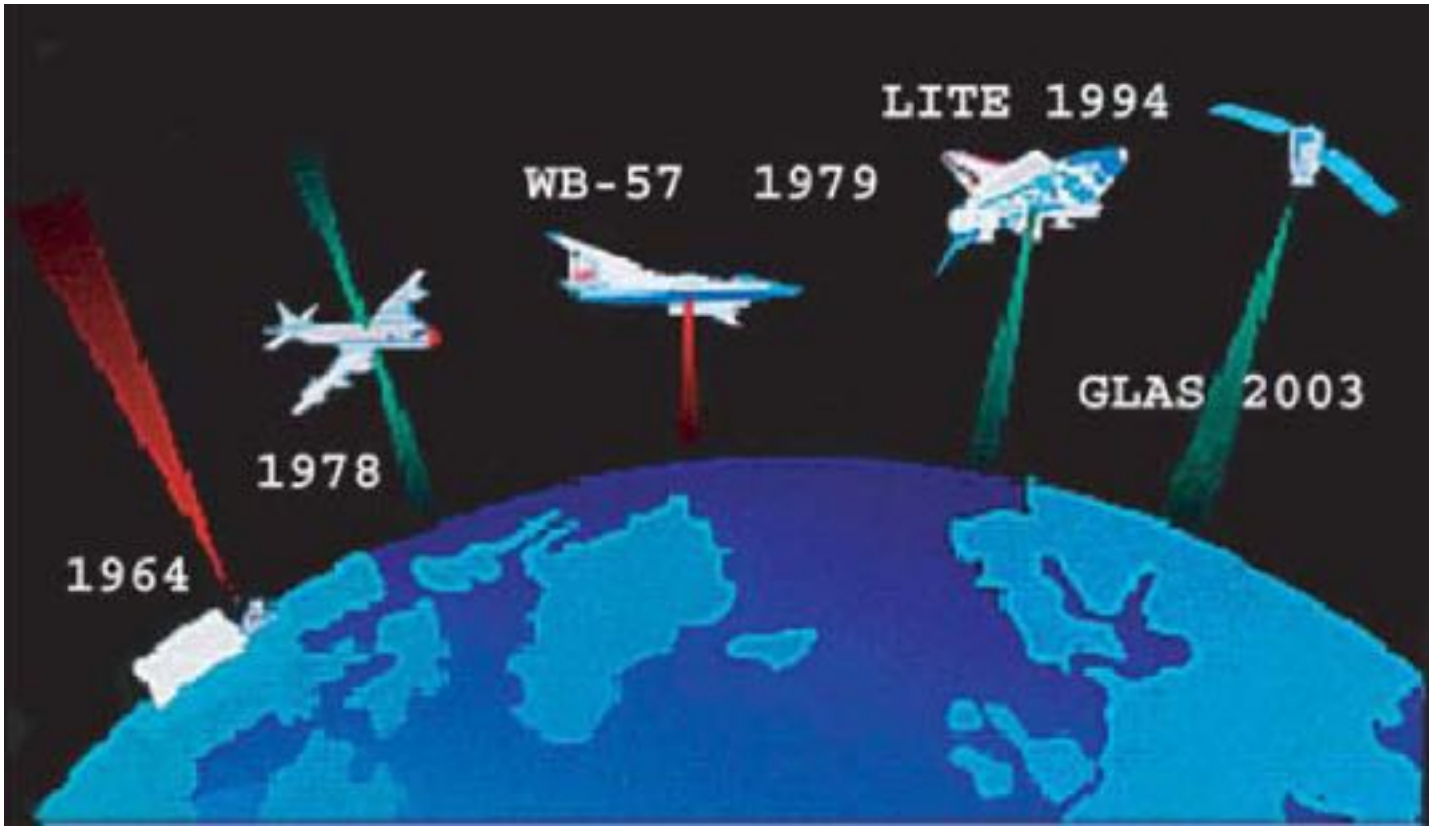

WEITKAMP, C. *Lidar Range-Resolved Optical Remote Sensing of the Atmosphere*. 1st. ed. New York: Springer, 2005.

LITE

Lidar In-space Technology Experiment (LITE) - 1994

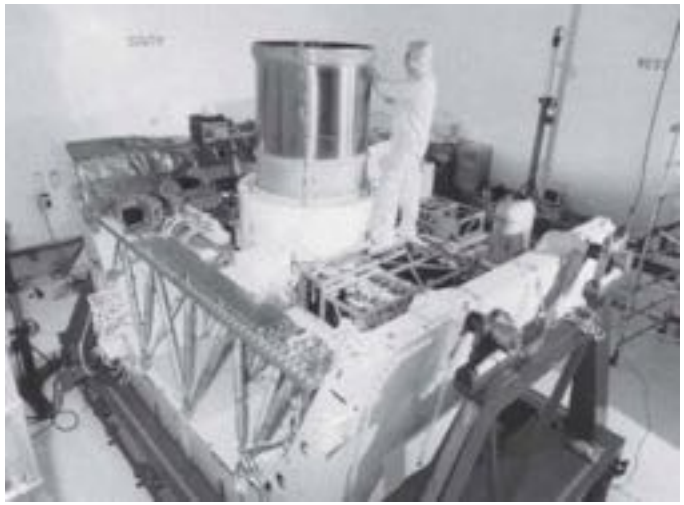

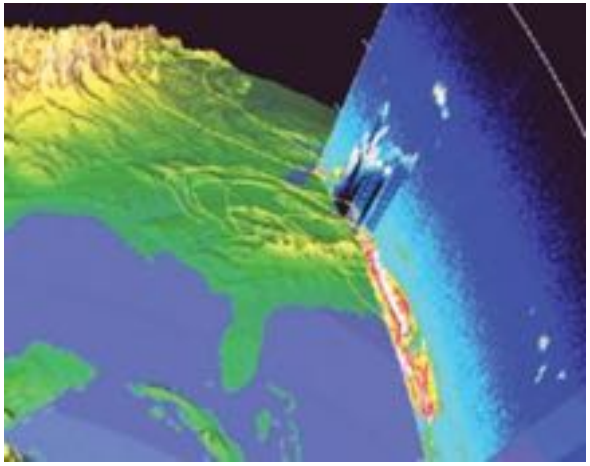

Primeiro Lidar em órbita a bordo de um ônibus espacial (10 dias em operação)

WEITKAMP, C. ***Lidar Range-Resolved Optical Remote Sensing of the Atmosphere*****. 1st. ed. New York: Springer, 2005.**

LITE

Lidar In-space Technology Experiment (LITE) - 1994

Observations of Biomass Burning by LITE

September 18, 1994 Orbit 134

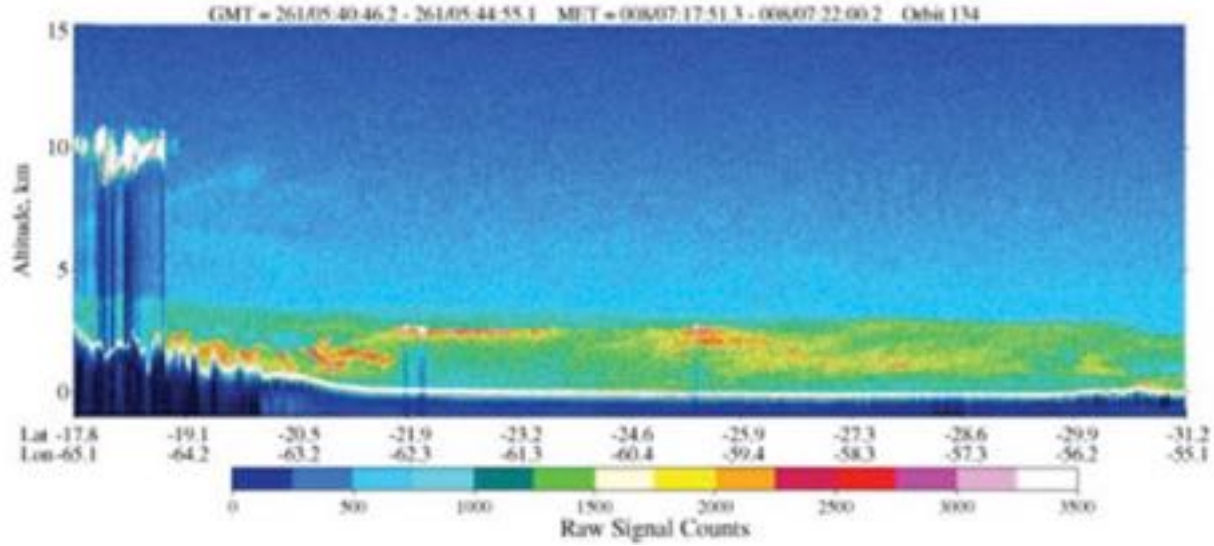

WEITKAMP, C. *Lidar Range-Resolved Optical Remote Sensing of the Atmosphere*. 1st. ed. New York: Springer, 2005.

LITE

Lidar In-space Technology Experiment (LITE) - 1994

Observations of
Saharan Dust
by LITE

September 15, 1994 Orbit 83

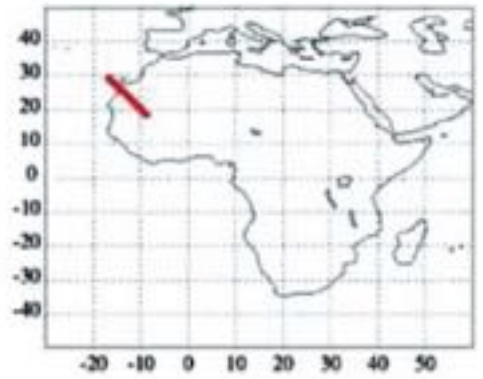

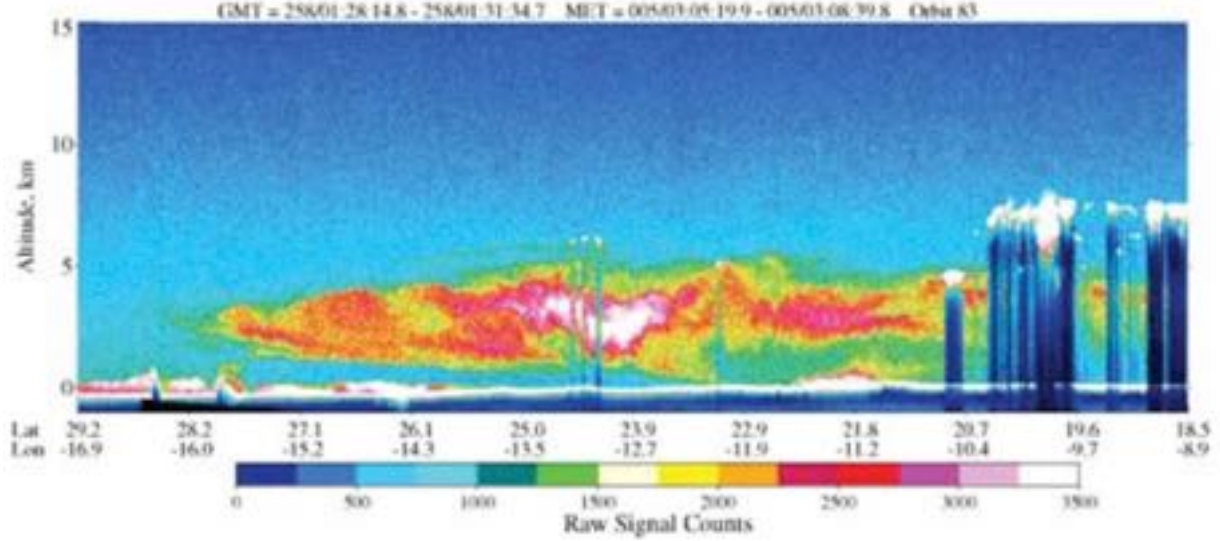

WEITKAMP, C. *Lidar Range-Resolved Optical Remote Sensing of the Atmosphere*. 1st. ed. New York: Springer, 2005.

GLAS

Satélite GLAS (Geoscience Laser Altimeter System) abordo do ICESat (Cloud and land Elevation Satellite) - 2003

Primeira missão de longa duração com um Lidar no espaço – 664 dias entre 20/02/2003 e 11/10/2009 († 30/08/2010)

WEITKAMP, C. *Lidar Range-Resolved Optical Remote Sensing of the Atmosphere*. 1st. ed. New York: Springer, 2005.

CALIPSO – Cloud-Aerosol Lidar and Infrared Pathfinder Satellite Observation

Lançado em 2006 – NASA e CNES

Estudo do perfil vertical das propriedades ópticas de aerossóis e nuvens em escala global

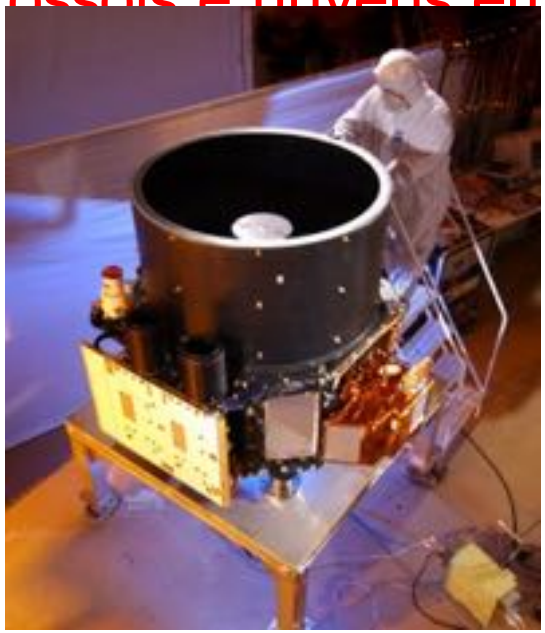

WEITKAMP, C. *Lidar Range-Resolved Optical Remote Sensing of the Atmosphere*. 1st. ed. New York: Springer, 2005.

A-Train Constellation

A-Train constellation – Afternoon constellation

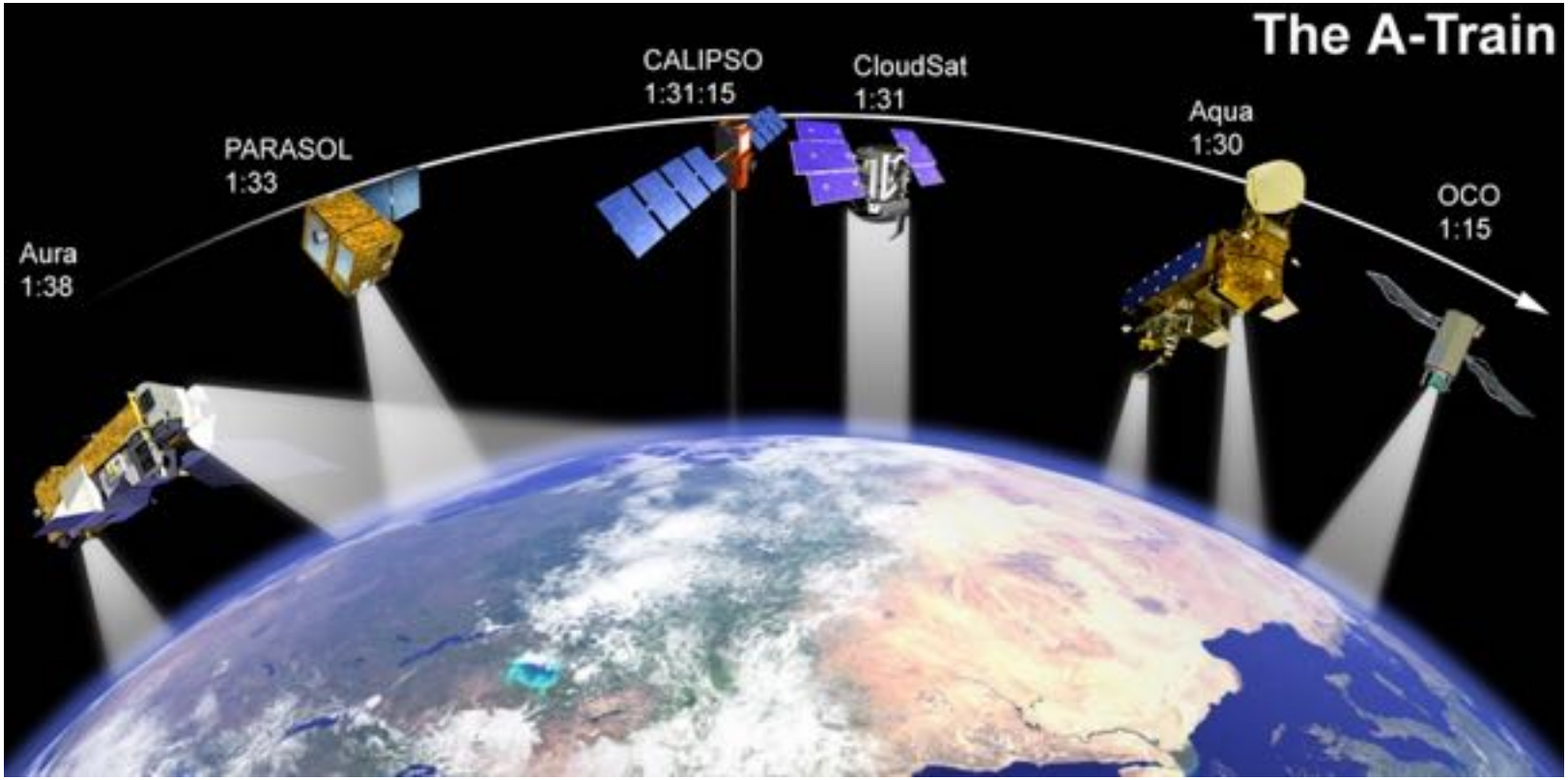

Canção de Jazz “Take the A-Train” composta por Billy Strayhorn e tocada pela banda de Duke Ellington

WEITKAMP, C. *Lidar Range-Resolved Optical Remote Sensing of the Atmosphere*. 1st. ed. New York: Springer, 2005.

CALIPSO

Lançado em Abril de 2006

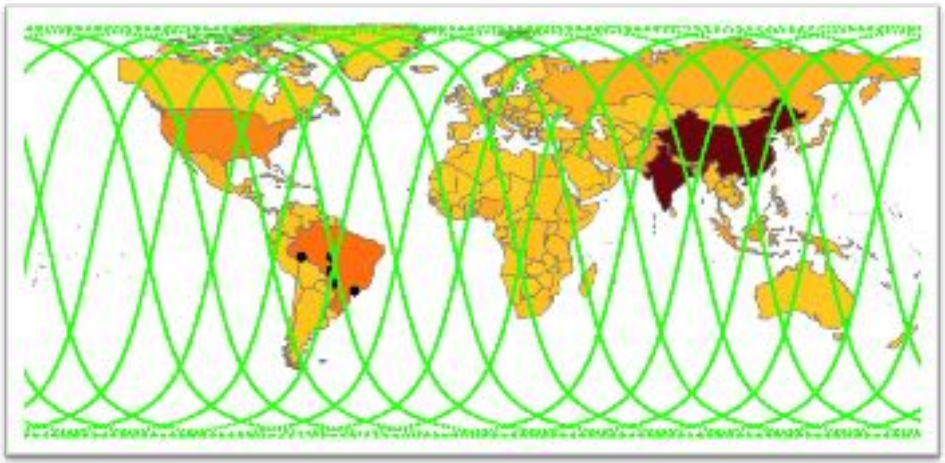

Altitude: 705 Km a 98° de inclinação.

Velocidade de órbita: 7 km/s

Órbitas: 14,55/dia - separação de 24,7° longitudinais por órbita.

Avanço de 10,8° a Oeste no fim de um ciclo diário.

Período de 16 dias para cobrir todo o globo terrestre.

Sistema CALIOP

CALIOP – Cloud Aerosol Lidar with Ortogonal Polarization

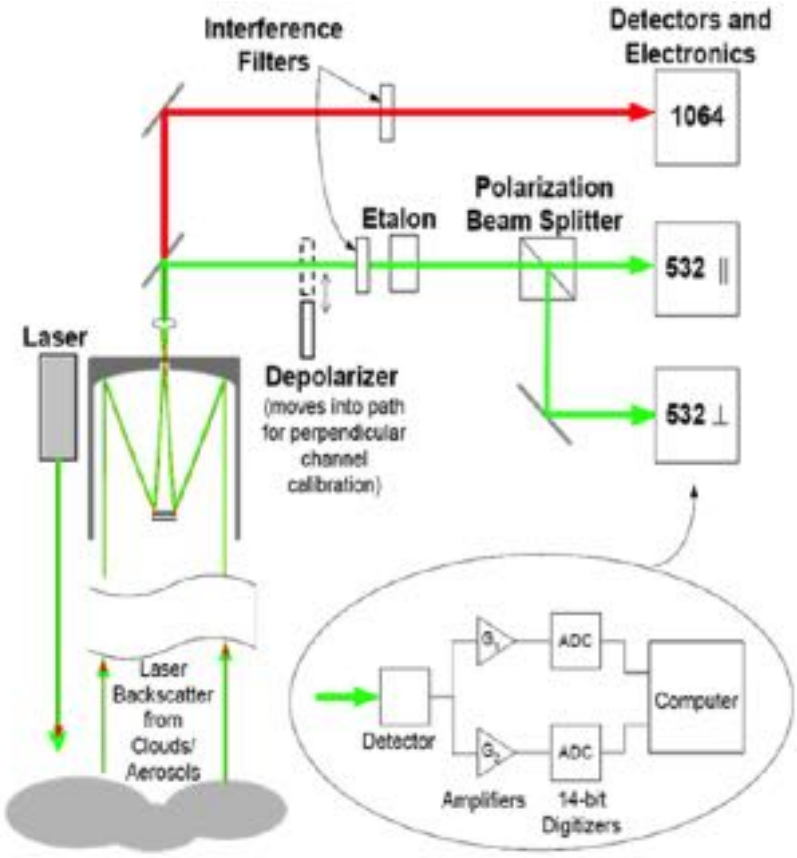

HOSTETLER, C. A.; LIU, Z.; REAGAN, J.; VAUGHAN, M. A.; WINKER, D. M.; OSBORN, M.; HUNT, W. H.; POWELL, K. A.; TREPTE, C. **CALIOP Algorithm Theoretical Basis Document - Calibration and Level 1 data products**. *Cloud-Aerosol Lidar Infrared Pathfinder Satellite Observations*, PC-SCI-201, p. 1–66, 2006.

CALIOP

Laser	Nd: YAG, 2x110 mJ
Comprimento de onda	532 nm, 1064 nm
Taxa de Repetição	20.25 Hz
Telescópio	1.0 m diâmetro
Polarização	532 ∥ e ⊥
FOV	130 μrad
Resolução Vertical	30 - 60 m
Resolução Horizontal	333 m

Câmera de ampla visão (WFC)

Comprimento de onda	645 nm
Largura de banda espectral	50 nm
FOV	125 m / 61 km

Radiômetro de Imagem (IIR)

Comprimento de onda	8.65, 10.6,12.05 μm
Resolução spectral	0.6-1.0 μm
FOV	1 km / 64 km

Como o CALIPSO mede nuvens e aerossóis na atmosfera?

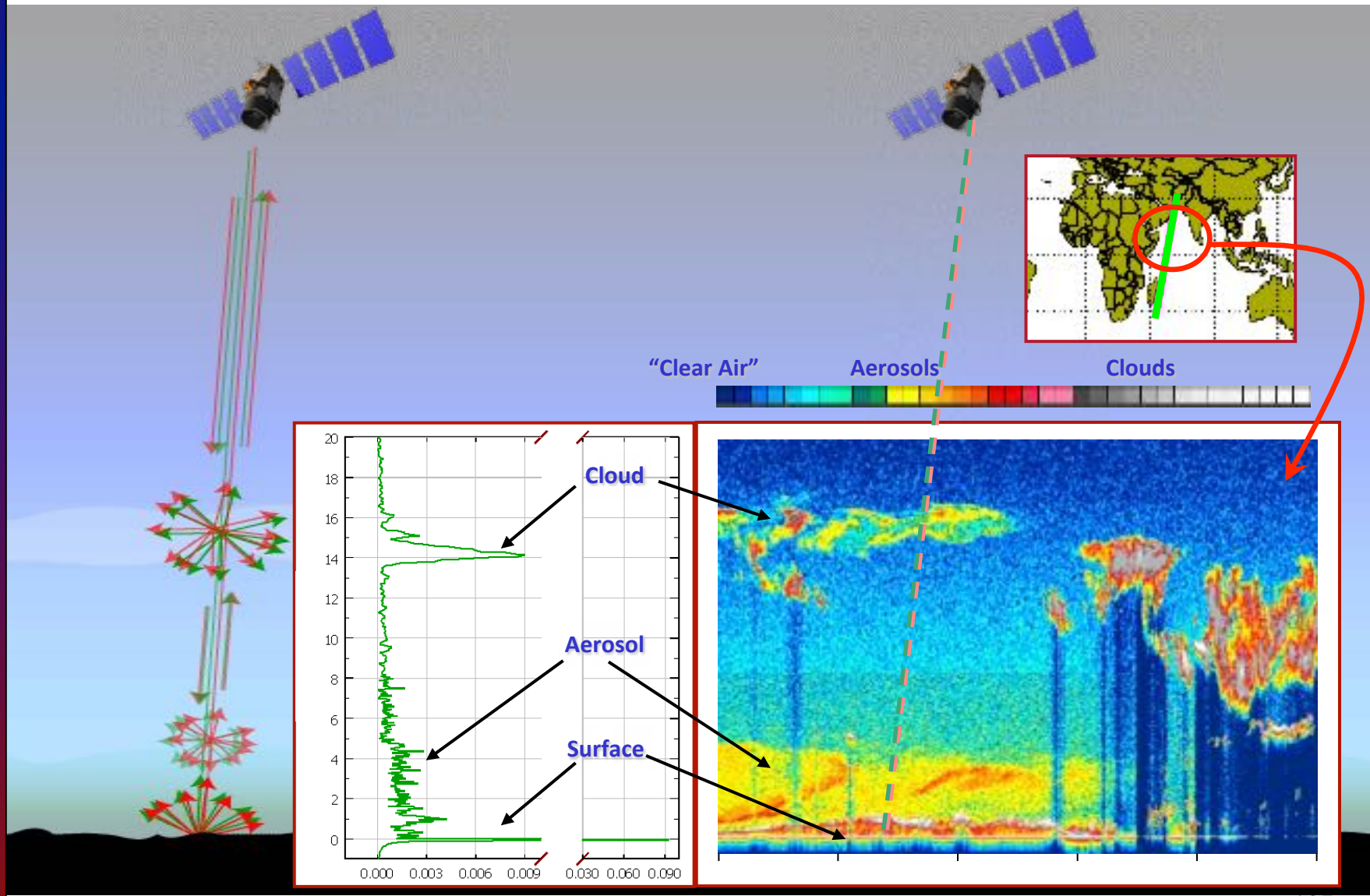

Produtos CALIPSO

Nível 1

- CALIOP profiles of attenuated backscatter (532, $532_{\perp}$, 1064 nm)
- IIR calibrated radiances (8.65, 10.6, 12.05 mm)
- WFC visible radiances (650 nm) (WFC)

Produtos CALIPSO

Nível 2

- **Cloud/Aerosol layer products**
  layer base and top heights, layer-integrated optical properties

- **Aerosol profile product**
  backscatter, extinction, & depolarization profiles; aerosol type & QA flags

- **Cloud profile product**
  backscatter, extinction, depolarization, & ice water content profiles; cloud phase & QA flags

- **Vertical mask**
  cloud/aerosol locations, cloud phase, aerosol type & QA flags

Produtos CALIPSO

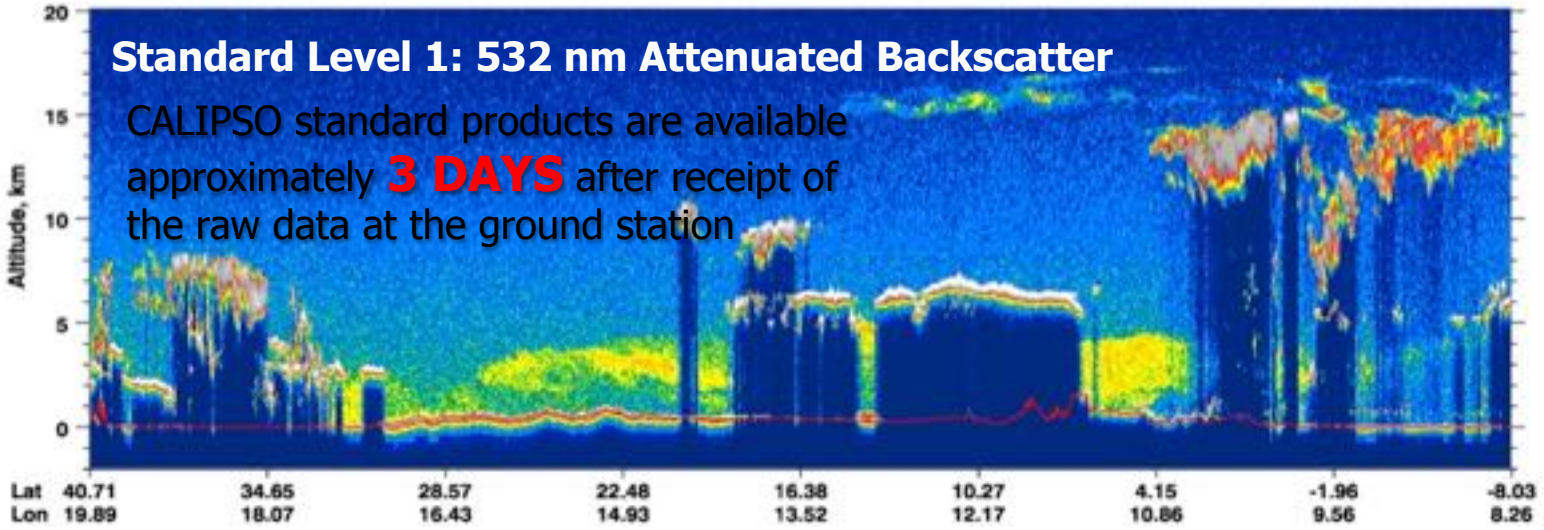

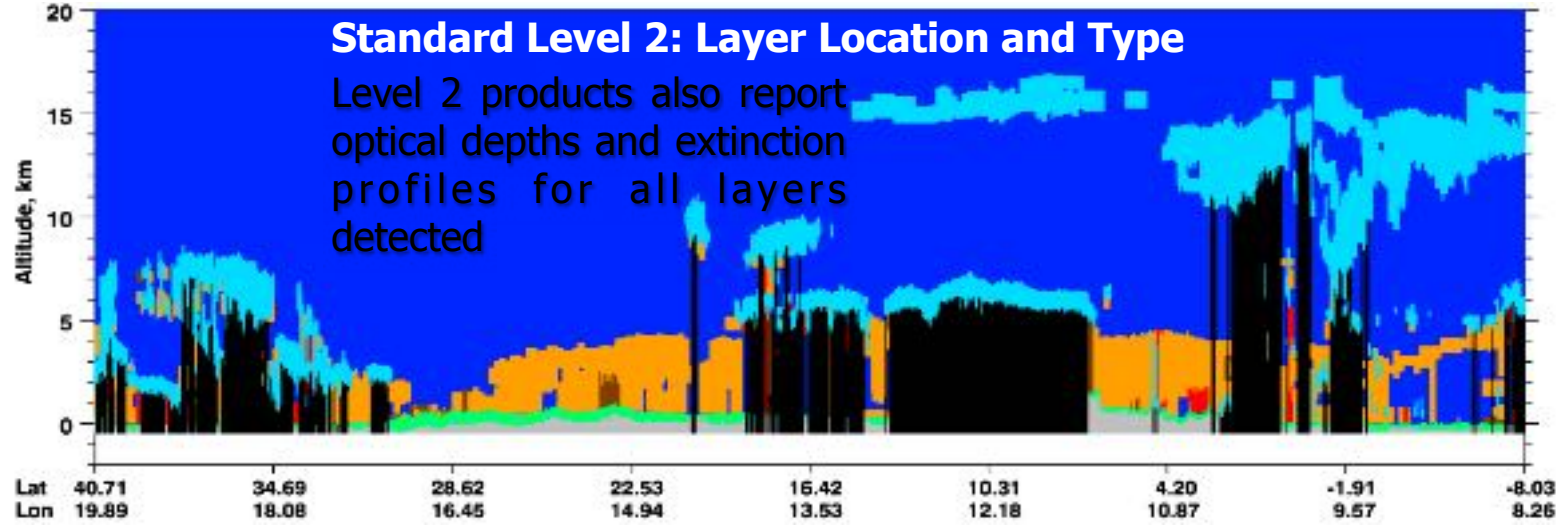

Produtos CALIPSO

Standard Level 1: 532 nm Attenuated Backscatter

14 October 2010, ~00:13:30 UTC

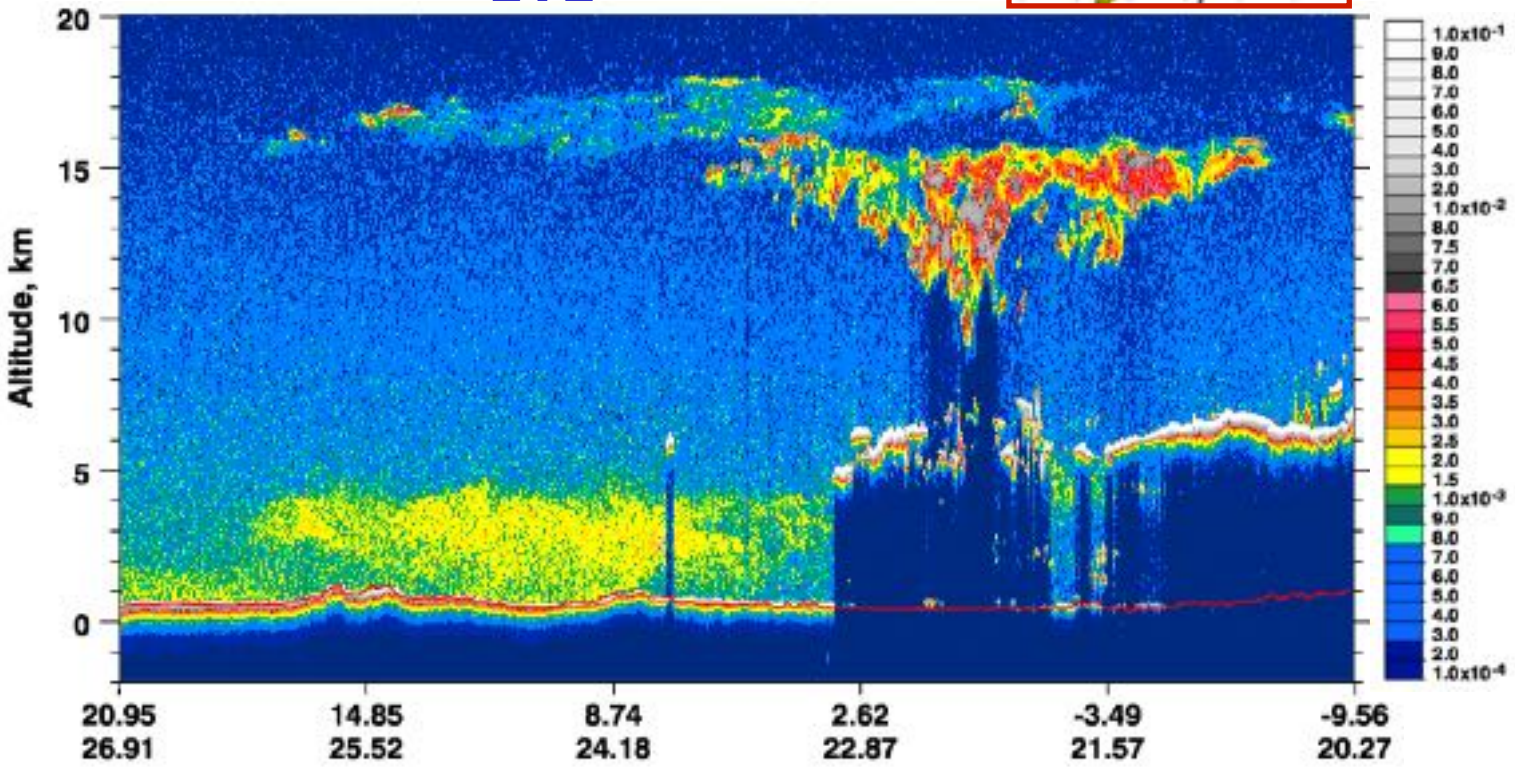

Calibrated, Geolocated, Altitude-Registered Raw Data

Produtos CALIPSO

14 October 2010, ~00:13:30 UTC

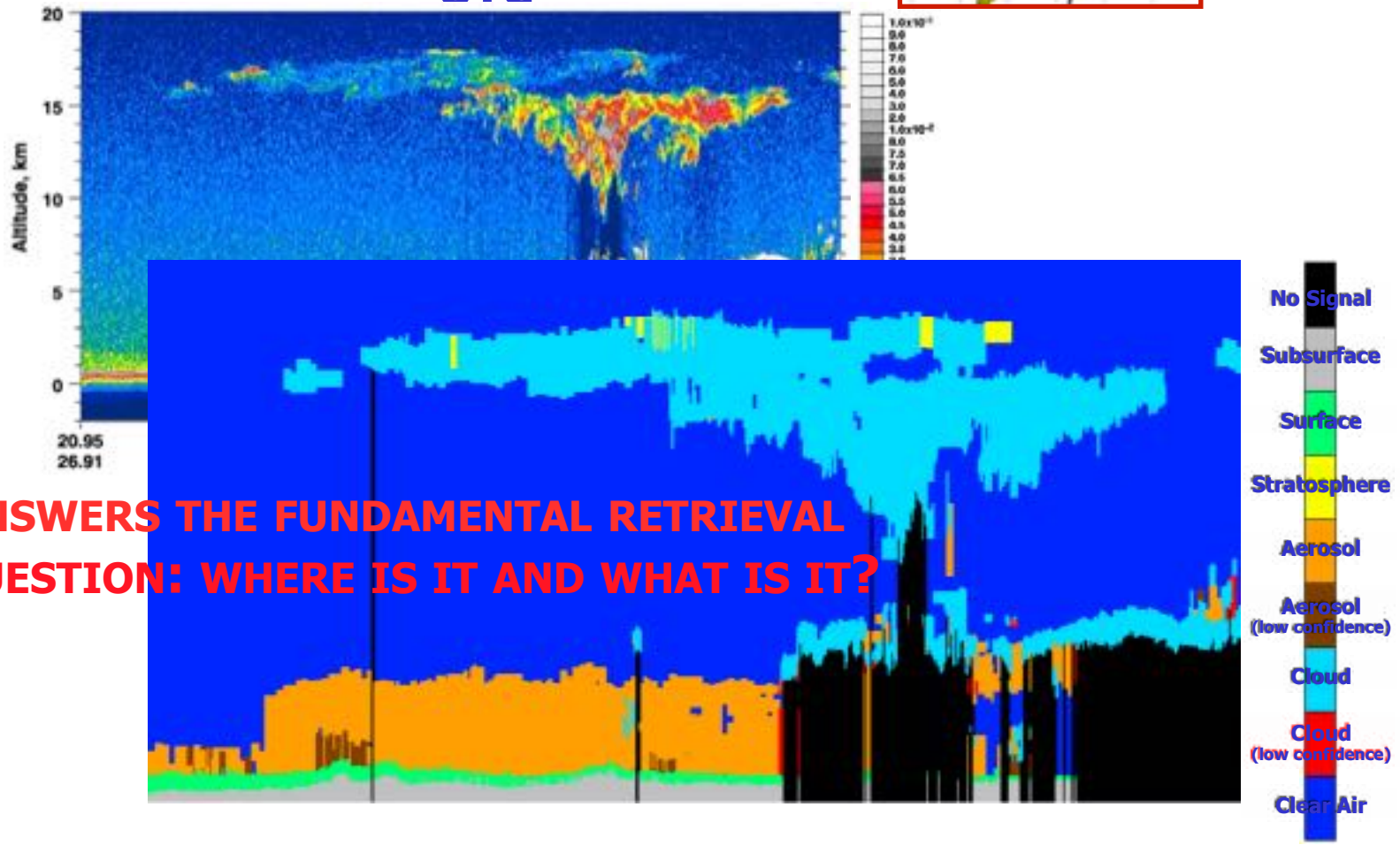

ANSWERS THE FUNDAMENTAL RETRIEVAL QUESTION: WHERE IS IT AND WHAT IS IT?

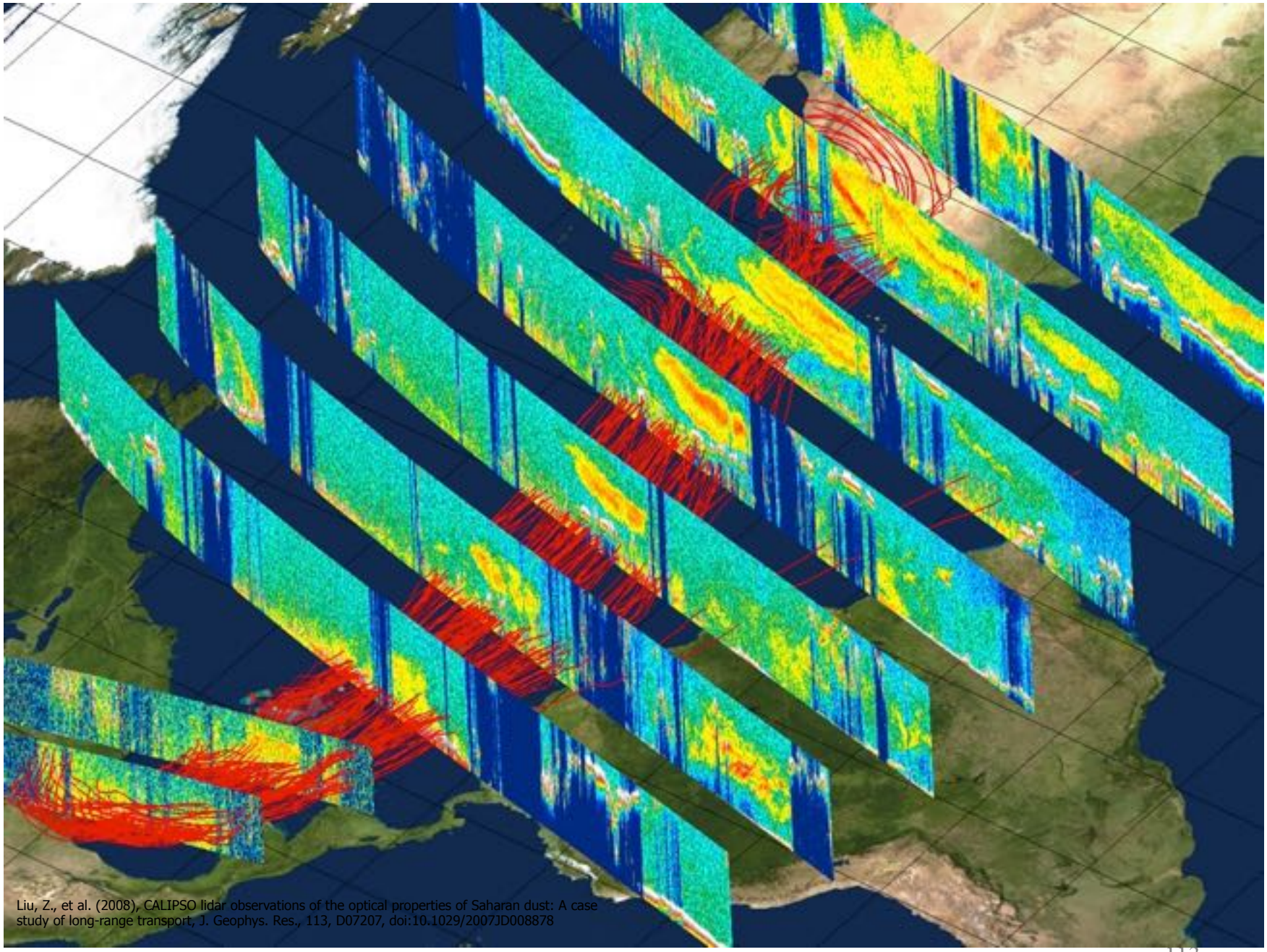

Liu, Z., et al. (2008), CALIPSO lidar observations of the optical properties of Saharan dust: A case study of long-range transport, J. Geophys. Res., 113, D07207, doi:10.1029/2007JD008878

Transporte de aerossóis

Mais de 101 mil focos de queimadas entre Agosto e Setembro de 2010*

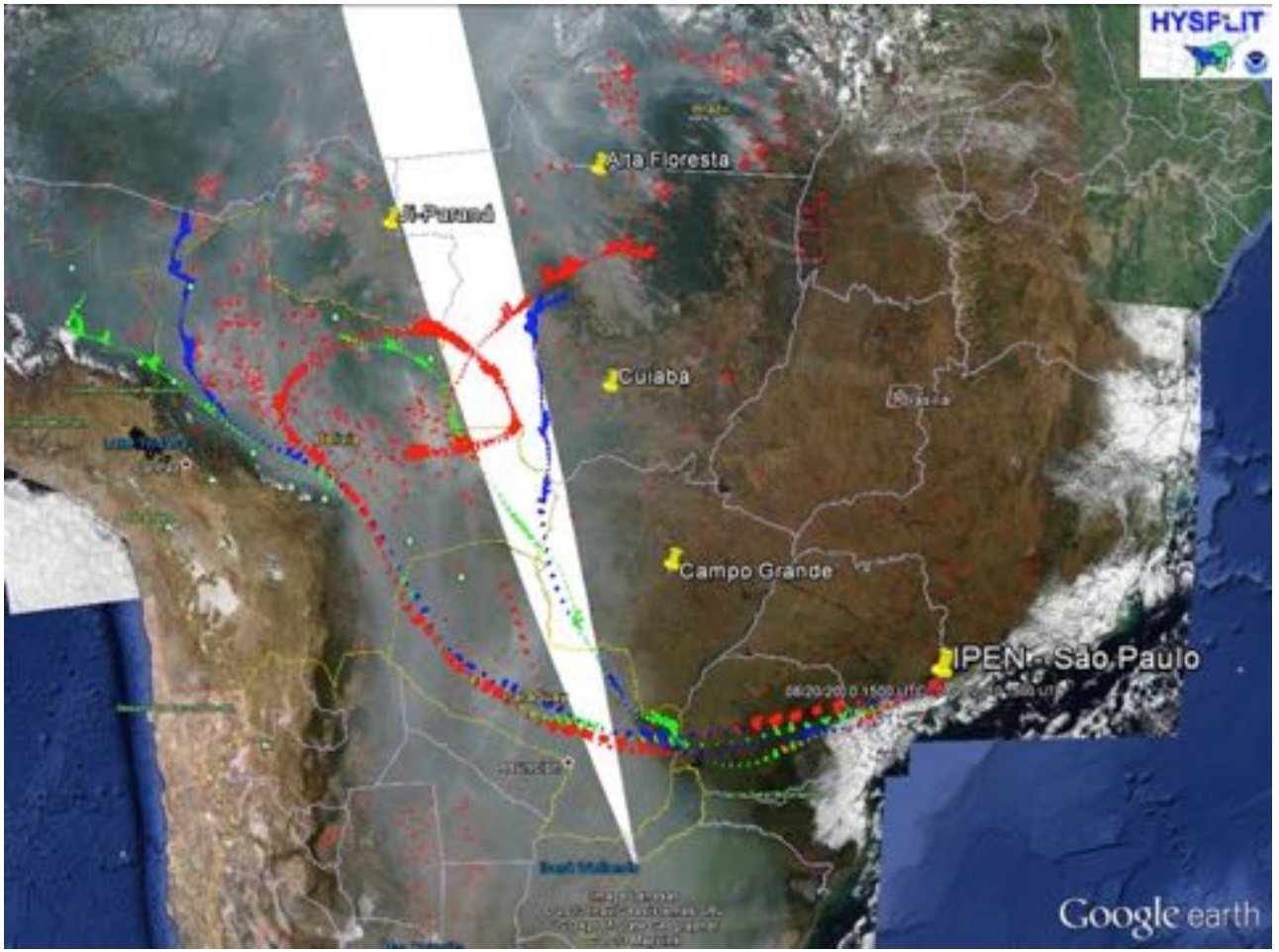

Transporte de aerossóis

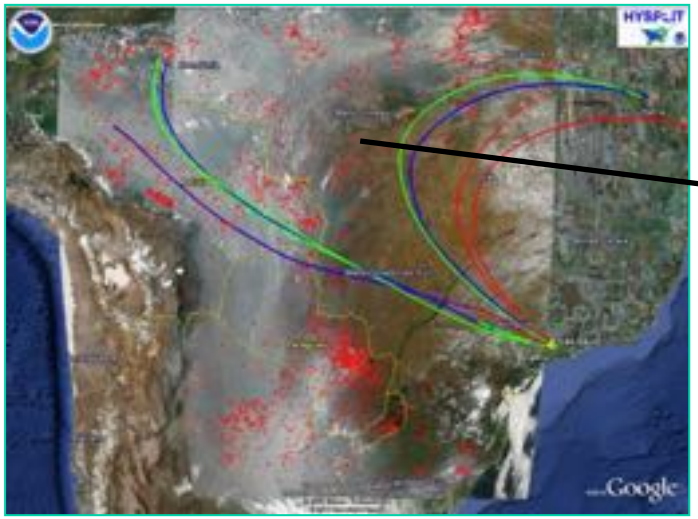

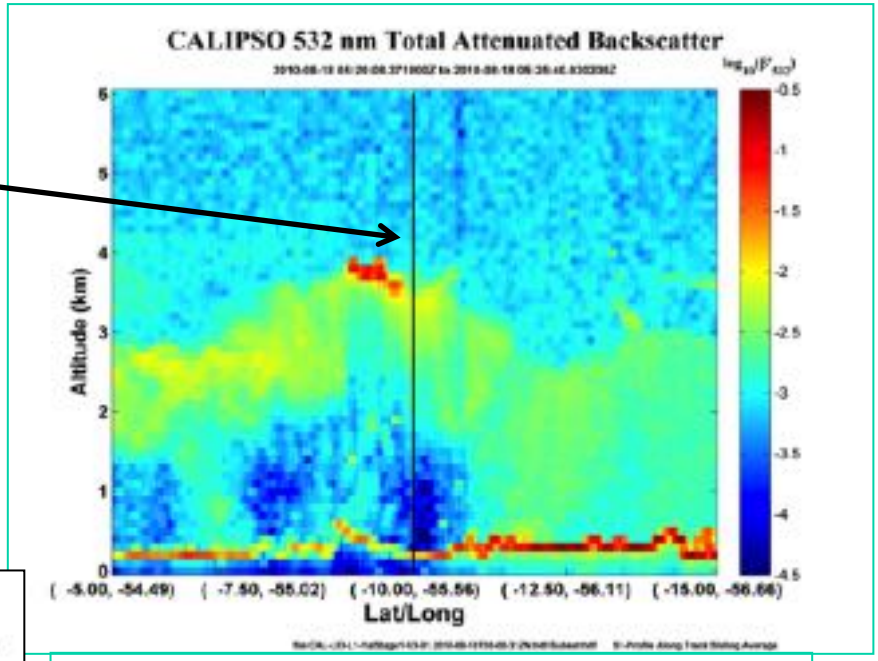

Sinal de retroespalhamento medido pelo Satélite CALIPSO

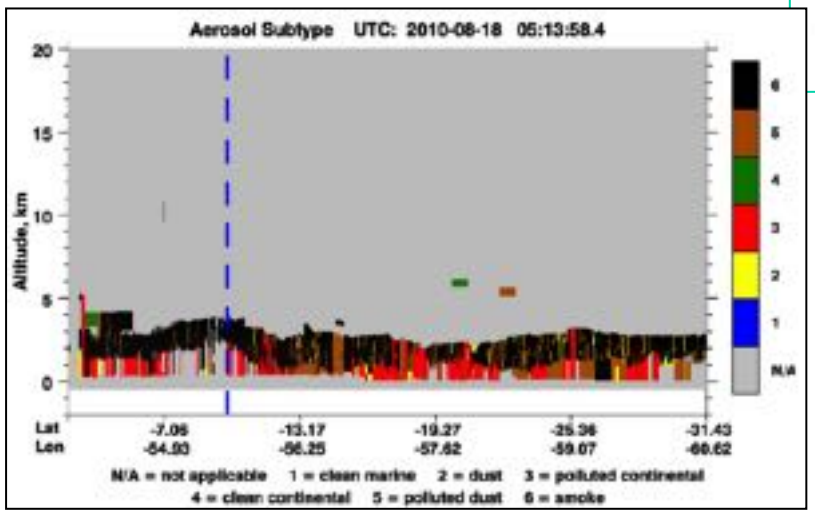

Razão Lidar = 70 sr

Transporte de aerossóis

Sinal de retroespalhamento lidar corrigido com a distância para o dia 20/08/2010

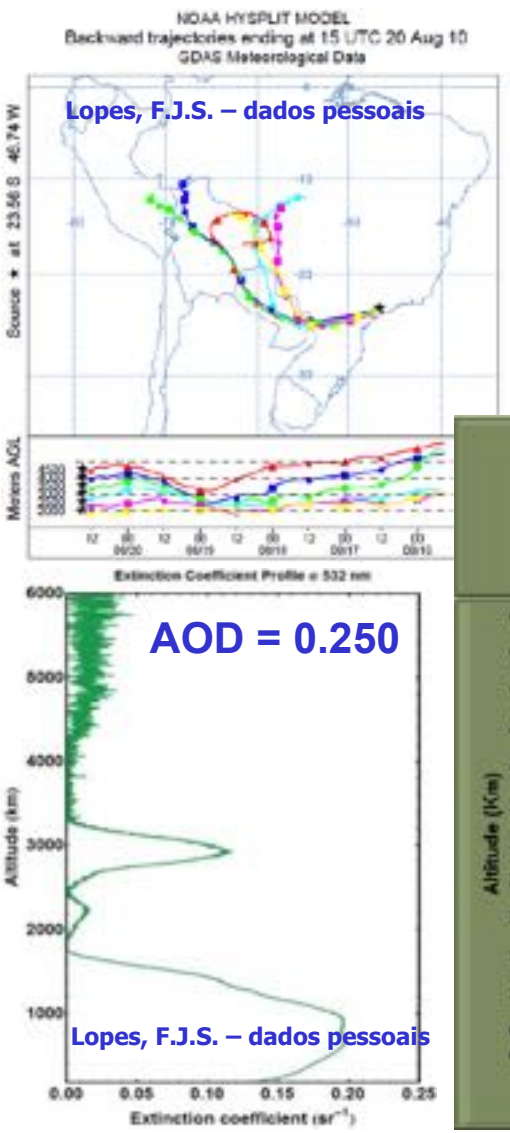

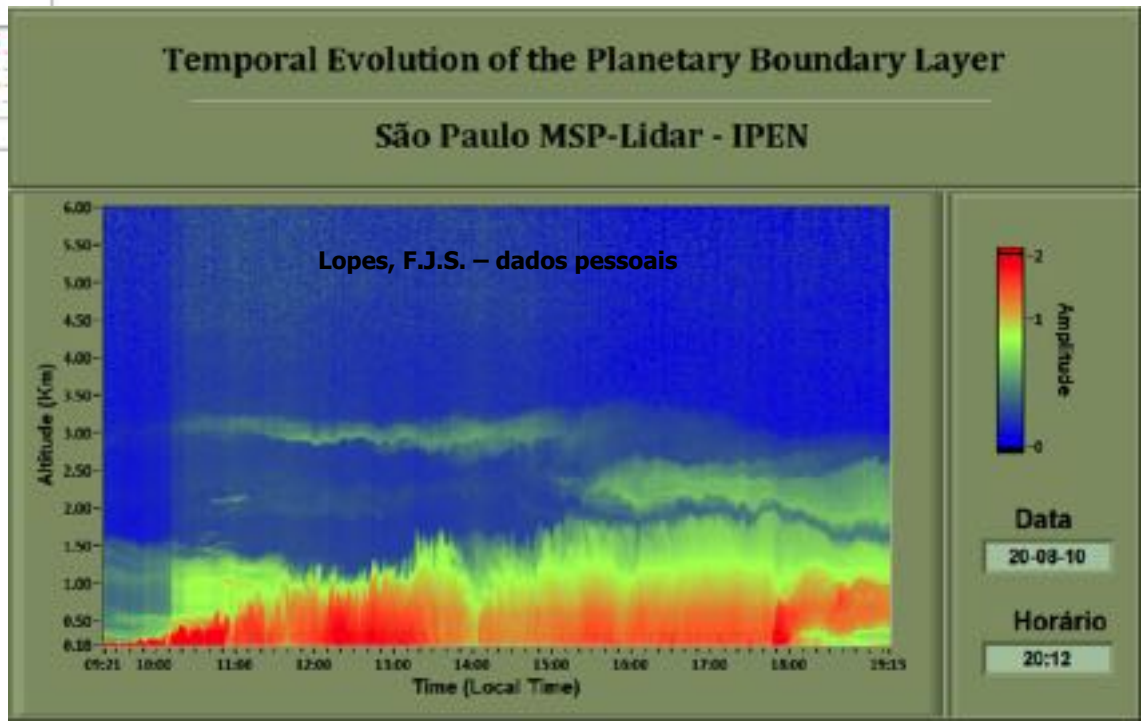

Transporte de aerossóis

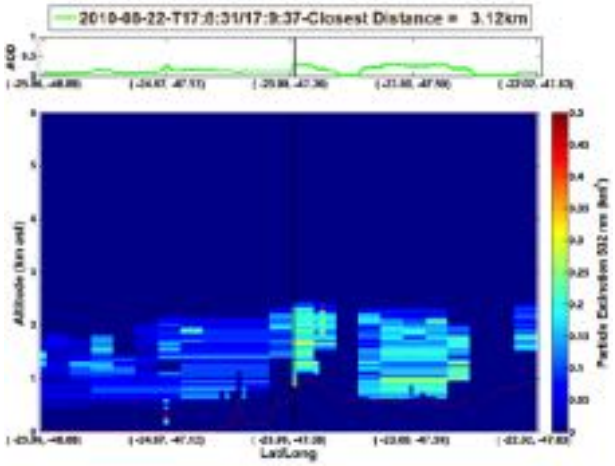

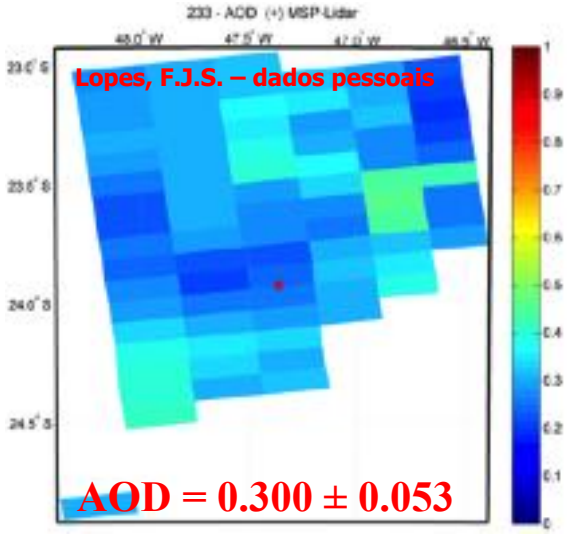

AOD AQUA-MODIS - 22 de Agosto de 2010 próximo a São Paulo – MT

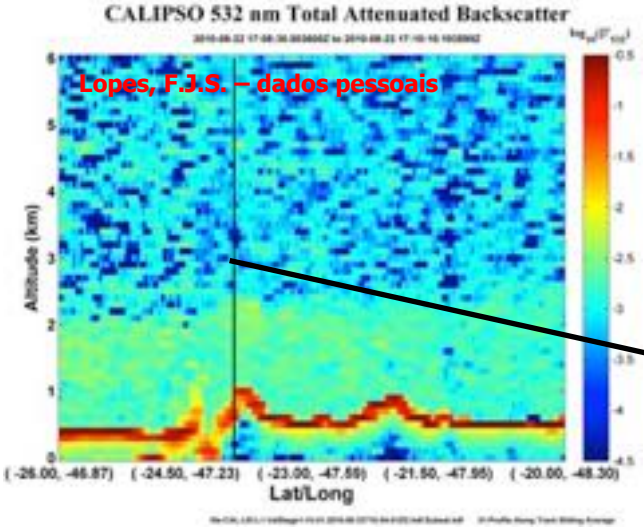

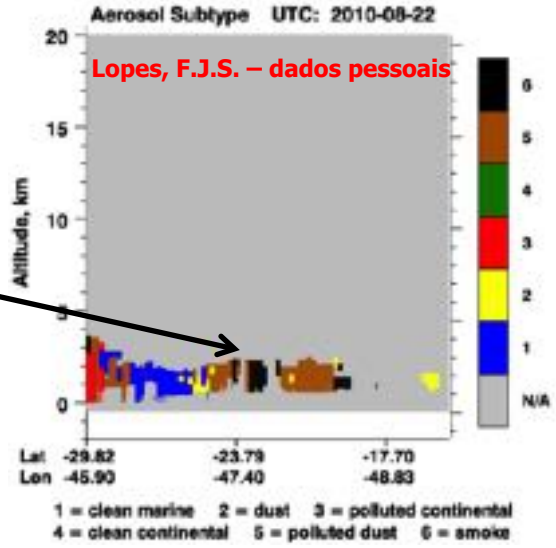

Transporte de aerossóis

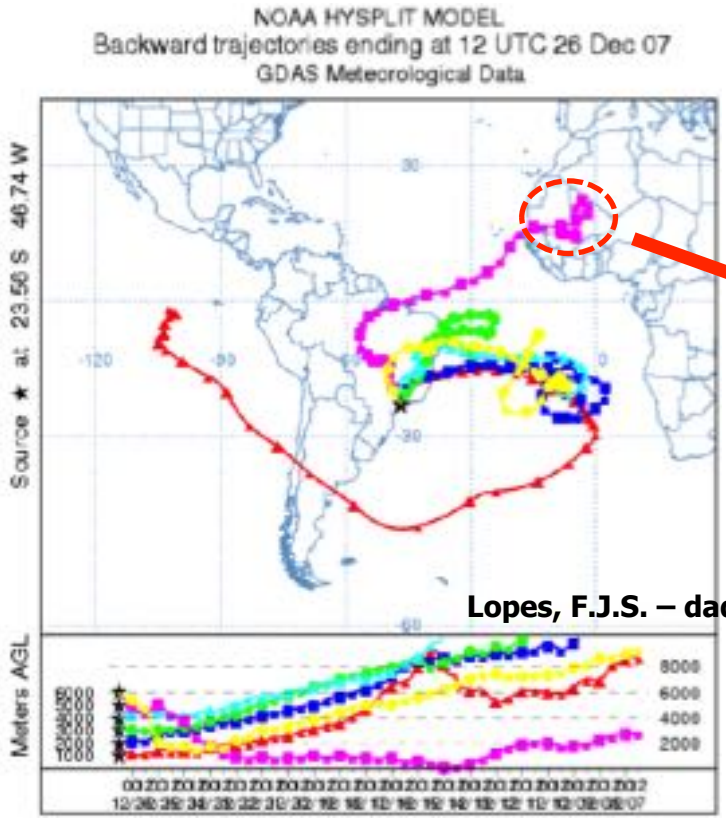

06/12/2007 ~13:45 UTC

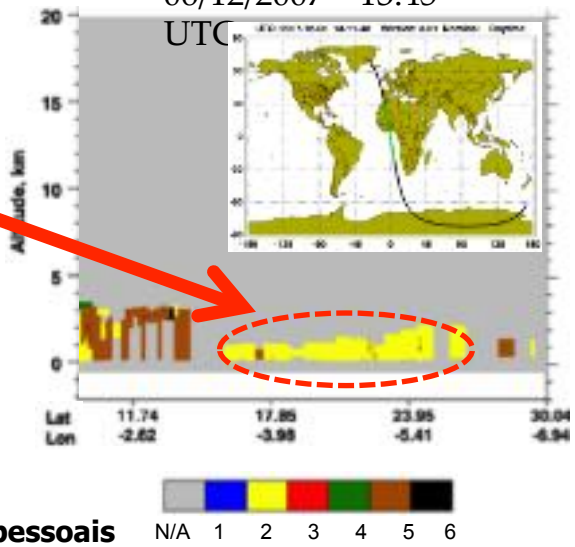

Lopes, F.J.S. – dados pessoais

N/A = not applicable
1 = clean marine
2 = dust
3 = polluted continental
4 = clean continental
5 = polluted dust
6 = smoke

Transporte de aerossóis

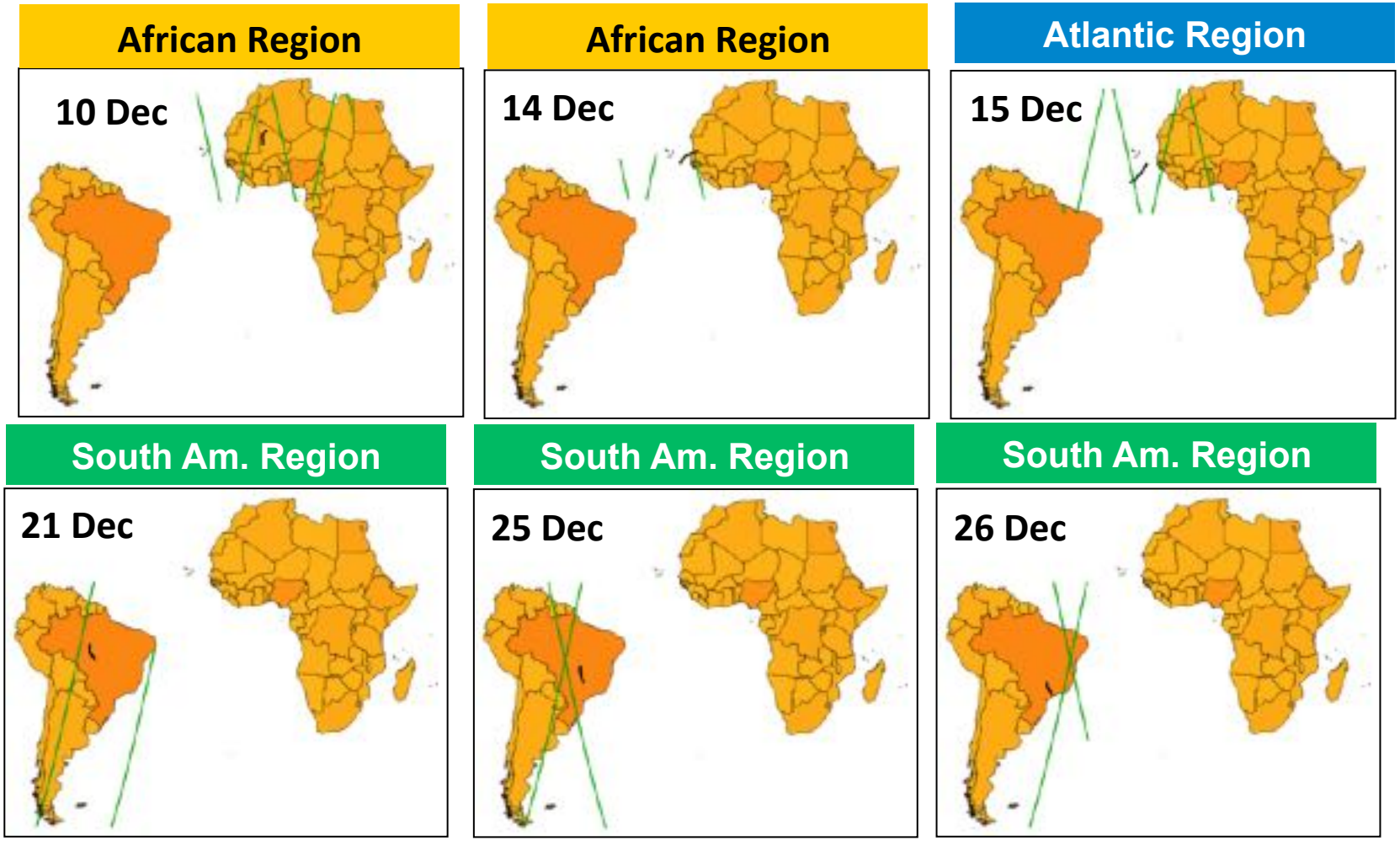

Transporte de aerossóis

South Am. Region

21 Dec

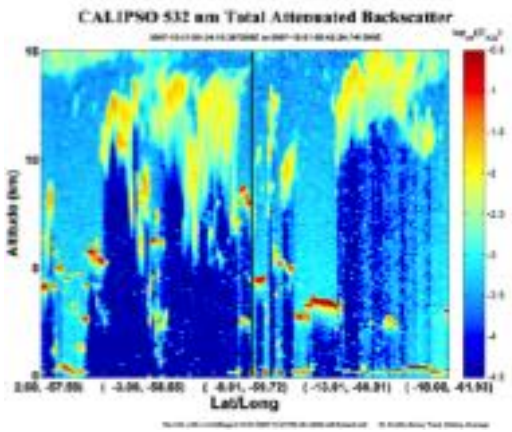

South Am. Region

25 Dec

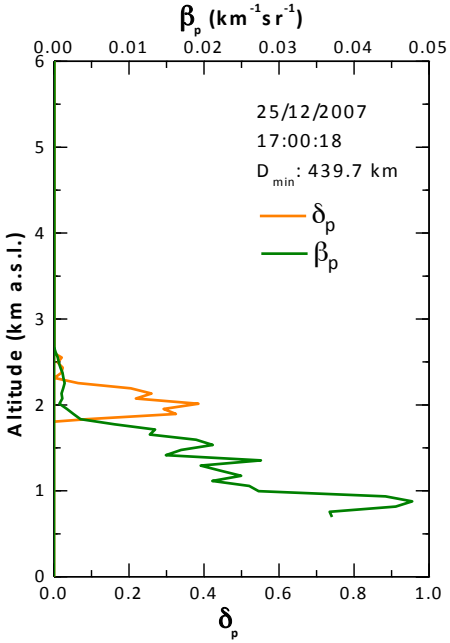

South Am. Region

26 Dec

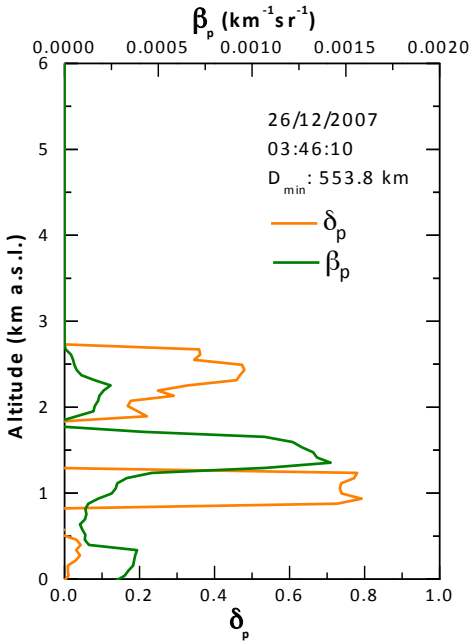

Transporte de aerossóis

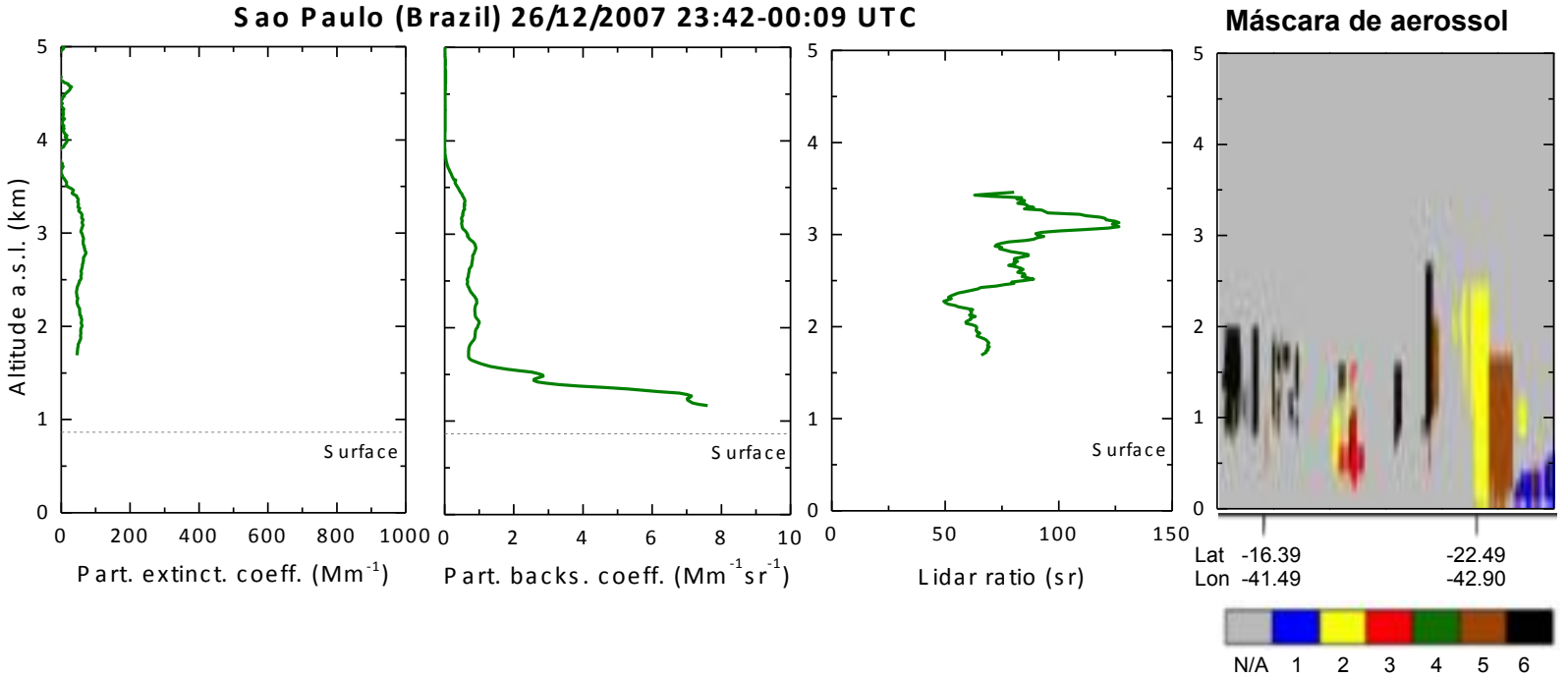

Dados do CALIPSO próximo de São Paulo detectou uma mistura de Poeira sahariana e poeira+poluição.

N/A = not applicable
1 = clean marine
2 = dust
3 = polluted continental
4 = clean continental
5 = polluted dust
6 = smoke

Validação

Necessidade de realização de processos de validação utilizando outros instrumentos

Desde 2007 diversos trabalhos de validação foram realizados

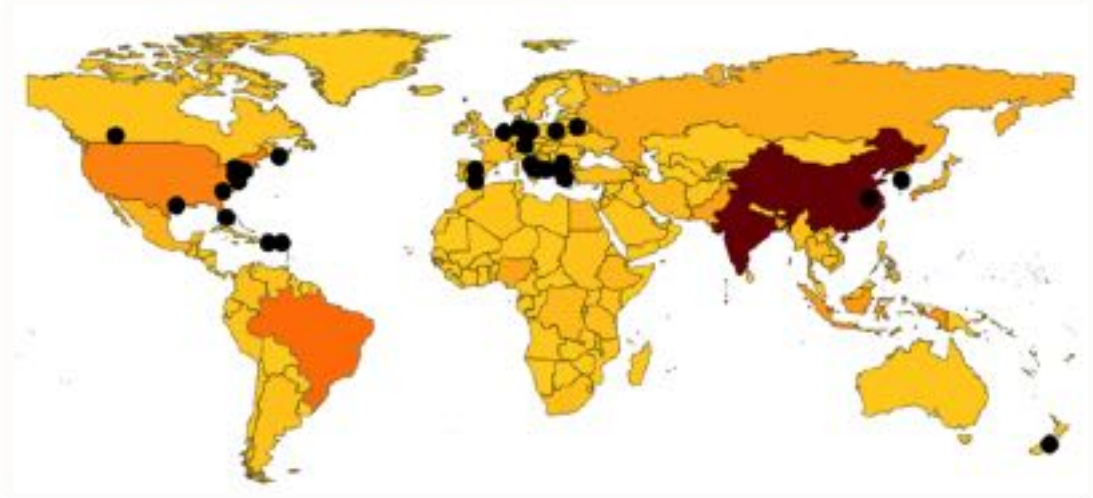

HUNT, W. H. et al. **CALIPSO Lidar Description and Performance Assessment.** ***Journal*** *of Atmospheric and Oceanic Technology, v. 26, p. 1214–1228, 2009.*

Anomalia do Atlântico Sul – SAA

Cinturão de radiação de Van Allen com a maior aproximação da superfície

Grande intensidade de radiação aumenta o ruído nos detectores do CALIOP

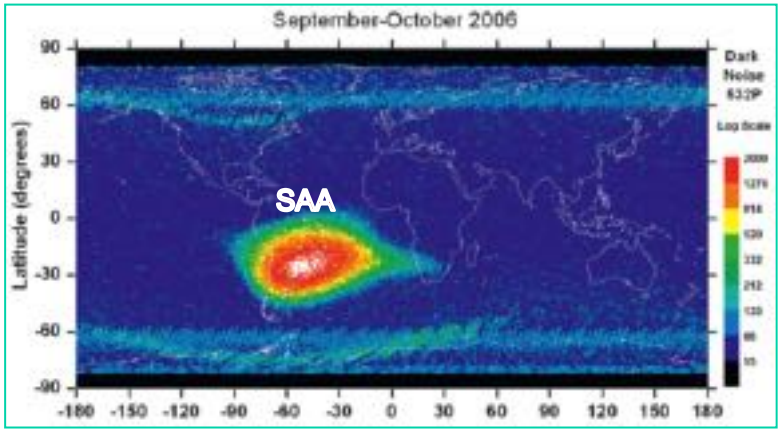

Validação

Necessidade de realização de processos de validação utilizando outros instrumentos

Desde 2007 diversos trabalhos de validação foram realizados

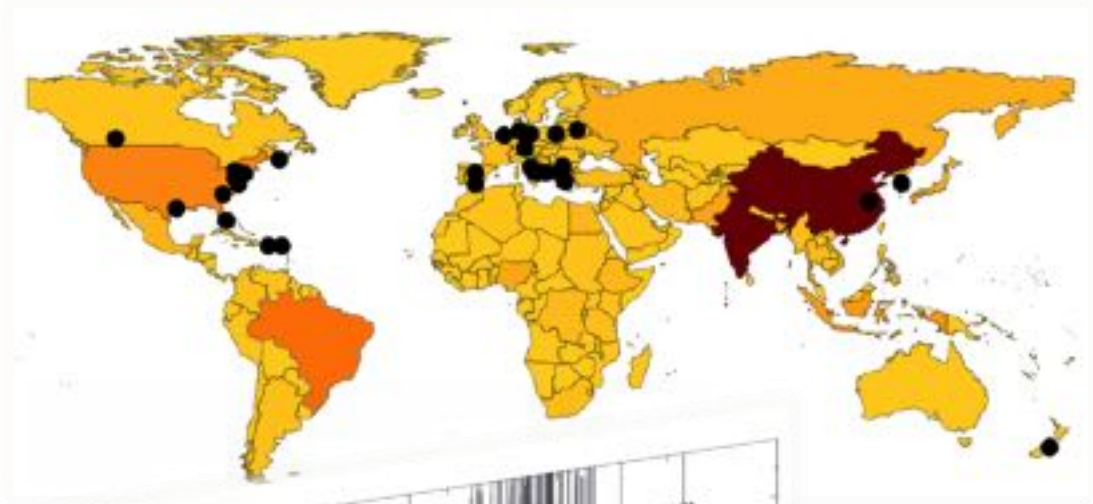

HUNT, W. H. et al. **CALIPSO Lidar Description and Performance Assessment.** ***Journal*** *of Atmospheric and Oceanic Technology, v. 26, p. 1214–1228, 2009.*

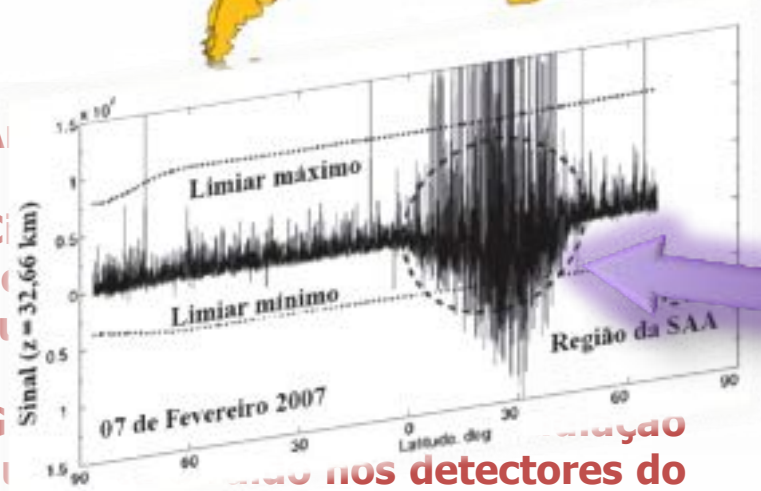

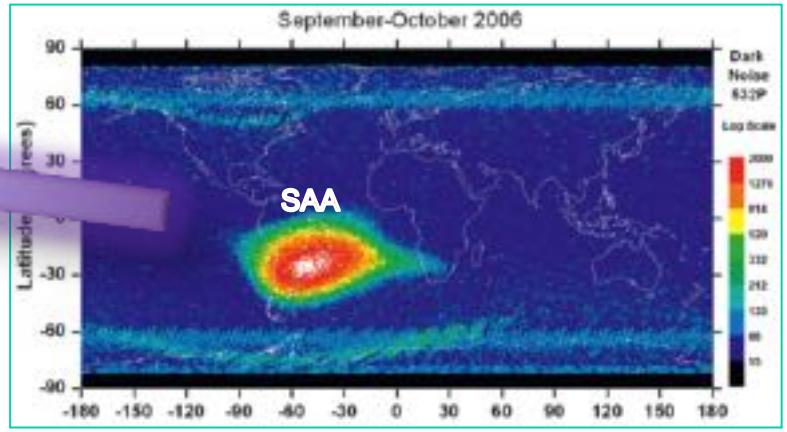

A

C

c

s

G

a

nos detectores do CALIOP

Validação

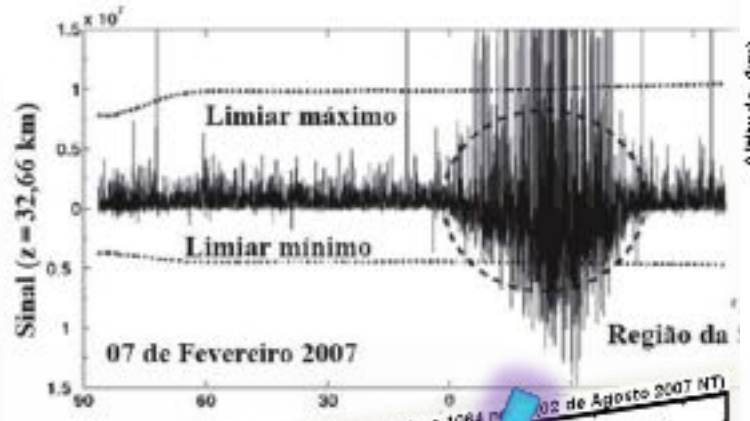
Limiar máximo
Limiar mínimo
Sinal (z = 32,66 km)
07 de Fevereiro 2007

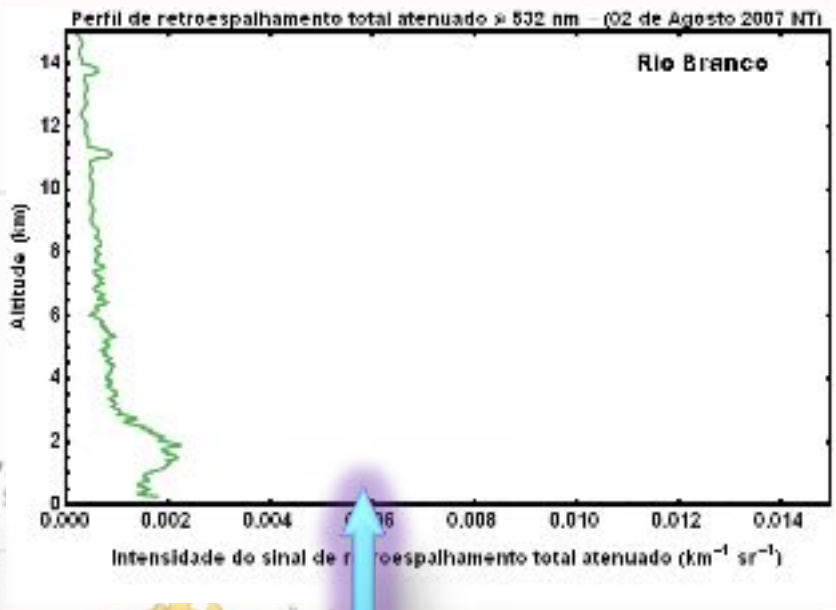
Perfil de retroespalhamento total atenuado @ 532 nm (02 de Agosto 2007 NT)
Rio Branco
Altitude (km)
Intensidade do sinal de retroespalhamento total atenuado (km⁻¹ sr⁻¹)

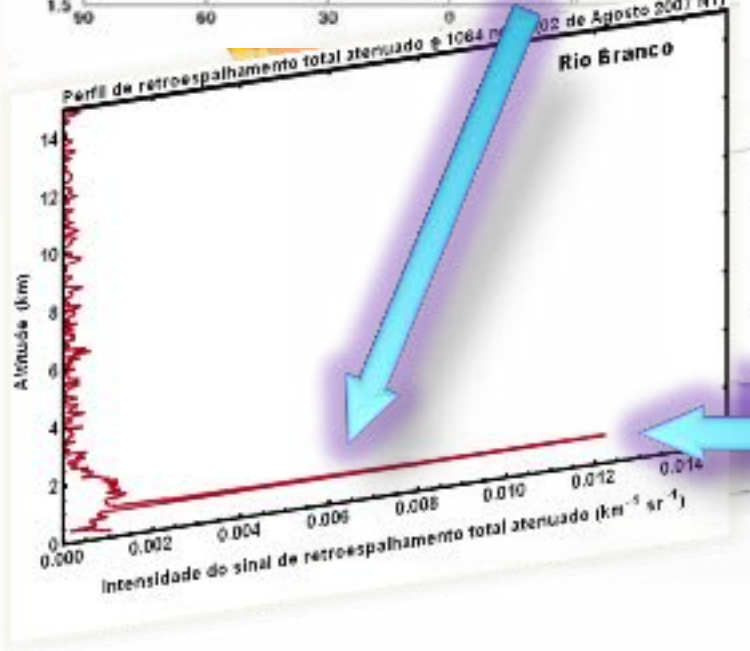
Rio Branco
Altitude (km)
Intensidade do sinal de retroespalhamento total atenuado (km⁻¹ sr⁻¹)

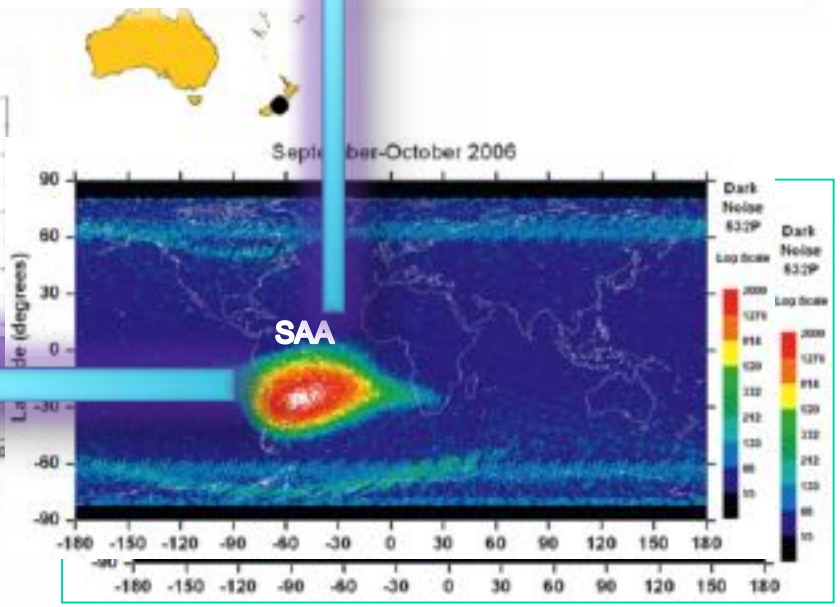
SAA
Dark Noise 532P
Dark Noise 532P

Validação

Locais de referências: Possuem sistema AERONET e/ou Lidar

RB, AF, CB e CG

Tipos de aerossóis característicos em determinadas épocas do ano

Aerossóis de fontes de queimadas

Quando o CALIPSO passou por essas localidades entre 2006 e 2009?

Validação

$$RL_{A/C} = \frac{1 - \exp(-2\,\tau_{aeronet})}{2\,\gamma_{caliop}}$$

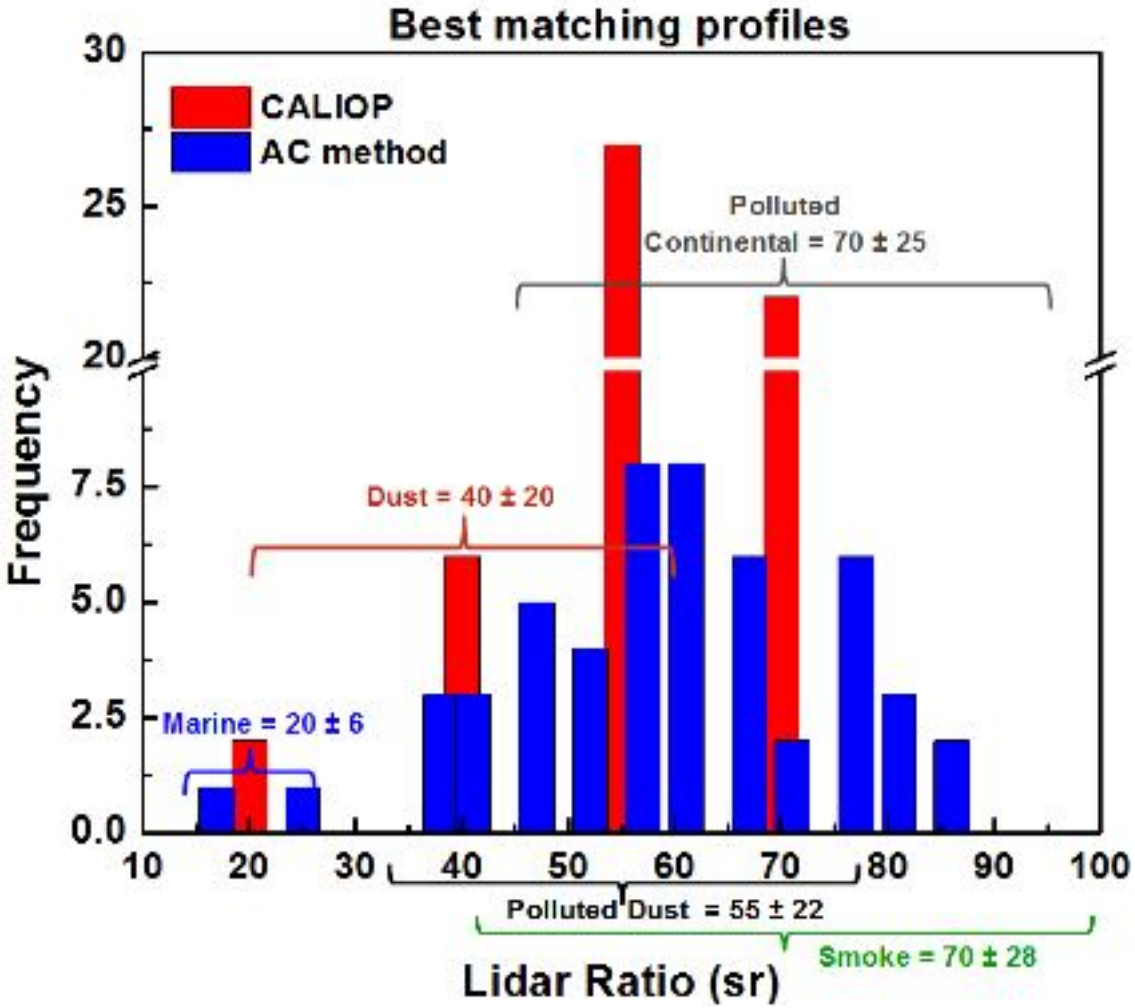

https://bit.ly/2l3n2XD

LALINET INTRODUCTION

Volume 98 No. 6
June 2017
ISSN: 0003-0007; eISSN: 1520-0477

LALINET

The First Latin American–Born Regional Atmospheric Observational Network

Juan Carlos Antuña-Marrero, Eduardo Landulfo, René Estevan, Boris Barja, Alan Robock, Elián Wolfram, Pablo Ristori, Barclay Clemesha, Francesco Zaratti, Ricardo Forno, Errico Armandillo, Álvaro E. Bastidas, Ángel M. de Frutos Baraja, David N. Whiteman, Eduardo Quel, Henrique M. J. Barbosa, Fabio Lopes, Elena Montilla-Rosero, and Juan L. Guerrero-Rascado

A Latin American community of scientists engaged in atmospheric research using lidar has created a regional lidar network.

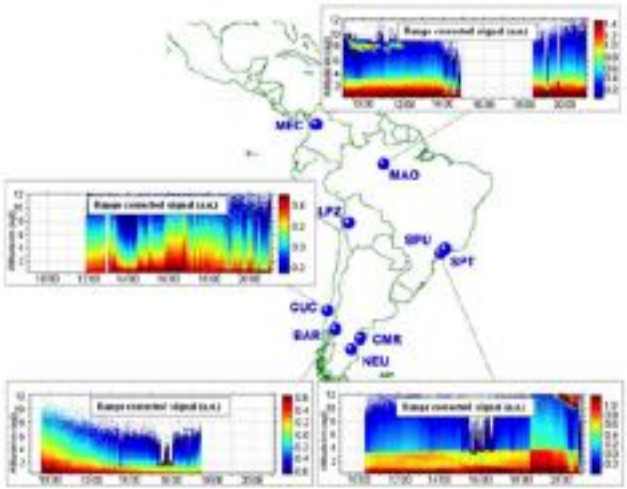

ELSEVIER
Journal of Atmospheric and Solar-Terrestrial Physics
Volumes 138–139, February 2016, Pages 112-120

Latin American Lidar Network (LALINET) for aerosol research: Diagnosis on network instrumentation

Juan Luis Guerrero-Rascado [a, b, c, *], Eduardo Landulfo [a], Juan Carlos Antuña [c], Henrique de

https://bit.ly/2l3n2XD

LALINET STATIONS

AREA GT 18 Mkm²

ST.	ID	LAT(S) LON(W)	Channels (nm)
Buenos Aires	*AEP*	34.56°S 58.42°W	*1064, 532P & 355P*
Buenos Aires	*VMA*	34.56°S 58.51°W	*1064, 607, 532P, 387 & 355P*
Neuquen	*NQN*	38.95°S 68.13°W	*1064, 532P & 355P*
Bariloche	*BRC*	41.15°S 71.16°W	*1064, 607, 532, 387 & 355*
Commodoro	*CDR*	45.79°S 67.46°W	*1064, 532 & 355*
Gallegos	*RGL*	51.61°S 69.31°W	*1064, 532P & 355P*
Punta Arenas	*PAR**	53.13°S 70.88°W	*1064, 607, 532P, 408, 387 & 355P*
S. Paulo	*SPU*	23°13' 46°28'	*1064, 607, 532, 408, 387 & 355*
S. Paulo	*SPT*	*VAR*	*607, 532*
Manaus	*MAO*	02.60°S 60.21°W	*408, 387, 355*
Natal	*NAT*	05.82°S 35.20°W	*1064, 532P & 355P*
*Temuco**	*TMU**	38.74°S 72.62°W	*1064, 532P & 355P*
Medellin	*MED*	06.26°N 75.58°W	*532 & 355*
La Paz	*LPZ*	16.54°S 68.07°W	*1064, 532P & 355P*

Eduardo Landulfo

https://bit.ly/2l3n2XD

NETWORK SCIENTIFIC DRIVES

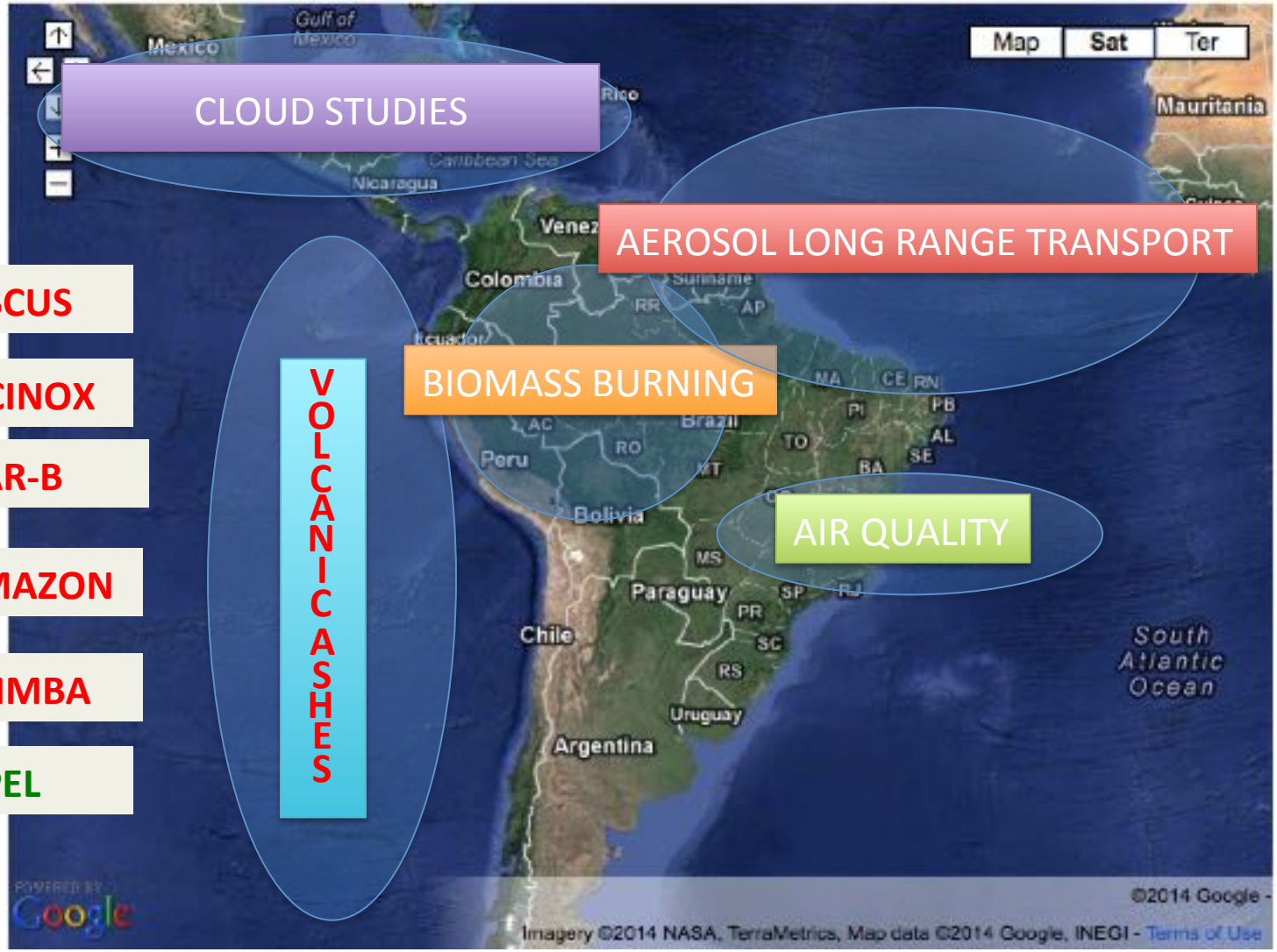

https://bit.ly/2l3n2XD

VOLCANIC ASHES & PLUMES

- 22nd – 23rd of April, 2015 – Calbuco volcano began eruption

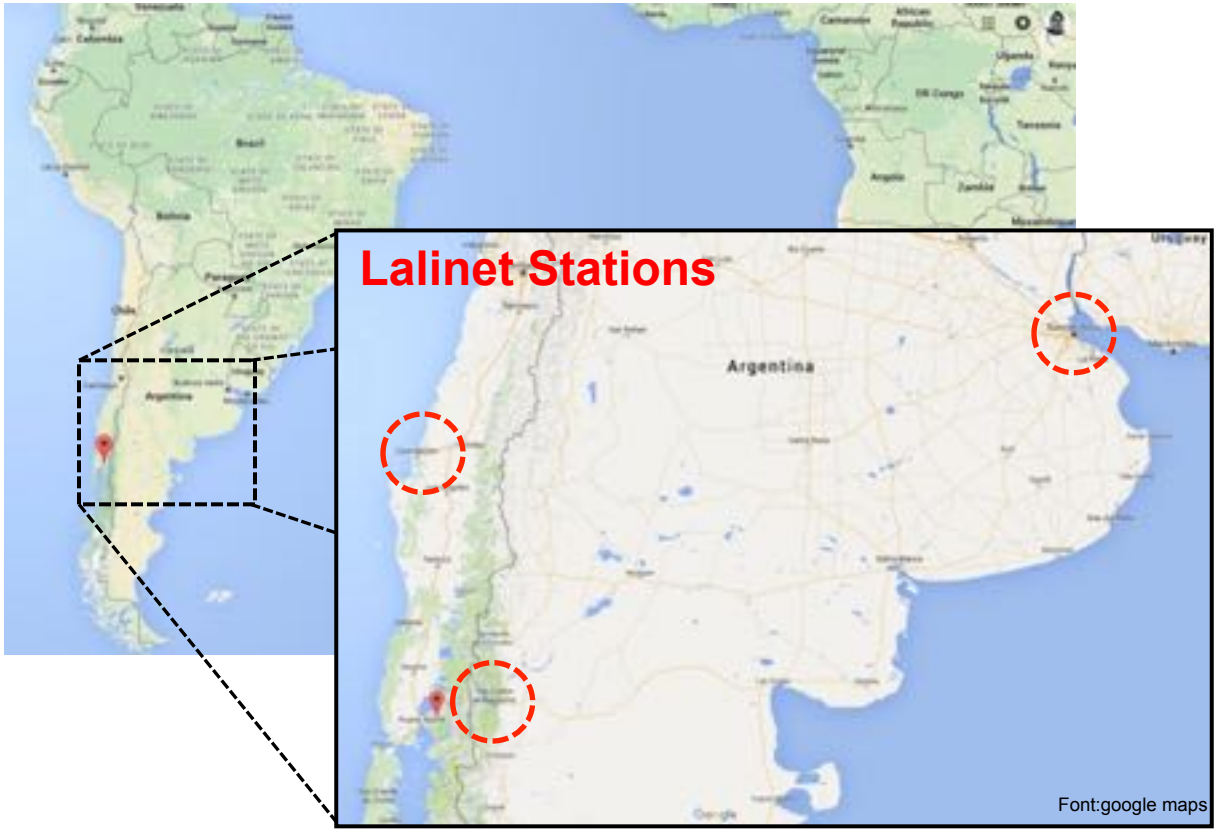

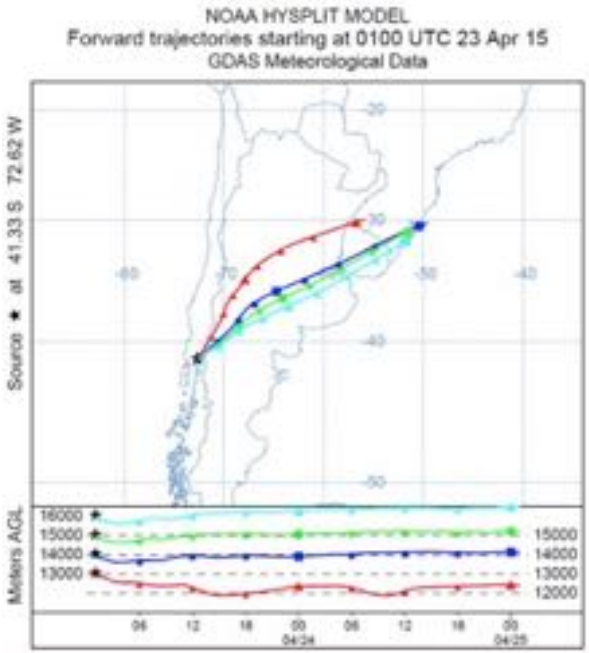

- First eruption since 1972
- Ash cloud achieved above 15 km of altitude

https://bit.ly/2l3n2XD

VOLCANIC ASHES & PLUMES

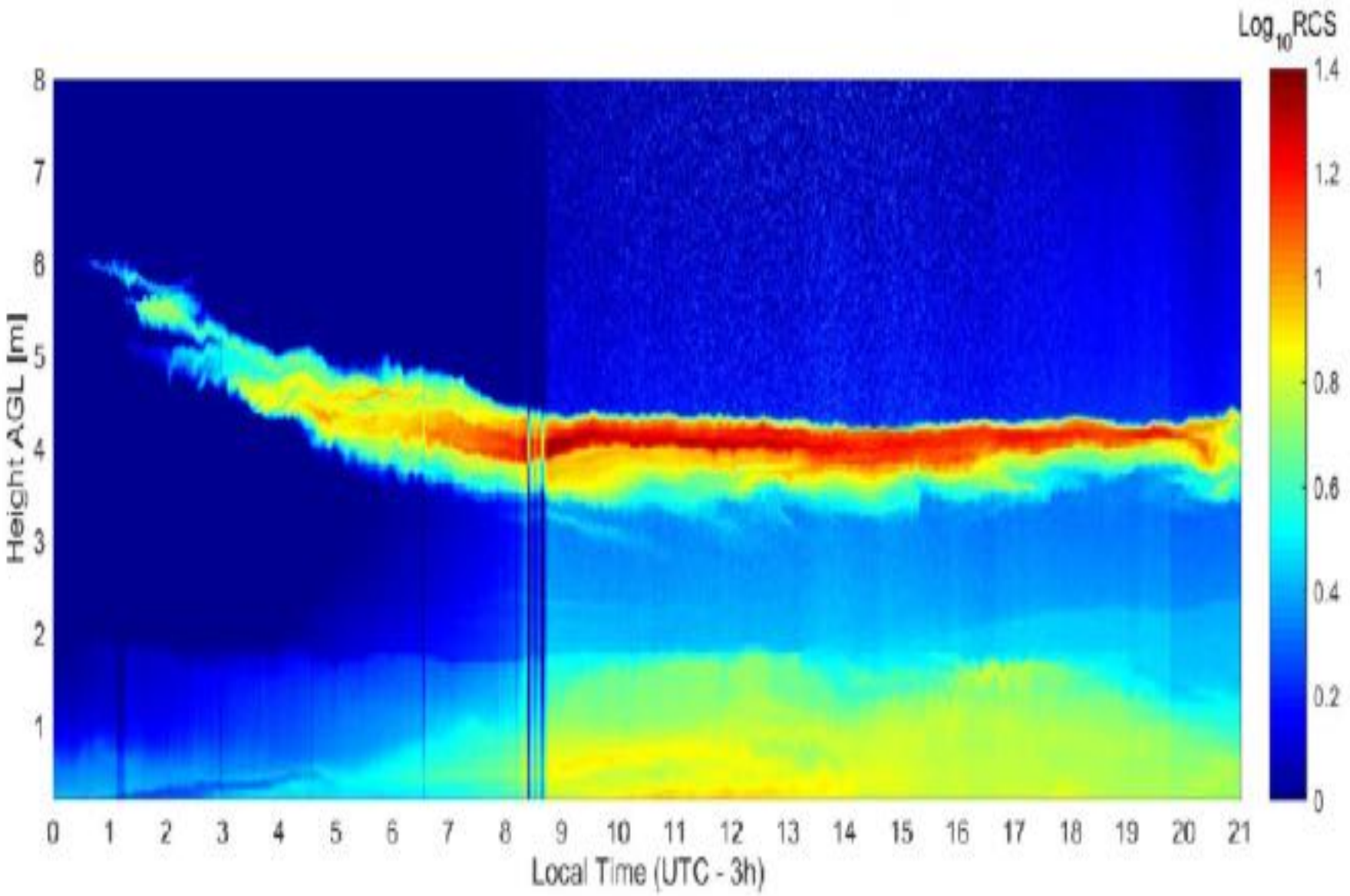

https://bit.ly/2l3n2XD

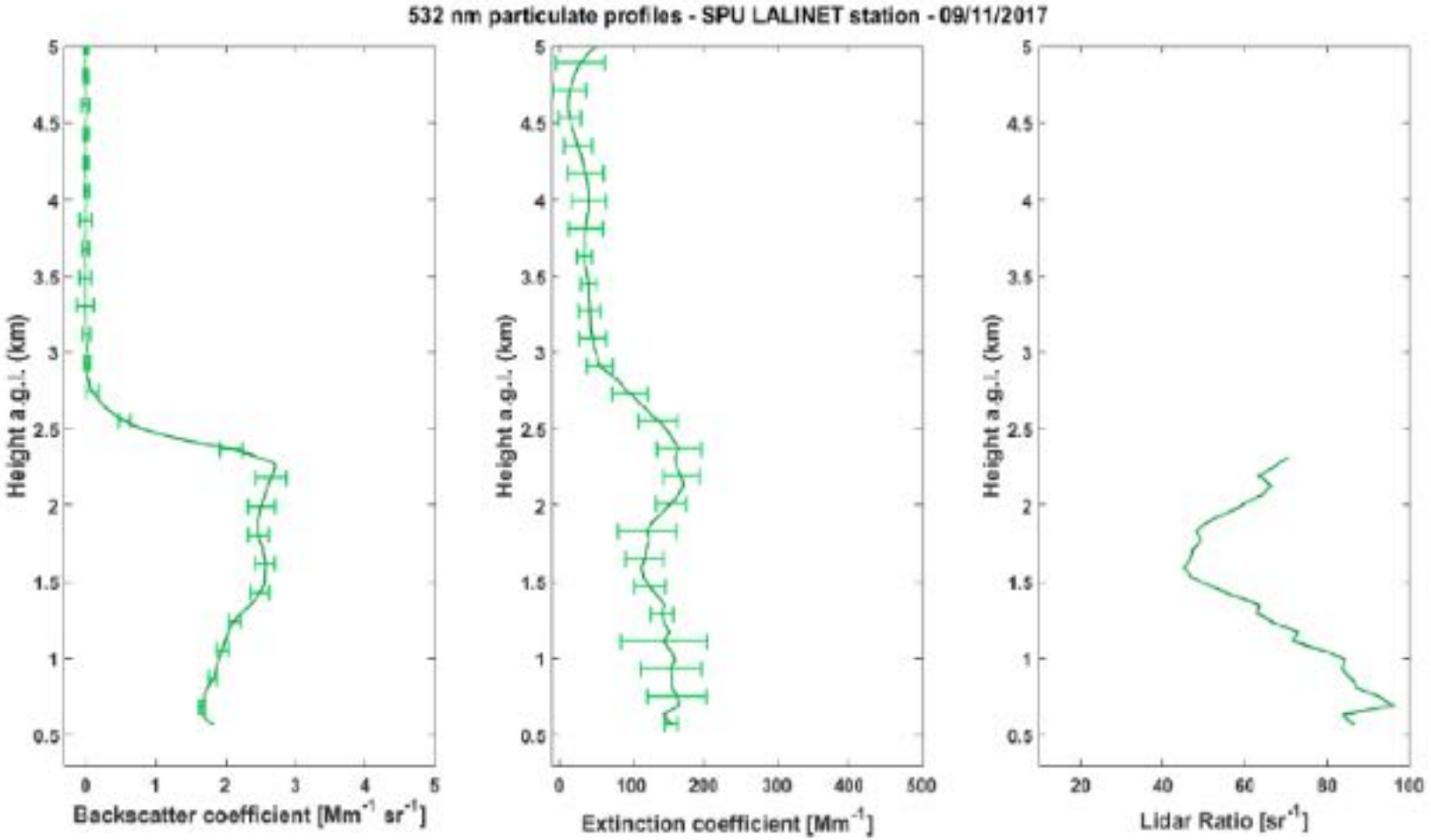

Eduardo Landulfo

https://bit.ly/2l3n2XD

LONG RANGE TRANSPORT STUDIES

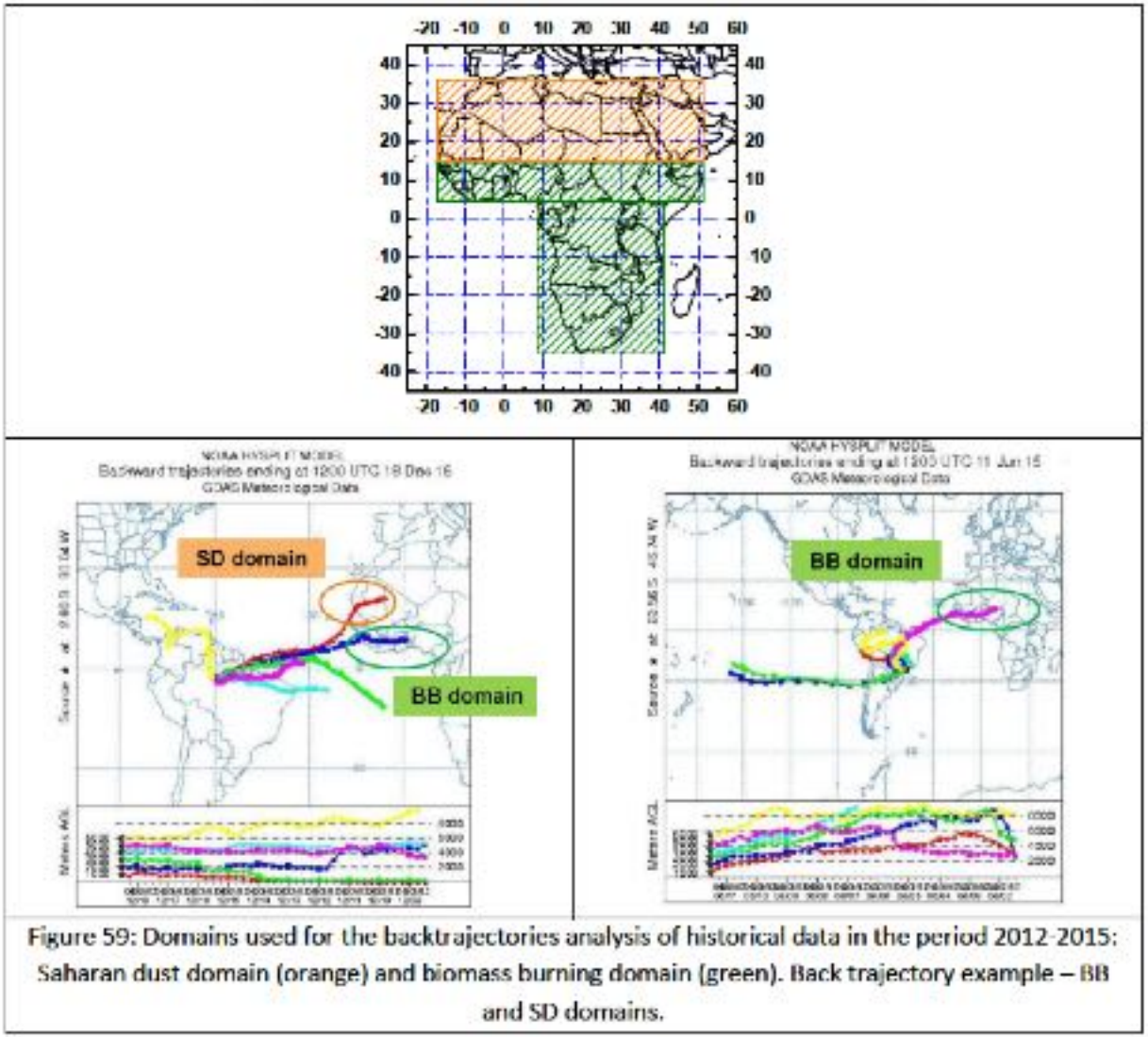

Figure 59: Domains used for the backtrajectories analysis of historical data in the period 2012-2015: Saharan dust domain (orange) and biomass burning domain (green). Back trajectory example – BB and SD domains.

https://bit.ly/2l3n2XD

AEROSOL TYPING

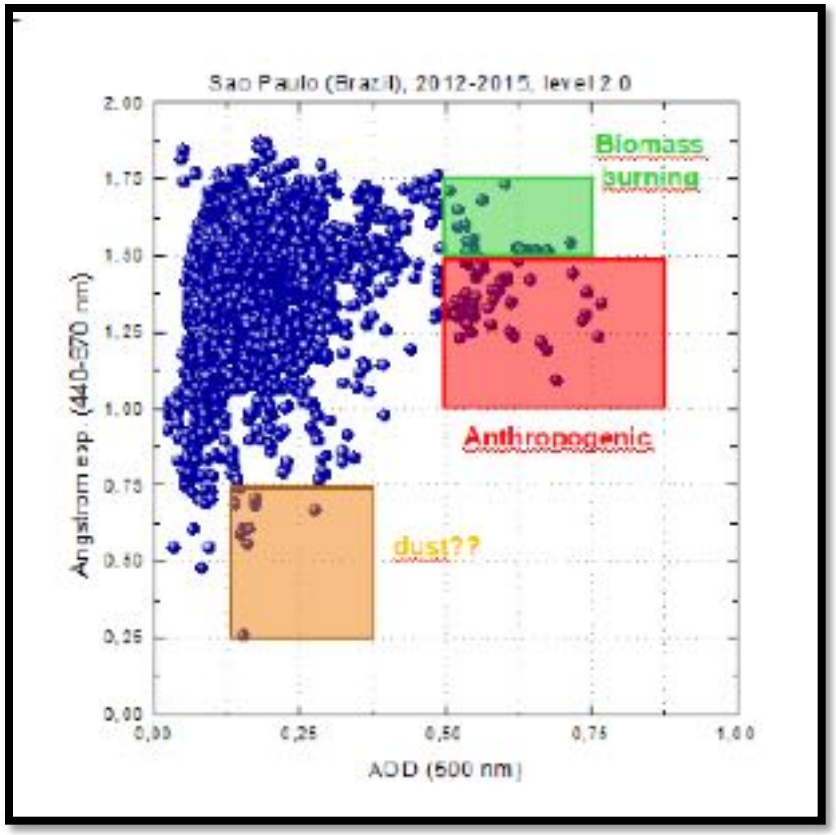

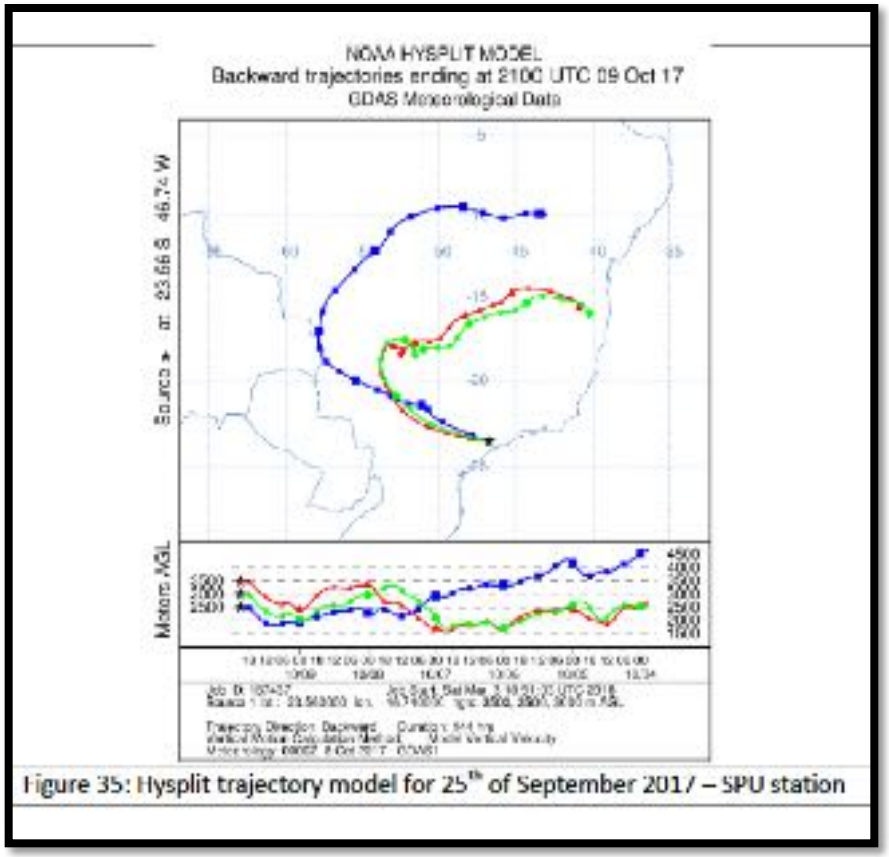

Figure 35: Hysplit trajectory model for 25th of September 2017 – SPU station

Eduardo Landulfo

European Space Agency

EarthCARE Mission

Announcement of Opportunity

External Calibration and Validation of the EarthCARE Mission

LALINET CAL/VAL PARTICIPATION

https://bit.ly/2ruZnD3

esa Earth Online

Login My Earthnet | Register | Google Custom Search

Need Help? Contact here | European Space Agency

Missions | Earth Topics | Data Access | PI Community | Explore more...

You are here Home › PI Community › Apply for Data › AO's

Follow | Share

Announcements of Opportunity

Aeolus CalVal Call | OSEO | Swarm SO | S5PVT | S3VT | G-POD | Previous AOs

Welcome to the submission area for the EarthCARE Calibration and Validation opportunity.

The deadline for the submission of EarthCARE Calibration and Validation proposals was 31 October 2017

First ESA EarthCARE Validation Workshop (11- 15 June 2018, Bonn, Germany)

EARTHCARE

PI Community

- PI Community Home
- Results
- Search Results and Projects
- Apply for Data
  - Fast Registration
  - Full Proposal
  - Service Request
  - Campaigns
  - AO's
  - 3rd Party

The Earth Clouds, Aerosol and Radiation Explorer (EarthCARE) Mission is being implemented as the sixth Earth Explorer Missions. EarthCARE has been specifically designed with the basic objective of improving the understanding of cloud-aerosol-radiation interactions, so as to include them correctly and reliably in climate and numerical weather prediction models. EarthCARE will achieve this by providing global observations of atmospheric cloud and aerosol profiles with collocated measured as well as modelled long-wave and short-wave radiation.

CLOUD-AEROSOL-INTERACTION

Atmospheric cloud and aerosol properties will be retrieved from EarthCARE's 355nm lidar with a high spectral resolution (HSR) receiver with co- and cross-polar channels (ATLID), 94GHz Doppler cloud profiling radar (CPR) and a multi-spectral imager (MSI). Radiative transfer models will be used to derive atmospheric radiative properties and heating rates from the retrieved cloud and aerosol observations. Reflected solar and emitted terrestrial thermal radiation will furthermore be observed by EarthCARE's broad-band radiometer (BBR) and compared to their modelled equivalents.

355 nm HRSL + CPR + MSI + BBR

esa

JAXA
Japan Aerospace Exploration Agency

https://bit.ly/2tOiU0U

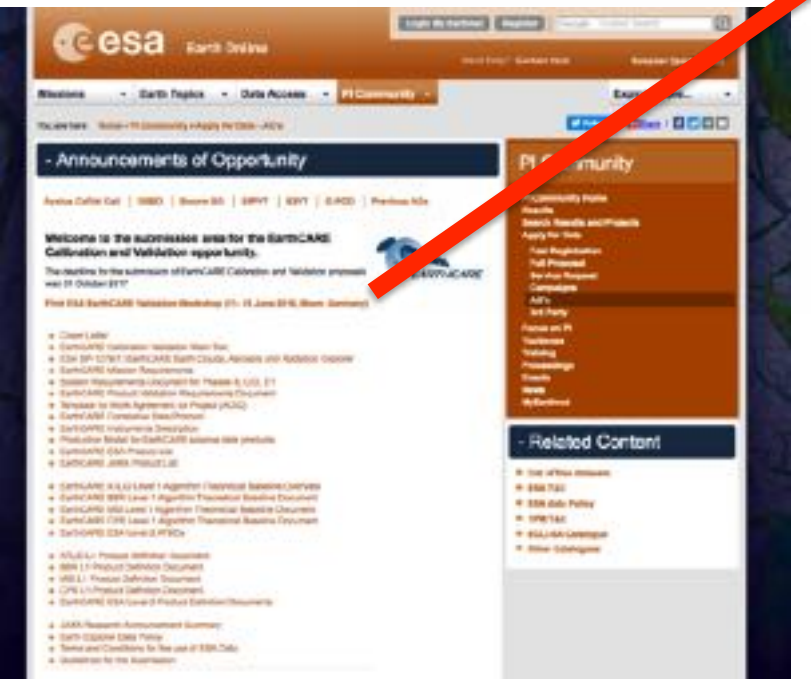

- Cover Letter
- EarthCARE Calibration Validation Main Text
- ESA SP-1279(1) EarthCARE Earth Clouds, Aerosols and Radiation Explorer
- EarthCARE Mission Requirements
- System Requirements Document for Phases B, C/D, E1
- EarthCARE Product Validation Requirements Document
- Template for Work Agreement for Project (AOID)
- EarthCARE Correlative Data Protocol
- EarthCARE Instruments Description
- Production Model for EarthCARE science data products
- EarthCARE ESA Product List
- EarthCARE JAXA Product List

- EarthCARE ATLID Level 1 Algorithm Theoretical Baseline Overview
- EarthCARE BBR Level 1 Algorithm Theoretical Baseline Document
- EarthCARE MSI Level 1 Algorithm Theoretical Baseline Document
- EarthCARE CPR Level 1 Algorithm Theoretical Baseline Document
- EarthCARE ESA Level 2 ATBOs

- ATLID L1 Product Definition Document
- BBR L1 Product Definition Document
- MSI L1 Product Definition Document
- CPR L1 Product Definition Document
- EarthCARE ESA Level 2 Product Definition Documents

- JAXA Research Announcement Summary
- Earth Explorer Data Policy
- Terms and Conditions for the use of ESA Data
- Guidelines for the Submission

VALIDAÇÃO

The European Space Agency is announcing the opportunity for interested groups to participate in these activities. Specific areas in which the contribution of the participants is sought are:

- validation using other satellite, airborne or ground-based experiments providing independent measurements;
- experiments to assess accuracy, resolution, and stability of the EarthCARE instruments;
- assessment and validation of the EarthCARE retrieval and processing

ÁREAS DE INTERESSE

- assessment of methods/algorithms for instrument calibration
- assessment of proposed methods/algorithms for external calibration
- independent estimates of achievable localisation and co-alignment errors
- independent determination of instrument stability
- comparison of geophysical products (cloud, aerosol, precipitation, and radiation properties) with independent ground-based, airborne or satellite measurements, including consideration of representativity errors
- impact of auxiliary information used in the processing (temperature, backscatter data bases, …)
- comparison with other space-borne sensors (at level 1 and level 2)
- characterisation of major error sources and their dependencies on secondary parameters (e.g. solar zenith angle, land-sea error dependency, etc.)
- error budget compilations

ATIVIDADES DOS PARTICIPANTES

- Integration of their proposed work within a wider scientific and technical framework, and the establishment of collaboration between specialists
- Participation in the establishment of detailed validation planning well in advance of the launch, presently planned for August 2019
- Participation in post-launch data product and retrieval algorithm validation, and independent monitoring of satellite performance and data quality
- Support to the Agency in the planning and execution of special satellite operations in conjunction with ground experiments
- Support to the Agency in the definition, in the light of post launch experience, of reprocessing algorithms to be applied to the level 1b, level 2a, and 2b data
- Support to ESA in dedicated ECVT meetings and workshops
- Participation in pre-launch rehearsal activities

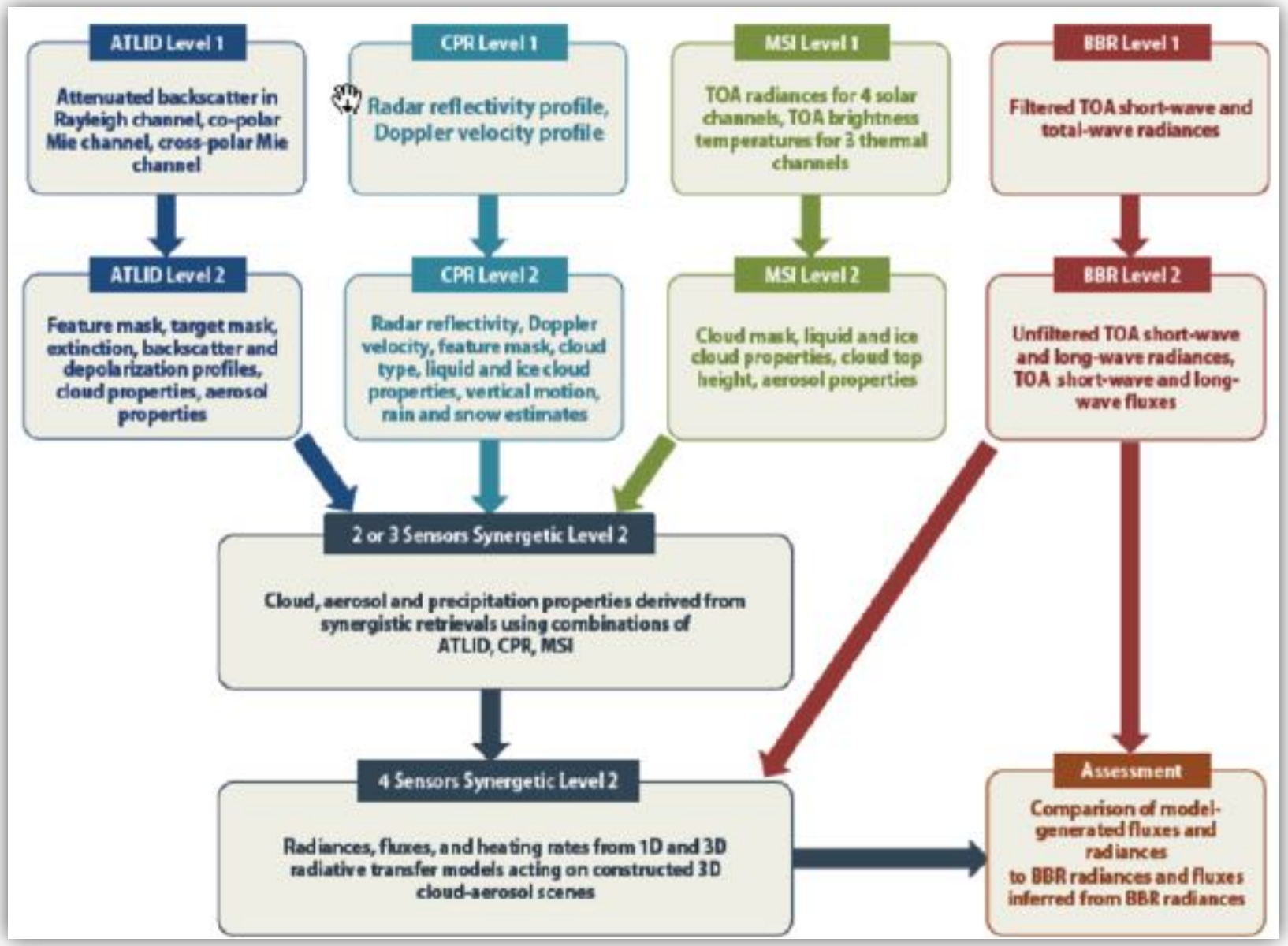
ATLID Level 1
Attenuated backscatter in Rayleigh channel, co-polar Mie channel, cross-polar Mie channel
CPR Level 1
Radar reflectivity profile, Doppler velocity profile
MSI Level 1
TOA radiances for 4 solar channels, TOA brightness temperatures for 3 thermal channels
BBR Level 1
Filtered TOA short-wave and total-wave radiances
ATLID Level 2
Feature mask, target mask, extinction, backscatter and depolarization profiles, cloud properties, aerosol properties
CPR Level 2
Radar reflectivity, Doppler velocity, feature mask, cloud type, liquid and ice cloud properties, vertical motion, rain and snow estimates
MSI Level 2
Cloud mask, liquid and ice cloud properties, cloud top height, aerosol properties
BBR Level 2
Unfiltered TOA short-wave and long-wave radiances, TOA short-wave and long-wave fluxes
2 or 3 Sensors Synergetic Level 2
Cloud, aerosol and precipitation properties derived from synergistic retrievals using combinations of ATLID, CPR, MSI
4 Sensors Synergetic Level 2
Radiances, fluxes, and heating rates from 1D and 3D radiative transfer models acting on constructed 3D cloud-aerosol scenes
Assessment
Comparison of model-generated fluxes and radiances
to BBR radiances and fluxes inferred from BBR radiances

LALINET VS CALVAL

Release of the call (opening of Submission Website)	**15 June 2017**
Closing of the call (closing of Submission Website)	**15 October 2017**
Notification of the evaluation results to PIs	**15 January 2018**
1st Validation Workshop (combined w. Science)	**June 2018**
Pre-launch ESA-JAXA validation workshop	**February 2019**
Validation Rehearsal	**March 2019**
Validation Rehearsal Review / Validation Readiness	**June 2019**
Launch	**August 2019**
Preliminary Validation Results Review	**February 2020**
Long-term Validation Phase	**February 2020 until End-of-Mission**


LEAL
Laser Environmental Applications Laboratory
HOME RESEARCH FIELD PROJECTS EQUIPMENTS CAMPAIGNS MEASUREMENTS PUBLICATIONS MEMBERS PARTNERS
ALLSKYCAM LIDAR DOPPLER
gescon.ipen.br/leal
ABOUT US

https://bit.ly/2JCvKqq

UNIVERSIDAD NACIONAL DE COLOMBIA

ciencias.medellin.unal.edu.co

HOME CONFERENCE REGISTRATION DEAD LINES COMMITTEES VENUE SEDES

aebastid@unal.edu.co

landulfo@gmail.com

Está aquí: Inicio / Institucional / The X Workshop Lidar Measurements in Latin America (WLMLA)

A- A A+

Servicios

The X Workshop Lidar Measurements in Latin America (WLMLA)

http://ciencias.medellin.unal.edu.co/eventos/wlmla/index.php/2-institucional/6-home